UNIVERSITÀ DEGLI STUDI DI MESSINA

DIPARTIMENTO DI SCIENZE CHIMICHE, BIOLOGICHE, FARMACEUTICHE ED AMBIENTALI

DOTTORATO DI RICERCA IN SCIENZE CHIMICHE

DOCTOR OF PHILOSOPHY IN CHEMICAL SCIENCES

Isotopic ratio mass spectrometry: from bulk analysis to the coupling with enantio-multidimensional gas chromatography for the authenticity assessment of premium products

PhD thesis of:
Lorenzo Cucinotta

Supervisor:
Prof. Danilo Sciarrone

Coordinator:
Prof. Concetta De Stefano

XXXV CICLO ANNO ACCADEMICO 2021/2022 SSD CHIM/01

Page intentionally left blank

Table of contents

Acknowledgments

I would like to express my sincere gratitude to Prof. Luigi Mondello and Prof. Paola Dugo for the opportunity given and the precious advice during my PhD.

I am deeply grateful to my esteemed supervisor Prof. Danilo Sciarrone for his invaluable support, patience, and for being a guide throughout all my PhD research activities.

My sincere gratitude extends to Fondazione Edmund Mach for the co-funding opportunity and to all the people involved in the research studies: Prof. Federica Camin, Dr Luana Bontempo, Dr Roberto Larcher, Dr Sergio Moser, Dr Mauro Paolini. I especially thank you for being part of the project we shared, and for your invaluable advice.

I would like to thank all the research team and colleagues at the University of Messina for the time spent together, especially my labmate Gemma for her precious support during these three years of research.

Last but not least, I would like to thank my family, Michela and my friends for their encouragement and support throughout all my studies.

Abstract

The PhD activity aimed to the evaluation of the applicability of isotopic ratio mass spectrometry for the authenticity assessment of premium products, from the analysis of whole samples by means of bulk stable isotope analysis to the development of advanced chromatographic approaches.

Starting from bulk analysis, a thorough investigation of Cannabis Sativa L. products was carried out, by analysing the main stable isotopes, namely $^{13}C/^{12}C$, $^{18}O/^{16}O$, $^{2}D/^{1}H$, $^{15}N/^{14}N$, $^{34}S/^{32}S$. (Chapter 2). This research allowed determining the characteristic isotopic distribution of different hemp parts, such as inflorescences, seeds and roots, representing a reliable authenticity range for genuine samples.

However, despite the renowned capability of bulk analysis to evaluate the isotopic distribution of a matrix, adulteration may sometimes involve only target components, thus requiring advanced analytical devices prior to IRMS detection. In this concern, gas chromatography is by far the preferred analytical method to evaluate the isotopic ratio of key separated volatile components. Nevertheless, the coupling of gas chromatography to isotopic ratio mass spectrometry (GC-C-IRMS) requires the condition of baseline resolution for the reliable detection of the isotopic ratios. Due to the uneven distribution of ^{13}C and ^{12}C isotopes along an entire peak of CO_2, co-elutions represent a critical matter and deny the achievement of reliable data. In this concern, a deep investigation was carried out to evaluate the applicability of monodimensional GC-C-IRMS in the analysis of complex samples, demonstrating the need for multidimensional gas chromatography to achieve reliable isotopic results (Chapter 5).

As well as isotopic ratio mass spectrometry, enantio-selective gas chromatography covers a key role in the field of authenticity assessment. The production of typical enantiomeric excesses for target volatiles is directly related to the biosyntheticpathways of the plant of origin, representing a valuable tool to discriminate between genuine and adulterated samples. Due to the capability of both techniques to investigate in depth the biochemical steps of the sample investigated, the main aim was to hyphen the enantio-selective GC separation to the IRMS detection. As well as for the monodimensional GC-C-IRMS application reported in Chapter 5, even in this case several issues were involved by applying a monodimensional enantio-selective GC-C-IRMS approach. To these aims, enantio-selective multidimensional gas chromatographic methods, with a simultaneous single quadrupole and IRMS detection, were developed for the analysis of different valuable products, such as Cannabis Sativa L. essential oils (Chapter 7), volatile organic components of

Moscato Giallo grapes (Chapter 8) and lemon essential oils (Chapter 9). This system allowed evaluating simultaneously the enantiomeric and isotopic ratios of key components, clearly reducing total time analysis.

Moreover, this coupling allows determining the specific isotopic ratio of each enantiomer separated. Whilst most of the literature references described how no isotopic differences should be expected between the enantiomers of the same couple, different isotopic signatures were registered for the dextro and levorotatory enantiomers of α and β-pinene in the case of lemon essential oils (Chapter 9). This finding paves the way for newer considerations in the field of authenticity assessment since different essential oil types may present typical chiral isotopic fractionation processes.

Chapter 1

Isotopic ratio mass spectrometry (IRMS)

1.1 IRMS: basic concepts

Isotopic ratio mass spectrometry (IRMS) is an analytical technique, which is spreading ever more for authenticity aims, since it is able to provide clearer information about the genuineness and provenance of a wide range of products. As highlighted by a review of Meier Augenstein in 1999, its application is covering various fields, from archaeology to forensic sciences, from geology to food traceability [Meier Augenstein 1999]. The main analytical concept is to provide precisely an accurate value of the abundance of the isotopic ratios in stable light elements, like carbon, oxygen, hydrogen, nitrogen and sulphur. In this concern, an IRMS is designed to measure with high precision small differences in the isotopic ratios of $^{13}C/^{12}C$, $^{18}O/^{16}O$, $^{2}D/^{1}H$, $^{15}N/^{14}N$, and $^{34}S/^{32}S$. As reported by Brenna *et al*., the term *high precision* needs to be intended as a standard deviation in the range of 4-6 significant figures, obtained at the expenses of the renowned flexibility of a common mass spectrometer [Brenna 1997]. In this concern, single quadrupoles, ion traps, and time-of-flight mass spectrometers do not provide the sensitivity required to detect the subtle differences in naturally-occurring isotopic abundances. For these reasons, the measurement of stable isotopic ratios requires a specialized instrument such as the multi-collector magnetic sector mass spectrometer, namely the IRMS system, developed for the first time by Nier in 40s [Nier 1940]. Moving to isotopic measurements, isotopic ratios are always labelled as delta (δ^{i} E) notations, calibrated with respect to international recognized materials, having a defined amount of stable isotopes. This procedure allows deleting any possible bias or systematic error in the measurement. About δ notation, this signature is expressed as the difference between the sample and the primary international standards, as reported in the following formula:

$$\delta^{i}E = \frac{{}^{i}R_{sample} - {}^{i}R_{standard}}{{}^{i}R_{standard}}$$

where R is the ratio between the heavier isotope with respect to the lighter one (e.g $^{13}C/^{12}C$). Moreover, R_{sample} is always corrected with respect to R_{standard}, whose value changes in relation to the element, and thus the international standard considered:

1) VSMOW (Vienna Standard Mean Ocean Water) for both $^{2}D/^{1}H$ and $^{18}O/^{16}O$
2) VPDB (Vienna Peedee Belemnite) for $^{13}C/^{12}C$
3) Atmospheric nitrogen for $^{15}N/^{14}N$

However, since international standards can or end up or become environmentally depleted, secondary standards have been calibrated over the time with respect to the primary ones. These reference materials are both natural and synthetic components, provided by both the International Atomic Energy Agency (IAEA; Vienna, Austria) and the National Institute of Standards and Technology (NIST; Washington, DC, USA). Most of these secondary standards have been discussed by several research groups [Valkiers 2007a, Valkiers 2007b, Brand 2014, Schimmelmman 2016, Qi 2016].

1.2 Natural abundances and main characteristics of stable isotope elements

Table 1.1 reports the average natural abundance of the main stable isotopes in bio-elements. After that, a brief description is provided about the characteristic isotopic distribution of such elements in nature.

Element	Stable Isotope	Mean natural abundance %
Hydrogen	^{1}H	99.99
	^{2}H	0.01
Carbon	^{12}C	98.89
	^{13}C	1.11
Nitrogen	^{14}N	99.63
	^{15}N	0.37
Oxygen	^{16}O	99.76
	^{17}O	0.04
	^{18}O	0.20
Sulphur	^{32}S	95.00
	^{33}S	0.76
	^{34}S	4.22
	^{35}S	0.02

Table 1.1 Average natural abundance of the main stable isotopes for hydrogen, carbon, nitrogen, oxygen and sulphur

Carbon

Dealing with carbon distribution in natural systems, the primary carbon source needs to be considered atmospheric CO_2. As reported by Longinelli *et al*., nowadays the $\delta^{13}C$ value of atmospheric CO_2 is gradually becoming more negative, until a value of -8.22 ‰ registered in 2003 [Longinelli 2005]. Moving to the photosynthetic cycles, once the plant absorbs the atmospheric CO_2, isotopic fractionation involves. As universally demonstrated, this process involves in a reduction of the resulting amount of ^{13}C in the plant, and to more negative $\delta^{13}C_{VPDB}$ values. Moreover, since the uptake of CO_2 by the plant is strictly related to the plant itself, isotopic fractionation will depend by the different photosynthetic cycle employed, such as Calvin (C_3), Hatch Slack (C_4) and Crassulacean acid metabolism (CAM). As reported by Winkler 1984, C_3 plants, such as grape, flowering plants, rice, wheat, show a higher depletion in ^{13}C with respect to C_4 ones, which follow the Hatch Slack cycle [Winkler 1984]. Therefore, as stated by Krueger, most of the C_3 plants had $\delta^{13}C_{VPDB}$ values covering a range from -24 ‰ to -34 ‰ [Krueger 1982]. Due to the minor isotopic fractionation with respect to Calvin cycle, C_4 plants, namely sugar cane, marine plants, corn, showed $\delta^{13}C_{VPDB}$ values from -10 ‰ to -16 ‰. Since CAM plants are able to use both the photosynthetic cycles, their $\delta^{13}C_{VPDB}$ values generally cover a range from -12 to -30 ‰.

Nitrogen

For nitrogen, as well as for carbon, only two stable isotopes exists in nature (^{14}N and ^{15}N). The main source of nitrogen is the atmosphere, from which it is converted to both inorganic forms and organic ones. As reported by Meier Augenstein, the main mechanisms related to the natural cycle of nitrogen include nitrogen fixation, assimilation, mineralisation, nitrification and denitrification [Meier Augenstein 2010]. In relation to which type of process involves, the nitrogen isotopic distribution in soil may vary between a range from -10 to +15 ‰. About plants, their $\delta^{15}N$ value may vary in relation to the type of fertiliser employed (synthetic or manure), as well as due to the isotopic fractionation during the uptake and organic compound assimilations [Bateman 2007].

Oxygen

The measurement of oxygen isotopic ratio ($\delta^{18}O$) refers to the abundance of the heavier isotope ^{18}O with respect to the ^{16}O. The variation in terms of oxygen isotopes strictly depends on the hydrological cycles: starting from the evaporation from the oceans, the transport of atmospheric vapour, until the precipitation and return of water in to the oceans. As reported by Clark, the $\delta^{18}O$ distribution of oceanic water has a range between -1 to +0.7 ‰ [Clark 1997]. In earth, several

factors affects oxygen isotopic fractionation. Among these, latitude plays surely a key role. After evaporation, water vapour moves from tropical zones to the poles, where it precipitates becoming more depleted in heavier isotopes. Contrarily, equatorial precipitations are more concentrated in terms of heavier isotopes. As well as latitude, also altitude affects oxygen isotopic fractionation. As reported by Förstel and Hutzen [Förstel and Hutzen 1984], different altitudes involves in a depletion of ^{18}O, since higher altitude corresponds to lighter vapour (differences of about -0.5‰ each 100 meter).

Hydrogen

Main considerations about ^{2}H variation in the hydrosphere are very similar to the pattern found for the ^{18}O, discussed previously [Craig 1961]. Dealing with hydrogen distribution in plants, metabolites originate from the water absorbed by the roots. In this concern, isotopic composition in xylem reflects that of ground water. Differently with respect to carbon distribution, no relevant differences involve for hydrogen isotopes for plants employing C_3, C_4 or CAM photosynthetic cycles [Bricout 1982]. Primary metabolites are relatively depleted in deuterium, resulting in $\delta^{2}H$‰ from – 90 to -180 ‰. This depletion is even more evident in secondary metabolites, where further depletion involves due to kinetic isotopic effects [Winkler 1984].

Sulphur

As reported in Table 1.1, sulphur exists as four stable isotopes. However, only $^{34}S/^{32}S$ is evaluated for isotopic determination, also due to the higher abundance of ^{34}S with respect to ^{33}S and ^{36}S. $\delta^{34}S$ in nature is strictly related to the availability of the inorganic compounds containing sulphur, namely sulphur, sulphate and hydrogen sulphide gas, and their distribution in global ecosystems. The content of heavier sulphides in the soil as well as aerobic and anaerobic growing conditions affects $\delta^{34}S$ in terrestrial plants [Rubenstein and Hobson 2004]. Other factors are related to microbial processes in the soil, fertilisation procedures as well as the sea-spray effect in coastal areas [Attendorn & Bowen 1997].

1.3 Bulk isotopic analysis performed by EA-IRMS and TC-EA/IRMS

As stated in the first paragraph, the capability to measure isotopic ratios of light stable elements requires an appropriate isotopic ratio mass spectrometer. In this concern, IRMS analysis can be performed by means of different modes, involving or the analysis of the entire sample, e.g., bulk analysis, or by means of a chromatographic separation step prior to the IRMS detection, e.g GC-C-IRMS (discussed in Chapter 4) or HPLC-C-IRMS. Dealing with bulk analysis, the value of isotopic ratio detected is directly dependent by all the molecules containing that specific isotope.

Since the first IRMS application on honey [Doner and White 1977], this approach demonstrated to be very useful to detect adulteration in various matrices. Nowadays, two different types of elemental analysers are available to detect the stable isotope composition of a matrix. For the analysis of carbon and nitrogen stable isotope ratios, an elemental analyser coupled to isotopic ratio mass spectrometer (EA-IRMS) is usually employed. In this analysis, samples are subjected to combustion in an oxygen atmosphere, and after that combustion products are transported by a flow of helium as carrier gas. In this concern, after the combustion process, a reduction step is required. While combustion produces CO_2, H_2O and NO_x from organic molecules, reduction aims to eliminate O_2 in excess and to reduce NO_x to N_2; for the elimination of water, a water trap is usually employed. Finally, the N_2 and CO_2 obtained by the organic molecules are separated by means of a packed GC column, and thus detected from the mass spectrometer (Figure 1A).

Dealing with the detection of hydrogen and oxygen stable isotopes, different elemental analysers were proposed. Samples are subjected to high thermal conversion (HTC) to produce CO and H_2 prior to IRMS detection. Figure 1B resumes the main components of such an instrument.

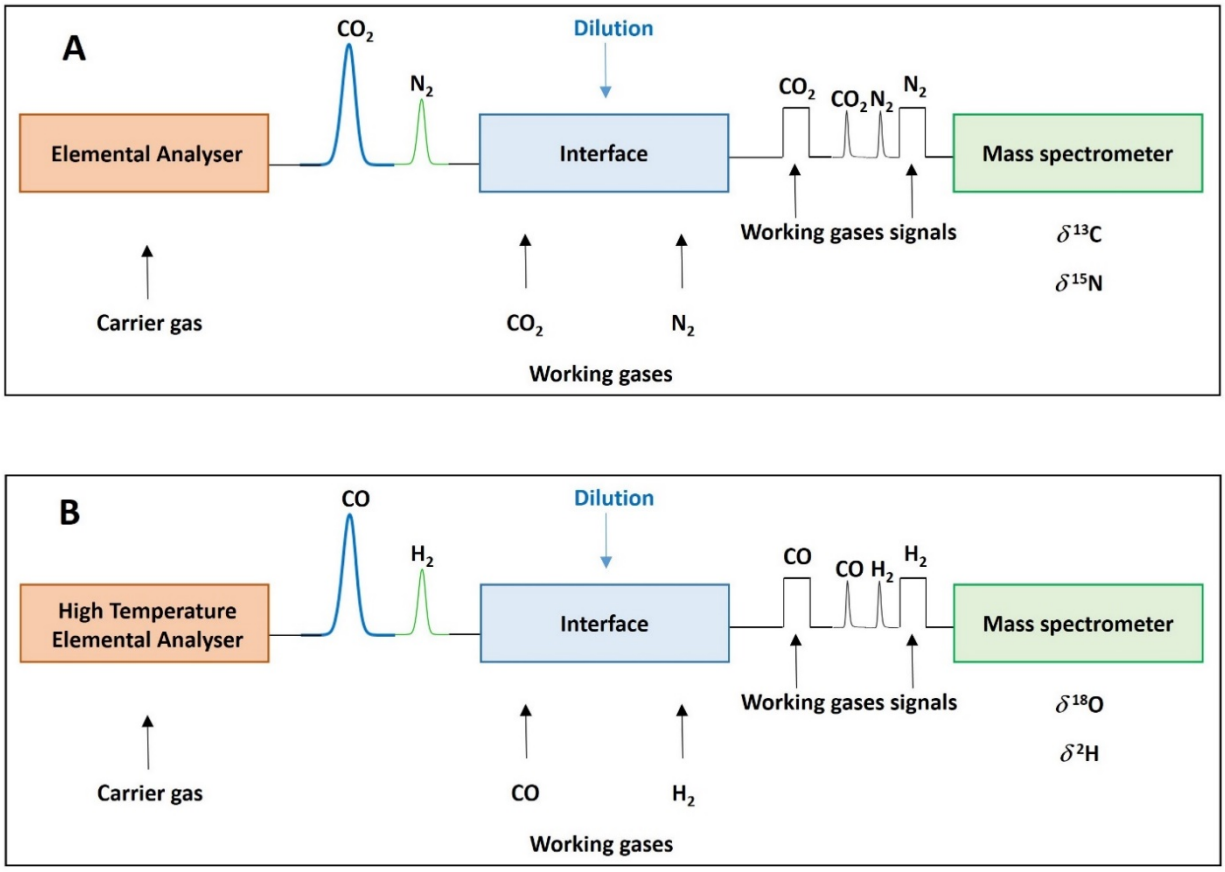

Figure 1.1 Scheme of elementar analyser (A) and high temperature elementar analyser (B)

In general, both the analysis are performed following a series of steps, namely: 1) combustion or thermal conversion of the sample analysed; 2) introduction of the gas into the ion source of the IRMS by means of the interface, which limits the gases entering the ion source ; 3) ionisation of the molecules and detection of the target ions.

1.4 Application

As reported, the employment of an EA-IRMS and of a HTC-EA-IRMS allows to provide a precise characterization of the typical $\delta^{i}E$ value of the main stable isotopes in nature. By these means, it is possible to define the natural distribution of high value products, in order to protect them against fraudulent actions. In this concern, adulteration is becoming an ever more spreading issue nowadays. Frauds can be associated to the employment of materials of different geographical origin or may be related to the substitution of key components with cheaper imitations. In this concern, traceability of products is becoming a common procedure to highlight the effective composition of high value matrices. In the light of what has been discussed above, the evaluation of isotopic composition is one of the key parameters to be evaluated for authenticity assessment, since it is affected by various environmental factors, as well as by climatic and geographic conditions. Several research works have demonstrated the usefulness of a thorough investigation of the stable isotopic pattern for a matrix. In this concern, Camin research group applied this multi stable isotope approach for the authenticity assessment of several food products [Bontempo 2016, Perini 2014, Camin 2012]. Dealing with the analysis of grated hard cheese, Camin was able to differentiate the most famous PDO Parmigiano Reggiano from nine European and two extra-European imitations [Camin 2012].

In the next chapter, a full investigation of the main stable isotopes ($^{2}H/^{1}H$, $^{18}O/^{16}O$, $^{13}C/^{12}C$, $^{15}N/^{14}N$, $^{34}S/^{32}S$) in Italian industrial hemp is discussed. Thanks to the approach developed, authenticity ranges for such a matrix were defined for the first time in literature.

References

Attendorn HG, Bowen R. Radioactive and Stable Isotope Geology, Chapman & Hall, New York, 1997

Bateman A.S., Kelly S.D., Woolfe M. Nitrogen isotope composition of organically and conventionally grown crops. J. Agric. Food Chem. 55 (2007) 2664.

Bontempo L, Camin F, Paolini M, Micheloni C, Laursen, K, H. Multi-isotopic signatures of organic and conventional Italian pasta along the production chain. J. Mass Spectrom (2016) 675-683

Brand WA, Coplen TB, Vogl J, Prohaska T. Assessment of international reference materials for stable isotope ratio analysis 2013 (IUPAC Technical Report). Pure Appl Chem 86 (2014) 425–467.

Brenna, JT, Corso, TN, Tobias, HJ, Caimi, RJ, High-Precision Continuous-Flow Isotope Ratio Mass Spectrometry, Mass Spectrom. Rev. 16 (1997) 227–258

Bricout J. Isotope ratios in environmental studies. Int. J. Mass Spec. Ion Phys. 45 (1982) 195.

Camin F, Larcher R, Perini M, Bontempo L, Bertoldi D, Gagliano G, Nicolini G, Versini G. Characterisation of authentic Italian extra-virgin olive oils by stable isotope ratios of C, O and H and mineral composition. Food Chem 118:4 (2010) 901–909.

Camin, F, Wehrens, R, Bertoldi, D, Bontempo, L, Ziller, L, Perini, M, Nicolini, G, Nocetti, M, Larcher, R. H, C, N and S stable isotopes and mineral profiles to objectively guarantee the authenticity of grated hard cheeses Anal. Chim. Acta 711 (2012) 54-59

Clark I., Fritz P. Environmental Isotopes in Hydrogeology, Lewis Publishers, New York, 1997.

Craig H. Isotopic variations in natural waters. Science. 133 (1961) 1702.

Doner LW, White JW. Carbon-13/carbon-12 ratio is relatively uniform among honeys. Science 197 (1977) 891–2.

Förstel H, Hutzen H. Variation des Verhaltnisses der stabilen Sauerstoff-isotope im Grundwasser der Bundesrepublik Deutschland. Gwf-wasser/abwasser. 125 (1984) 21.

Krueger H.W., Reesman R.H. Carbon isotope analyses in food technology. Mass Spec. Rev. 1 (1982) 206.

Longinelli A, Lenaz R, Ori C, Selmo E. Concentrations and δ 13 C values of atmospheric CO_2 from oceanic atmosphere through time: polluted and non-polluted areas. Tellus B 57:5 (2005) 385–390.

Meier-Augenstein W. Applied gas chromatography coupled to isotope ratio mass spectrometry. J Chromatogr A 842 (1999) 351–371.

Meier-Augenstein W. Stable Isotope Forensics. UK: John Wiley & Sons Ltd, 2010.

Nier AO. A mass spectrometer for routine isotope abundance measurements. Rev Sci Instrum 11:7 (1940) 212–216.

Qi, H., Coplen, T.B., Mroczkowski, S.J., Brand, W.A., Brandes, L., Geilmann, H., Schimmelmann, A. A new organic reference material, l -glutamic acid, USGS41a, for δ13C and δ15N measurements - A replacement for USGS41, Rapid Commun Mass spectrum 30:7 (2016) 859-866

Rubenstein D.R., Hobson K.A. From birds to butterflies: animal movement patterns and stable isotopes. Trends Ecol. Evol. 19 (2004) 256.

Schimmelmann, A., Qi, H., Coplen,T.B., Brand, W. A., Fong, J., Meier-Augenstein, W., Kemp, H. F., Toman, B., Ackermann, A., Assonov, S., Aerts-Bijma, A.T., Brejcha, R. Organic Reference Materials for Hydrogen, Carbon, and Nitrogen Stable Isotope-Ratio Measurements: Caffeines, n-Alkanes, Fatty Acid Methyl Esters, Glycines, l -Valines, Polyethylenes, and Oils, Anal Chem 88:8 (2016) 4294-4302

Valkiers, S., Varlam, Russe, M. K, Berglund, M., Taylor, P., Wang, J., Milton M., De Bievre, P, Int J Mass Spectrom, 264 (2007) 10–21.

Valkiers, S., Varlam, Russe, M. K, Berglund, M., Taylor, P., Wang, J., Milton M., De Bievre, P, Int J Mass Spectrom, 263 (2007), 195–203.

Winkler F.J. Chromatography and mass spectrometry in nutrition science and food safety, (Eds: A. Frigerio, H. Milon), Elsevier Science Publishers BV, Amsterdam, 1984.

Chapter 2

Isotopic Characterization of Italian Industrial Hemp (Cannabis sativa L.) Intended for Food Use: A First Exploratory Study

2.1 Introduction

Cannabis sativa L., commonly named hemp, is an annual and mainly dioecious plant based on the C_3 photosynthetic cycle, belonging to the family of *Cannabaceae* [Landi 1997]. Hemp covers a high number of traditional and innovative application in various fields, leading to its global distribution as an emerging high-value specialty crop [Amaducci *et al*., 2015; Ryz *et al.*, 2017]. Currently, due to the increased interest by consumers on healthy food products, including alternative gluten-free, vegan, and vegetarian diets, the consumption of hemp flour-based products, as well as hemp seeds and oil, is spreading more and more.

From an historical point of view [Giupponi *et al.*, 2020], since the Second World War Italy was among the main hemp producers [Baldini *et al.*, 2016], and after that it was still considered as one of the most important global Cannabis industries [Cacchioni 2021]. However, different years of plating ban have limited its commercialization so far. Only by means of the Italian Law 242/2016, cultivation has been legalized again, only for those varieties having a content in delta-9-Tetrahydrocannabinol (THC) lower than 0.2%. Consequently, this law allowed an increased hemp fields' extension from less than 500 hectares in 2013 to 4000 hectares in 2018 [Coldiretti 2020].

Due to the increased interest of the Italian market for hemp and its derived food products [Crini *et al.*, 2020; Giupponi *et al.*, 2020], the Italian hemp Federation in 2021 has established the first guidelines for its production. These documents referred to both plants employed for the production of extracts as well as those for food use. In this concern, and to highlight the authenticity of such evaluable product, different analytical methods were evaluated. These approaches would be useful in the case of adulteration, especially related to the employment of foreign hemp seed oils of doubtful origin and quality [Federcanapa, 2021a; 2021b].

Accordingly, isotopic ratio mass spectrometry (IRMS) is surely one of the most recognized analytical approaches for the authentication and traceability of food products [Altieri *et al.*, 2020;

Bontempo *et al.*, 2020a; Wadood *et al.*, 2019]. In literature, isotopic ratio signatures demonstrated to be a suitable method to discriminate between biological and environmental processes, allowing to provide typical fingerprints of a product, directly related to its geographical and ecological origin [Portarena *et al.*, 2014]. Dealing with *Cannabis Sativa*, literature references are mainly related to the analysis of the light stable isotopes (*i.e.* H, C, N, O) of marijuana samples [Booth *et al.*, 2010; Hurley *et al.*, 2010; Shibuya *et al.*, 2007], in order to investigate illicit traffic by tracking the origin of the drug plantations. In this concern, multiple applications on *Cannabis Sativa*, as the possibility to describe stable isotope ratio analysis of Italian industrial hemp has never been explored.

To these aims, this study determined a specific range of light stable isotope ratios in Italian industrial hemp intended for food use, allowing to contribute a first isotopic database for this plant, paving the way for further research studies on authentication and traceability of food products obtained by hemp.

2.2 Materials and methods

2.2.1 Sampling and cultivation sites

Eighty-four samples of hemp grown in open fields, namely eight roots, twenty-six stems, thirty-eight inflorescences, twelve seeds, and five hemp seed oil samples were hand-collected in eight different regions of Italy between 2018 and 2019 (Figure 2.1). In relation to the Udine sampling site in Friuli Venezia Giulia region (NE Italy; point No. 14 in Figure 2.1), all the parts of the hemp plant (roots, stem, inflorescences, and seeds) were sampled from two different cultivations: one grown under synthetic (nitrogen-phosphorus-potassium, NPK) and one under manure fertilization.

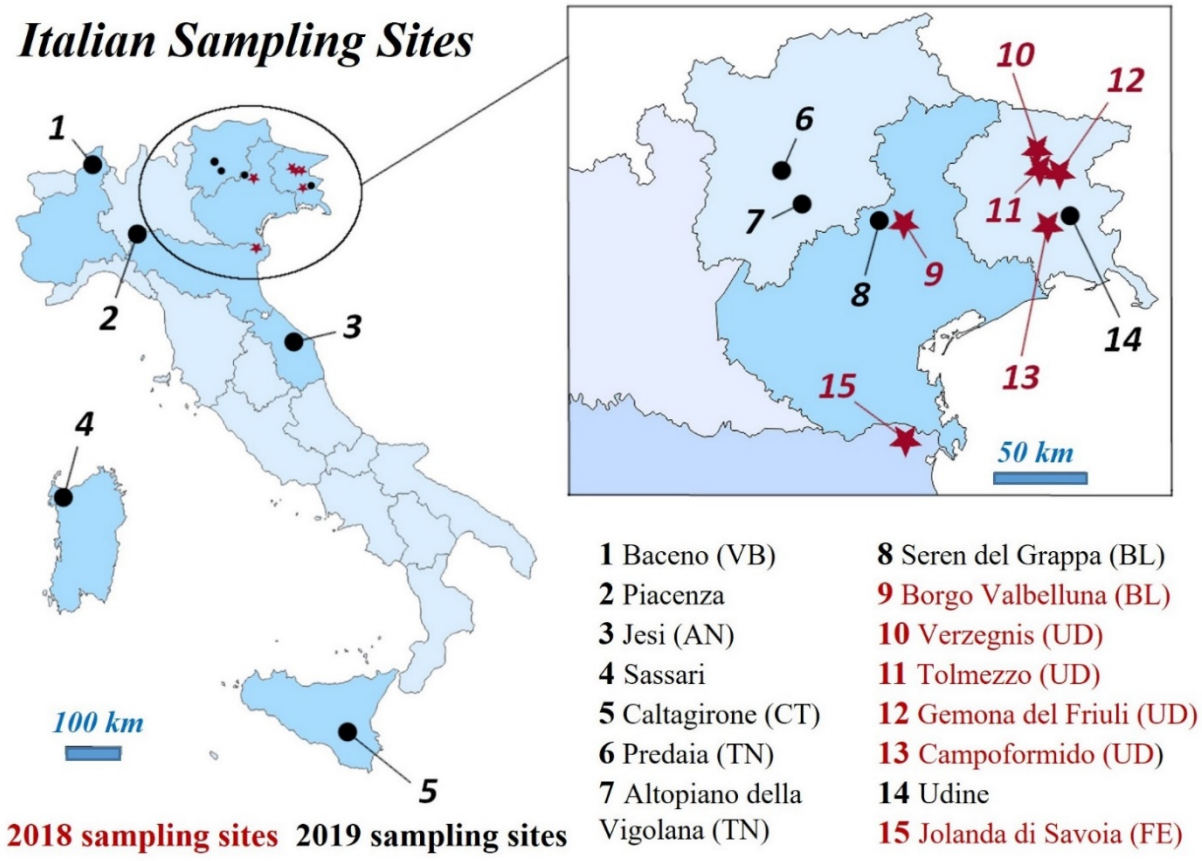

Figure 2.1 Map of 2018 (red stars) and 2019 (black circles) sampling sites.

Every sample analyzed consists of a pool of five-six plants separated into their different parts, which were then stored in polyethylene bags and kept at -20°C until their treatment.

2.2.2 Stable isotope ratio analysis

Isotopic analysis was carried out on freeze-dried, ground, and homogenized samples, except oils that were directly analyzed.

About 0.25 ± 0.05 mg of duplicate powdered sample were weighed into silver capsules for hydrogen ($^{2}H/^{1}H$) and oxygen ($^{18}O/^{16}O$) isotopic ratio analysis and introduced into a High Temperature Conversion Elemental Analyzer (TC/EA), coupled with a Delta Plus XP Isotope Ratio Mass Spectrometer (IRMS; Thermo Fisher Scientific GmbH, Bremen, Germany). For the analyses of carbon ($^{13}C/^{12}C$), nitrogen ($^{15}N/^{14}N$), and sulfur ($^{34}S/^{32}S$) isotopic ratios, about 2.5 mg of triplicate powdered sample were weighed into tin capsules and introduced into a vario EL cube EA, coupled with an isoprime precisION IRMS (Elementar Analysensysteme GmbH, Langenselbold, Germany).

The isotopic ratios were reported in delta notation and calculated according to Brand & Coplen (2012):

$$\delta^{i}E = \frac{{}^{i}R_{sample} - {}^{i}R_{standard}}{{}^{i}R_{standard}}$$

where the superscript *i* indicates the mass number of the heavier isotope of element *E* (*e.g.*, ^{18}O) and *R* the isotopic ratio of *E* (*e.g.*, $^{18}O/^{16}O$) in the sample and in an internationally recognized standard: Vienna-Standard Mean Ocean Water (V-SMOW) for $\delta^{2}H$ and $\delta^{18}O$, Vienna-Pee Dee Belemnite (V-PDB) for $\delta^{13}C$, Air nitrogen for $\delta^{15}N$, and Vienna-Canyon Diablo Troilite (V-CDT) for $\delta^{34}S$. The delta values were multiplied by 1000 and expressed in ‰.

Isotopic values for $\delta^{2}H$ and $\delta^{18}O$ were calculated against the United States Geological Survey (USGS) international reference materials USGS54 (Canadian lodgepole pine; $\delta^{2}H$ and $\delta^{18}O$ recommended values) and USGS56 (South African red ivorywood; $\delta^{2}H$, $\delta^{18}O$). Isotopic values for $\delta^{13}C$, $\delta^{15}N$, and $\delta^{34}S$ were calculated against in-house working standards, which were themselves calibrated against the International Atomic Energy Agency (IAEA) and USGS international reference materials IAEA-CH-6 (sucrose; $\delta^{13}C$ certified/recommended value), NBS22 (mineral oil; $\delta^{13}C$), USGS40 (L-glutamic acid; $\delta^{13}C$, $\delta^{15}N$), IAEA-NO-3 (potassium nitrate; $\delta^{15}N$), IAEA-SO-5 (barium sulfate; $\delta^{34}S$), NBS127 (barium sulfate; $\delta^{34}S$), USGS42 (Tibetan human hair; $\delta^{34}S$), and USGS43 (Indian human hair; $\delta^{34}S$). For $\delta^{2}H$, $\delta^{13}C$, $\delta^{15}N$, $\delta^{18}O$, and $\delta^{34}S$ the uncertainty of measurements (± 1 standard deviation) was 1, 0.1, 0.2, 0.3, and 0.3‰, respectively.

2.2.3 Statistical analysis

To examine trends among different stable isotope ratios, only sampling sites with a minimum number of two samples were considered. Non-parametric statistical tests were performed. The Kruskal-Wallis test by ranks ($p < 0.05$) was employed for multiples comparisons, while possible rank correlation was assessed by means of Spearman's rank correlation coefficient. Non-parametric tests highlighted statistically significant differences among the different hemp sample populations and correlations among variables.

2.3 Results and discussion

Dealing with the stable isotope composition of Italian industrial hemp, no research studies have been carried out until now. Consequently, these results are the first ones obtained for hemp samples harvested in Italy. Stable isotope composition of investigated samples is presented in Table 2.1, divided in relation to the area and the isotopic ratios investigated. Bulk samples of hemp seed oil were analyzed only for hydrogen and oxygen isotopes. Figures 2.2 and 2.3 show isotopic results retrieved from inflorescences, since this was the only part of the Cannabis plant that was sampled in all the considered areas.

Samples			δ^2H		$\delta^{13}C$		$\delta^{15}N$		$\delta^{18}O$		$\delta^{34}S$	
Area	**Type***	**n**	**Mean**	**S.Dev**	**Mean**	**S.Dev**	**Mean**	**S.Dev**	**Mean**	**S.Dev**	**Mean**	**S.Dev**
Tolmezzo (UD)	I	1	-117		-29.3		1.9		22.0		2.0	
Verzegnis (UD)	I	7	-107	13	-28.8	1.1	2.4	0.9	22.1	0.5	6.6	1.7
	S	7	-85	5	-28.4	0.8	0.8	0.9	23.9	0.7	3.9	1.7
	R	1	-94		-28.5		0.9		24.1		4.7	
Predaia (TN)	O	1	-197						17.9			
	SD	1	-149		-30.4		5.1		20.9		5.5	
	I	1	-98		-28.4		2.8		22.7		5.9	
Gemona del Friuli (UD)	I	6	-96	5	-29.9	0.4	1.1	1.0	21.4	0.7	5.3	2.4
	S	6	-103	10	-29.5	0.2	1.5	0.5	22.9	1.1	4.3	2.6
	R	1	-110		-29.1		1.7		23.4		4.1	
Baceno (VB)	I	1	-95		-28.0		6.3		22.2		3.1	
Udine	SD*f*	2	-117	1	-27.9	1.4	2.7	0.01	24.0	0.8	8.7	0.5
	SD*m*	1	-134		-29.3		4.8		23.7		9.5	
	I*f*	2	-89	4	-28.5	0.3	2.0	0.2	23.1	1.0	12.7	1.2
	I*m*	1	-100		-28.2		4.6		23.3		11.5	
	S*f*	2	-94	5	-28.0	0.7	2.7	0.6	23.6	0.2	9.3	1.5
	S*m*	2	-113	0.1	-29.2	0.9	5.2	1.9	22.2	0.4	10.9	0.4
	R*f*	2	-105	9	-27.5	0.7	2.9	0.6	24.2	0.6	10.2	0.7
	R*m*	2	-125	0.1	-28.9	0.3	4.9	0.5	22.8	0.2	11.1	0.4
Borgo Valbelluna (BL)	I	2	-100	4	-27.8	0.4	4.9	0.2	23.2	0.4	5.3	0.1
Campoformido (UD)	I	6	-103	10	-29.1	0.8	0.6	0.8	22.6	0.6	10.8	1.0
	S	6	-103	8	-28.7	0.5	1.1	0.5	23.2	0.3	8.6	1.6
	R	1	-117		-28.6		1.9		23.9		8.7	
Altopiano della Vigolana (TN)	SD	1	-141		-29.4		2.6		22.3		6.3	
	I	1	-101		-28.7		1.3		23.5		6.1	
Seren del Grappa (BL)	SD	1	-138		-30.9		3.6		21.5		4.5	
	I	1	-116		-30.3		3.5		21.7		5.4	
Piacenza	SD + I	2	-104	16	-27.5	0.4	5.0	0.3	23.4	0.4	0.7	1.4
	S	2	-84	2	-26.7	0.1	4.7	0.8	24.5	0.4	-1.2	0.8

Samples			***$\delta^{2}H$***		***$\delta^{13}C$***		***$\delta^{15}N$***		***$\delta^{18}O$***		***$\delta^{34}S$***	
Area	***Type****	***n***	***Mean***	***S.Dev***	***Mean***	***S.Dev***	***Mean***	***S.Dev***	***Mean***	***S.Dev***	***Mean***	***S.Dev***
Jolanda di Savoia (FE)	O	1	-200						20.9			
	I	3	-85	18	-27.5	0.4	11.3	7.2	23.3	1.1	4.1	0.7
Jesi (AN)	O	1	-181						22.4			
	SD	1	-118		-28.5		10.7		23.7		2.8	
	I	1	-68		-23.6		8.3		28.6		-9.9	
Sassari	O	1	-179						24.5			
	SD	2	-99	7	-27.8	0.4	3.1	0.7	27.3	0.2	10.5	0.2
	I	2	-86	15	-26.9	0.4	2.7	0.1	25.7	0.2	12.9	0.6
Caltagirone (CT)	O	1	-173						25.6			
	SD	1	-104		-25.8		7.3		28.7		1.4	
	I	1	-80		-26.2		8.7		25.4		1.4	
	S	1	-88		-27.6		7.9		26.5		0.5	
	R	1	-93		-27.3		7.1		27.8		2.6	
Minimum value			-200		-30.9		0.6		17.9		-9.9	
Maximum value			-68		-23.6		11.3		28.7		12.9	

Table 2.1 Stable isotope ratios (mean values and Standard Deviation (S.Dev) expressed in ‰) of Italian industrial hemp samples (*Cannabis sativa* L.) ordered according to the latitude of the sampling areas (from the highest to the lowest). *n* refers to the number of samples analyzed.

*Samples are labeled as follow: O = Oils, SD = Seeds, I = Inflorescences, S = Stems, R = Roots. Only for the Udine sampling area: *f* = grown under synthetic fertilization, *m* = grown under bovine manure fertilization.

2.3.1 Carbon, nitrogen, and sulfur stable isotope ratios in hemp

Carbon isotope ratio signatures are directly related to the photosynthetic cycle of the plant considered, as well as to the climatic conditions of the harvesting place of the plant involved [Bontempo *et al.*, 2020b]. According to the biochemical pathway of the C_3 plants [Carter & Chesson, 2017], $\delta^{13}C$ values were found to be between −30.9 and −23.6‰ (Table 2.1). Moreover, these results were in agreement with those obtained in other studies led on hemp samples harvested outdoor in Brazil [Shibuya *et al.*, 2007] and USA [Hurley *et al.*, 2010]. About our data, Figure 2.2 showed an evident increasing trend according to the latitude decrease, since the most negative values were found for samples collected in Northern Italy. This finding was found in agreement with the geographical and climatic conditions of the harvesting place of the *Cannabis Sativa* plant. According to previous literature studies [Bateman & Kelly, 2007], nitrogen stable isotope ratio was considered as a marker to differentiate crops produced under conventional and organic regime, since it is related to the type of fertilizer used for their growth. The $\delta^{15}N$ values may vary from 0.3 to 14.6‰ in plants harvested under organic fertilization, while from −4.0 to 8.7‰ for those harvested under conventional fertilization [Inácio *et al.*, 2015]. However, a different behavior is shown for those crops organically grown with a fertilization strategy consisting of nitrogen fixing plants, which involve in lower $\delta^{15}N$ values, within the range of conventionally grown crops [Bontempo *et al.*, 2020b]. In this research $\delta^{15}N$ values fell inside the range between 0.6 and 11.3‰, corresponding to the Cannabis inflorescences harvested at Campoformido (Friuli Venezia Giulia) and Jolanda di Savoia (Emilia Romagna), respectively (Table 2.1), labelled as organically grown samples. However, mean $\delta^{15}N$ values obtained for samples produced at Campoformido, Seren del Grappa (Veneto), and Sassari (Sardinia), all labeled as organically grown, fell into the conventional range (Table 2.1; Fig. 2.2). This behavior may be linked to a fertilization strategy consisting of leguminous plants, which affected nitrogen values of samples, lowering them [Bontempo *et al.*, 2020b].

Noteworthy is the mean $\delta^{15}N$ value (10.7‰) obtained for the seed sample harvested at Jesi (Fig. 2.1; Table 2.1). Although it was produced in a cultivation area under conventional regime, its nitrogen isotopic data fell within the organic range, probably due to the employment of organic fertilizers. As highlighted in several papers [Paolini 2017; Zazzo *et al.*, 2011; Zhou *et al.*, 2021], sulfur stable isotope ratios is influenced by different elements, like distance from the sea, microbial reactions, kind of soil, fertilizers employed, and anthropogenic inputs.

About this study, most of the hemps had positive $\delta^{34}S$ values ranging between 0.5 and 12.9‰, except for Piacenza (Emilia Romagna) and Jesi sampling sites, which had negative values, −1.2 and −9.9‰, respectively (Table 2.1).

The values obtained for sulphur were found in agreement with previous results by Paolini [Paolini 2017]. Moreover, since a limited isotopic fractionation process involves for sulfur isotopes in plants [Carter & Chesson, 2017], $\delta^{34}S$ values were related to those found in the soil, and thus in relation to the geographical origin of the samples investigated. However, some similarities were found also between sampling sites having a different geographic origin. This example was evident for the inflorescence samples of Udine and Sassari, and Piacenza and Caltagirone (Sicily), which had similar mean $\delta^{34}S$ values (12.7 and 12.9‰, 0.7 and 1.4‰, respectively), even if they were sampled in different places in Italy. This similar behavior could be explained by the common nature of bedrocks: carbonate for Udine and Sassari sites, and clay/calcareous for Piacenza and Caltagirone ones [Costantini *et al.*, 2012].

Also the sampling area of Jesi represented an exception, since the inflorescence sample had a quite negative mean (−9.9‰; Table 2.1; Fig. 2.2), very different from the values registered for the other hemps. This finding is maybe related to the geology of this area of Central Italy, as highlighted by Costantini *et al*.

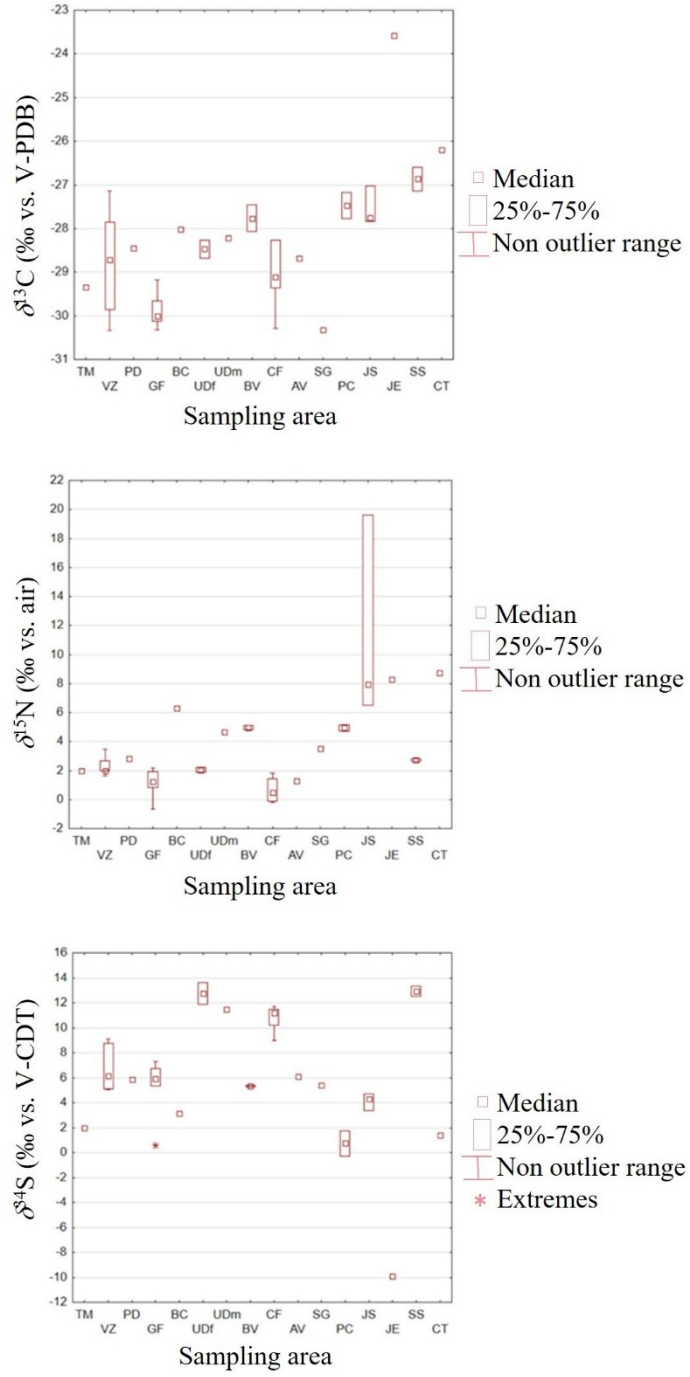

Figure 2.2 Box-plots of $\delta^{13}C$, $\delta^{15}N$, and $\delta^{34}S$ values, expressed in ‰, of Italian industrial hemp inflorescence samples (*Cannabis sativa* L.) ordered according to the latitude of the sampling areas (from the highest to the lowest).

V-PDB = Vienna-Pee Dee Belemnite, V-CDT = Vienna-Canyon Diablo Troilite, TM = Tolmezzo (UD), VZ = Verzegnis (UD), PD = Predaia (TN), GF = Gemona del Friuli (UD), BC = Baceno (VB), UD = Udine (*f* = grown under synthetic fertilization, *m* = grown under bovine manure fertilization), BV = Borgo Valbelluna (BL), CF = Campoformido (UD), AV = Altopiano della Vigolana (TN), SG = Seren del Grappa (BL), PC = Piacenza, JS = Jolanda di Savoia (FE), JE = Jesi (AN), SS = Sassari, CT = Caltagirone (CT).

2.3.2 Hydrogen and oxygen stable isotope ratios in hemp

Dealing with hydrogen and oxygen isotope ratios, their distribution is strongly affected by climatic and geographical processes, which may alternatively deplete or enrich their values [Gat 1996]. Moreover, δ^2H and δ^{18}O values in plant organic matter depend from its primary source of water, or irrigation or soil, since they are subjected to an enrichment process along evapotranspiration and the cellulose synthesis by the plant [Carter & Chesson 2017].

In this research, hydrogen isotope ratios ranged from −200 to −68‰, with the lower values registered in all the five hemp seed oils analyzed. Dealing with oxygen isotope ratios, values ranged from 17.9 to 28.7‰ (Table 2.1). Moreover, inflorescence samples showed an increasing mean δ^{18}O values moving from North to South, as shown in Figure 2.3. This behavior was related to meteorological conditions and dynamic fractionation in the hydrological cycle [Gat 1996]. The highest δ^{18}O values were found for hemps sampled in Central and Southern Italy, as in Jesi, Sassari and Caltagirone (Table 2.1; Fig. 2.3). This behavior may be linked to two main factors: i) the precipitation δ^{18}O values [Giustini *et al.*, 2016], and ii) the effects of warmer climates on evapotranspiration processes, which may further enrich hydrogen and oxygen isotopic ratios. As well as for δ^{18}O, positive tendency was shown also by the mean δ^2H values, which are strongly affected both by the isotopic composition of the water taken up by the plant [Silveira Lobo Sternberg, 1989], as well as by the photosynthetic metabolism of cellulose [Yakir & De Niro, 1990]. Also in this case, the sample harvested at Jesi was an outlier for hydrogen isotopic composition. In this concern, its less negative mean value (−68‰; Table 2.1; Fig. 2.3) could be related to precipitation values characteristic for coastal areas [Giustini *et al.*, 2016].

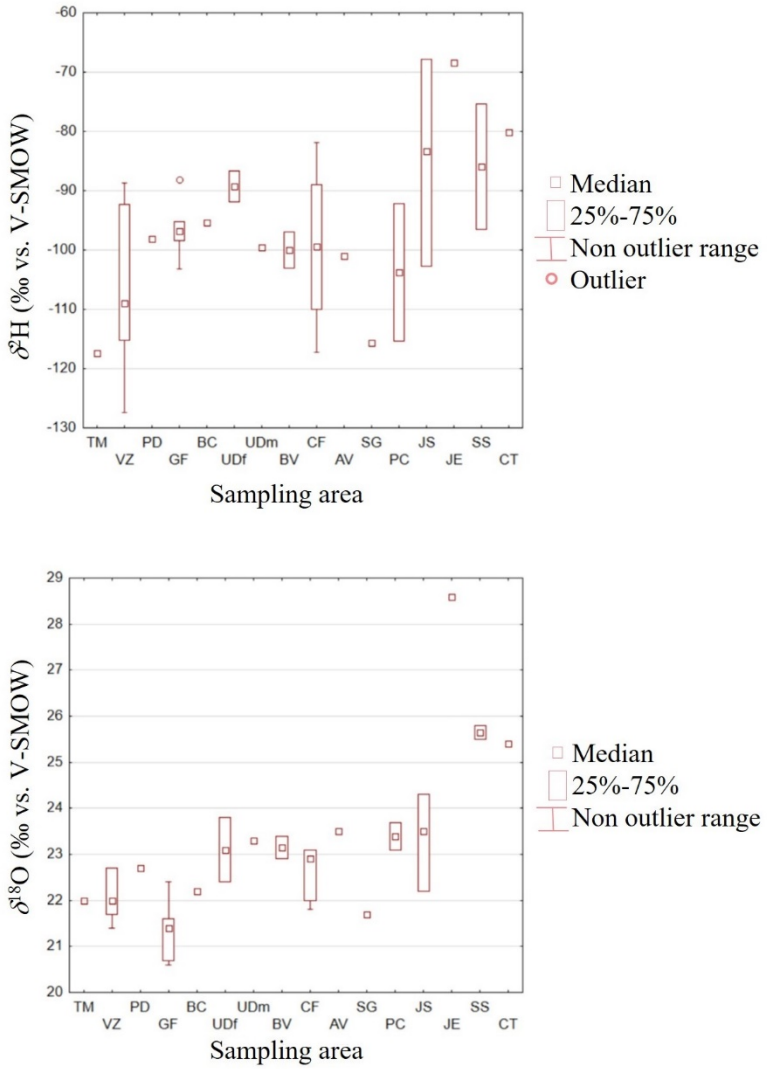

Figure 2.3 Box-plots of δ^2H and δ^{18}O values, expressed in ‰, of Italian industrial hemp inflorescence samples (*Cannabis sativa* L.) ordered according to the latitude of the sampling areas (from the highest to the lowest).

V-SMOW = Vienna-Standard Mean Ocean Water, TM = Tolmezzo (UD), VZ = Verzegnis (UD), PD = Predaia (TN), GF = Gemona del Friuli (UD), BC = Baceno (VB), UD = Udine (*f* = grown under synthetic fertilization, *m* = grown under bovine manure fertilization), BV = Borgo Valbelluna (BL), CF = Campoformido (UD), AV = Altopiano della Vigolana (TN), SG = Seren del Grappa (BL), PC = Piacenza, JS = Jolanda di Savoia (FE), JE = Jesi (AN), SS = Sassari, CT = Caltagirone (CT).

2.3.3 Hydrogen and oxygen stable isotope ratios in hemp seed oil

Beside the analysis of eighty-four samples of hemp, in this study hydrogen and oxygen stable isotope ratios were investigated in hemp seed oils. These samples were collected in five different sampling sites, namely from North to South, Predaia, Jolanda di Savoia, Jesi, Sassari, and Caltagirone.

As already shown in Section 2.3.2, hydrogen and oxygen isotopic ratios were mainly influenced by climatic and geographical conditions of the sampling areas [Tarapoulouzi *et al.*, 2021]. This behavior was evident also in mean $\delta^{2}H$ and $\delta^{18}O$ values detected for hemp seed oil samples (Table 2.1). In this concern, the mean $\delta^{18}O$ values showed a clear trend, since increasing values were found from Predaia (Trentino-South Tyrol, NE Italy; 17.9‰) to Caltagirone (Sicily, S Italy; 25.6‰). As well as for oxygen isotope ratios, also for hydrogen isotope values Predaia (−197‰) had more negative value with respect to Caltagirone (−173‰). The only exception was found for Jolanda di Savoia (Emilia Romagna, N Italy) sampling site, which had the lowest mean value detected in this study (−200‰; Table 2.1).

Marked differences have been detected, as expected, in mean $\delta^{2}H$ and $\delta^{18}O$ values moving from seeds to oil samples. A mean depletion of 65‰ was found for hydrogen signature, while of 2.6‰ for oxygen. In this concern, this trend is related to the depletion of the cellulosic component with respect to the lipidic one, which is largely ^{2}H depleted relative to the bulk of the organic matter [Schmidt *et al.*, 2003].

2.3.4 Insight on stable isotope ratios in hemp collected at Udine sampling site

Dealing with Udine sampling area in Friuli Venezia Giulia region (NE Italy; point No. 14 in Fig. 2.1), all the parts of the hemp plant were considered, starting from roots to seeds. In addition, samples were taken from two different cultivations: or produced under synthetic (NPK) or under bovine manure fertilization. In this concern, a marked enrichment for $\delta^{15}N$ values (with a mean increase of about 2.3‰) was evident for all the parts of the Cannabis plant grown under organic fertilization, as shown in Figure 2.4. Differently, all the parts of the Cannabis plant grown under organic fertilization showed lower mean $\delta^{2}H$ values with respect to those produced under conventionally fertilized cultivation. This behavior was highlighted also, with a less evidence, also by carbon and oxygen stable isotope ratios, except for inflorescences (Figure 2.4).

These trends have been reported in literature in other plants like wheat [Bontempo *et al.*, 2016; Georgi *et al.*, 2005; Laursen *et al.*, 2013], and their behavior was supposed to be influenced by a higher transpiration and water evaporative loss with respect to conventionally grown plants. Additional hypotheses was related to differences in cultivation processes, related to plant density and growth rates, affecting respiration, water uptake, and evapotranspiration. Dealing with $\delta^{34}S$ results, more positive mean values were found for organically fertilized hemps, except for inflorescences samples (Figure 2.4).

Moreover, a pronounced depletion was found in terms of hydrogen stable ratios in inflorescences and seeds (with a mean decrease of about 32‰, Table 2.1), probably related to the lower cellulose

content. As discussed by Schmidt *et al*. [Schmidt *et al.*, 2003], this behavior is also related by a higher content of lipids in seeds, observed for both organically and conventionally fertilized cultivations (Figure 2.4). About $\delta^{13}C$ values, a slight decrease was observed moving from roots to inflorescences in conventionally grown plants; differently, a slight increase was found in seeds. However, this trend was not evident also in organically grown hemp (Figure 2.4). Moving to nitrogen isotope ratio, no evident differences were registered in plant parts, regardless of the fertilization strategy. Differently, in conventionally grown plants, a slight decrease for $\delta^{18}O$ values was found starting from roots to inflorescences. Dealing with organically grown Cannabis, a decrease was found from roots to stems, while a further increase from inflorescences to seeds. This uneven behavior between $\delta^{2}H$ and $\delta^{18}O$ may be linked to additional biochemical or source effects [Yakir & De Niro, 1990], due to water evaporation in leaves or in relation to organic matter synthesis [Dawson *et al.*, 2002]. About mean $\delta^{34}S$ values, no evident patterns were highlighted, regardless of the fertilization process (Figure 2.4). However, $\delta^{34}S$ values detected in Cannabis inflorescence have been found higher with respect to those highlighted in all the other parts of the plant, as visible in Figure 2.4.

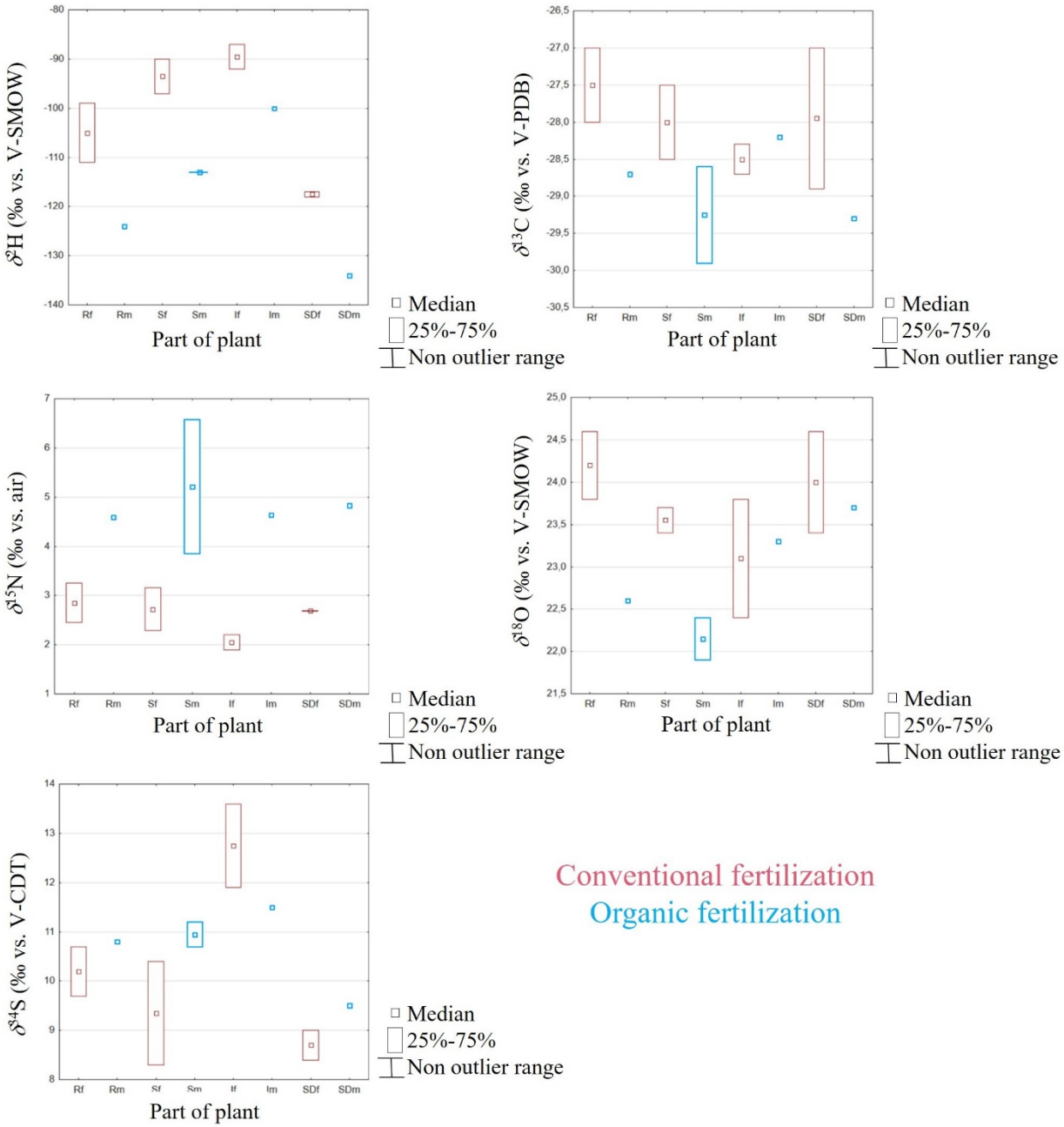

Figure 2.4 Box-plots of $\delta^{2}H$, $\delta^{13}C$, $\delta^{15}N$, $\delta^{18}O$, and $\delta^{34}S$ values, expressed in ‰, of Italian industrial hemp samples (*Cannabis sativa* L.) collected at Udine sampling site in Friuli Venezia Giulia region (NE Italy), ordered according to the part of plant and the fertilization strategy (conventional in red, organic in blue).

V-SMOW = Vienna-Standard Mean Ocean Water, V-PDB = Vienna-Pee Dee Belemnite, V-CDT = Vienna-Canyon Diablo Troilite, R = Roots, S = Stems, I = Inflorescences, SD = Seeds, *f* = grown under synthetic fertilization, *m* = grown under bovine manure fertilization.

2.4. Conclusions

This research provided for the first time in literature a broad knowledge about the stable isotope composition of the Italian industrial hemp intended for food use, representing a first reliable range able to evaluate authenticity and traceability of this high value plant. In this concern, stable isotope ratios demonstrated typical characteristics related to the geographical origin, fertilization processes, and climatic conditions of the hemp growth areas. In detail, $\delta^{13}C$ signatures, and partially $\delta^{2}H$ and $\delta^{18}O$, highlighted how isotopic values were affected by climatic conditions, as well as by the latitude of the investigated places. Differently, $\delta^{15}N$ reflected conventional or organic fertilization processes, while $\delta^{34}S$ values clustered different samples, probably in relation to the common nature of bedrocks. Dealing with hemp seed oil bulk samples, a relevant depletion in mean $\delta^{2}H$ and $\delta^{18}O$ values was registered, due to the high amount of lipids in the oil. Future studies will involve a wider sampling, with more representative areas, involving different climatic conditions, in order to have a more robust method to trace the origin of hemp. Moreover, it will make easier to understand the behavior of light stable isotopes in the biogeochemical processes of the plant.

References

Altieri, S.; Saiano, K.; Biondi, M.; Ricci, P.; Lubritto, C. Traceability of 'Mozzarella di Bufala Campana' production chain by means of carbon, nitrogen and oxygen stable isotope ratios. J. Sci. Food Agric.100, (2020) 995–1003.

Amaducci, S.; Scordia, D.; Liu, F.H.; Zhang, Q.; Guo, H.; Testa, G.; Cosentino, S.L. Key cultivation techniques for hemp in Europe and China. Ind. Crops Prod. 68 (2015) 2–16.

Baldini, L.; Scognamiglio, M.; Reverchon, E. Supercritical fluid technologies applied to the extraction of compounds of industrial interest from Cannabis sativa L. and to their pharmaceutical formulations: A review. J. Supercrit. Fluids 165 (2020) 104960.

Bateman, A.S.; Kelly, S.D. Fertilizer nitrogen isotope signature. Isot. Environ. Health Stud. 43 (2007) 237–247.

Bontempo, L.; Camin, F.; Paolini, M.; Micheloni, C.; Laursen, K.H. Multi-isotopic signatures of organic and conventional Italian pasta along the production chain. J. Mass Spectrom. 51 (2016) 675–683.

Bontempo, L.; Camin, F.; Perini, M.; Ziller, L.; Larcher, R. Isotopic and elemental characterisation of Italian white truffle: A first exploratory study. Food Chem. Toxicol. 145 (2020) 111627.

Bontempo, L.; van Leeuwen, K.A.; Paolini, M.; Laursen, K.H.; Micheloni, C.; Prenzler, P.D.; Ryan, D.; Camin, F. Bulk and compound-specific stable isotope ratio analysis for authenticity testing of organically grown tomatoes. Food Chem. 318 (2020) 126426.

Booth, A.L.; Wooller, M.J.; Howe, T.; Haubenstock, N. Tracing geographic and temporal trafficking patterns for marijuana in Alaska using stable isotopes (C, N, O and H). Forensic Sci. Int. 202 (2010) 45–53.

Brand, W.A.; Coplen, T.B. Stable isotope deltas: Tiny, yet robust signatures in nature. Isot. Environ. Health Stud. 48 (2012) 393–409.

Cacchioni, D. Hemp and Industry in Italy: Between Pasts and Present. AGER J. Depopulation Rural. Dev. Stud. 32 (2021) 93–115.

Carter, J.F.; Chesson, L.A. Food Forensics. Stable Isotopes as a Guide to Authenticity and Origin; CRC Press: Boca Raton, FL, USA, 2017; ISBN 9780367782085.

Coldiretti—Italian National Confederation of Direct Farmers. Via Libera alla Cannabis a Tavola, Campi Decuplicati. Available online: https://www.coldiretti.it/economia/via-libera-alla-cannabis-tavola-campi-decuplicati

Costantini, E.A.C.; L'Abate, G.; Barbetti, R.; Fantappié, M.; Lorenzetti, R.; Magini, S. Soil Map of Italy; National Research Council and Minister of Agriculture Food and Forestry: Rome, Italy, 2012. Available online: https://esdac.jrc.ec.europa.eu/content/carta-dei-suoli-ditalia-soil-map-italy

Crini, G.; Lichtfouse, E.; Chanet, G.; Morin-Crini, N. Applications of hemp in textiles, paper industry, insulation and building materials, horticulture, animal nutrition, food and beverages, nutraceuticals, cosmetics and hygiene, medicine, agrochemistry, energy production and environment: A review. Environ. Chem. Lett. 18 (2020) 1451–1476.

Dawson, T.E.; Mambelli, S.; Plamboeck, A.H.; Templer, P.H.; Tu, K.P. Stable Isotopes in Plant Ecology. Annu. Rev. Ecol. Syst. 33 (2002) 507–559.

Federcanapa—Italian Hemp Federation. Linee Guida per la Coltivazione Della Canapa da Estrazione. Available online: https://www.federcanapa.it/coltivazione-canapa-industriale-estrazione

Federcanapa—Italian Hemp Federation. Linee Guida per il Seme di Canapa ad Uso Alimentare. Available online: https: //www.federcanapa.it/linee-guida-canapa-alimentare

Gat, J.R. Oxygen and hydrogen isotopes in the hydrologic cycle. Annu. Rev. Earth Planet. Sci. 24 (1996) 225–262.

Georgi, M.; Voerkelius, S.; Rossmann, A.; Graßmann, J.; Schnitzler, W.H. Multielement Isotope Ratios of Vegetables from Integrated and Organic Production. Plant Soil 275 (2005) 93–100.

Giupponi, L.; Leoni, V.; Carrer, M.; Ceciliani, G.; Sala, S.; Panseri, S.; Pavlovic, R.; Giorgi, A. Overview on Italian hemp production chain, related productive and commercial activities and legislative framework. Ital. J. Agron. 15 (2020) 194–205.

Giustini, F.; Brilli, M.; Patera, A. Mapping oxygen stable isotopes of precipitation in Italy. J. Hydrol. Reg. Stud. 8 (2016) 162–181.

Hurley, J.M.; West, J.B.; Ehleringer, J.R. Tracing retail cannabis in the United States: Geographic origin and cultivation patterns. Int. J. Drug Policy 21 (2010) 222–228.

Inácio, C.T.; Chalk, P.M.; Magalhães, A.M.T. Principles and Limitations of Stable Isotopes in Differentiating Organic and Conventional Foodstuffs: 1. Plant Products. Crit. Rev. Food Sci. Nutr. 55 (2015) 1206–1218.

Landi, S. Mineral nutrition of Cannabis sativa L. J. Plant Nutr. 20 (1997) 311–326.

Laursen, K.H.; Mihailova, A.; Kelly, S.D.; Epov, V.N.; Bérail, S.; Schjoerring, J.K.; Donard, O.F.X.; Larsen, E.H.; Pedentchouk, N.; Marca-Bell, A.D. Is it really organic?—Multi-isotopic analysis as a tool to discriminate between organic and conventional plants. Food Chem. 141 (2013) 2812–2820.

Law 242/2016. Disposizioni per la Promozione della Coltivazione e della Filiera Agroindustriale della Canapa. Law 2nd December 2016, n. 242; 2016. Available online: https://www.gazzettaufficiale.it/eli/id/2016/12/30/16G00258/sg

Paolini, M. Development and Implementation of Stable Isotope Ratio Analysis in Bulk Products and Sub-Components to Ensure Food Traceability. Ph.D. Thesis, University of Udine, Udine, Italy, 2017. Available online: https://hdl.handle.net/10449/37884

Portarena, S.; Gavrichkova, O.; Lauteri, M.; Brugnoli, E. Authentication and traceability of Italian extra-virgin olive oils by means of stable isotopes techniques. Food Chem. 164 (2014) 12–16.

Ryz, N.R.; Remillard, D.J.; Russo, E.B. Cannabis Roots: A Traditional Therapy with Future Potential for Treating Inflammation and Pain. Cannabis Cannabinoid Res. 2 (2017) 210–216.

Schmidt, H.-L.; Werner, R.A.; Eisenreich, W. Systematics of 2 H patterns in natural compounds and its importance for the elucidation of biosynthetic pathways. Phytochem. Rev. 2 (2003) 61–85.

Shibuya, E.K.; Sarkis, J.E.S.; Negrini-Neto, O.; Martinelli, L.A. Carbon and nitrogen stable isotopes as indicative of geographical origin of marijuana samples seized in the city of São Paulo (Brazil). Forensic Sci. Int. 167 (2007) 8–15.

Silveira Lobo Sternberg, L. Oxygen and Hydrogen Isotope Ratios in Plant Cellulose: Mechanisms and Applications. In Stable Isotopes in Ecological Research; Rundel, P.W., Ehleringer, J.R., Nagy, K.A., Eds.; Springer: Berlin/Heidelberg, Germany, 1989; pp. 124–141.

Tarapoulouzi, M.; Skiada, V.; Agriopoulou, S.; Psomiadis, D.; Rébufa, C.; Roussos, S.; Theocharis, C.R.; Katsaris, P.; Varzakas, T. Chemometric Discrimination of the Geographical Origin of Three Greek Cultivars of Olive Oils by Stable Isotope Ratio Analysis. Foods 10 (2021) 336.

Wadood, S.A.; Boli, G.; Yimin, W. Geographical traceability of wheat and its products using multielement light stable isotopes coupled with chemometrics. J. Mass Spectrom. 54 (2019) 178–188.

Yakir, D.; DeNiro, M.J. Oxygen and Hydrogen Isotope Fractionation during Cellulose Metabolism in Lemna gibba L. Plant Physiol. 93 (1990) 325–332.

Zazzo, A.; Monahan, F.J.; Moloney, A.P.; Green, S.; Schmidt, O. Sulphur isotopes in animal hair track distance to sea. Rapid Commun. Mass Spectrom. 25 (2011) 2371–2378.

Zhou, X.; Wu, H.; Pan, J.; Chen, H.; Jin, B.; Yan, Z.; Xie, L.; Rogers, K.M. Geographical traceability of south-east Asian durian: A chemometric study using stable isotopes and elemental compositions. J. Food Compos. Anal. 101 (2021) 103940.

Chapter 3

Basic concepts of gas chromatography and the development of multidimensional gas chromatographic systems

Gas chromatography (GC) is a technique of choice for the separation of volatile and semi-volatile components, which are thermally stable at the temperature required for their vaporization. Its application covers the fields of scientific investigation, environmental pollution, flavour and fragrances, as well as modern biology and medicine. Starting from the first work in 1952 by Martin and James with the employment of packed columns [Martin and James 1952], several step forwards were done in terms of improved efficiency six years later by Golay, thanks to the introduction of open-tubular capillaries [Golay 1958]. In Figure 3.1 is reported a scheme of a typical gas chromatographic system, characterized by three independently controlled thermal zones (injector, GC oven and detector).

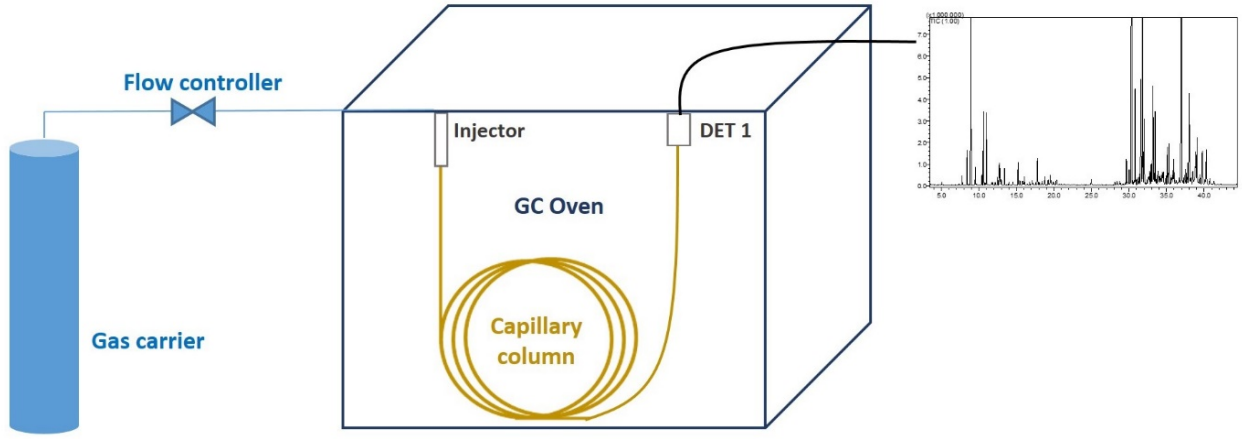

Figure 3.1 Basic configuration of a GC system

Briefly, once the injection takes place, analytes are delivered from the injector to the column thanks to a flow of mobile phase, which is a gas flowing from a pressurized cylinder. The column is the heart of the system. Herein, the separation processes involve due to the different physicochemical interactions between the stationary phase and the analytes. In relation to the different affinities for the stationary phases, each analyte forms its own concentration band, which ends its elution

process at different times. The end of the analytical column is directly connected to the detector, which can provide specific information about each separated analytes (chromatogram), in relation to its main features (quali and/or quantitative analysis).

3.1 GC figures of merit

In the present paragraph, a brief description of the main GC figures of merit will be provided.

Retention time

This term is strictly related to the time elapsed between the injection and the maximum of a chromatographic peak. The elution of each analyte in a mixture is recorded in a chromatogram, whose example is reported in Figure 3.2.

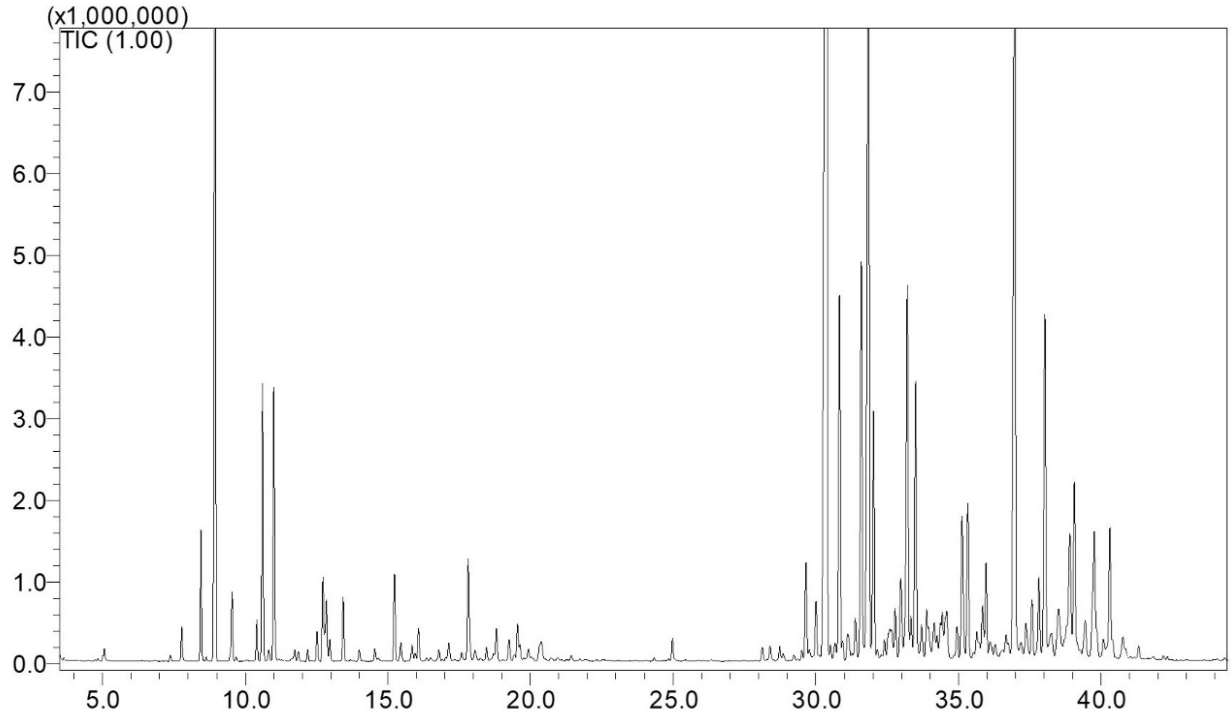

Figure 3.2 GC-MS chromatogram: x axis refers to retention time, y axis refers to detector response

A chromatogram shows the elution order (time domain) of each component in a mixture (x axys), and the relative detector response (y axis). In the case of apolar stationary phase, elution order often follows the increasing boiling points of the analytes in the mixture.

In order to evaluate retention properties, a suitable term is the *retention factor*, namely k':

$$k' = \frac{t_R - t_0}{t_0} \qquad \textit{eq 3.1}$$

This term is composed by the ratio of the time of the interactions between the analyte and the stationary phase (t_R), and the time required for a totally un-retained analyte to travel along the entire chromatographic column (t_0). From these observations, it's clear that analytes having small *k'* will have low affinity with the stationary phase; differently, analytes with high *k'* will have high affinity with the stationary phase with longer t_R.

Another term related to retention in chromatography is the selectivity (α):

$$\alpha = \frac{k'}{k''} \qquad eq3.2$$

, which compares the retention time of two different eluting components. Since the relative retention reflects the behaviour of the two different solutes, it is frequently employed to evaluate the solute–column interactions. In order to have a good separation, α must have values ≥1. Otherwise (α =1), a major co-elution involves.

Among the chromatographic concepts related to the retention of target analytes, the retention index assumes a crucial importance. This approach is very useful for inter-laboratory comparison, since it compares the retention time of a solute with respect to those of reference standard analytes, always employed as homologous series. In the case of isothermal conditions, retention index (*I*) can be calculated by means of the following formula

$$I = 100_z + 100\,\frac{\log t_R(x) - \log t_R(z)}{\log t_R(z+1) - \log t_R(z)} \qquad eq\ 3.3$$

, where *z* corresponds to the number of carbon atoms related to the homologous series, while *x* is related to the target component. When using a series of n-alkanes, an incremental index value is assigned in relation to the total carbon number, namely 100 for methane, 200 for ethane, exc. As an example, if an analyte elutes from the analytical column exactly halfway between heptane and octane, its retention index will be of 750.

Band broadening

The main aim of a GC run is to obtain a suitable separation of each individual analyte in a mixture, based on the differences in retention times. According to basic principle of chromatography, analytes are initially injected in a sharp band, which starts naturally broadening along each step of a GC analysis. This behaviour involves in a Gaussian distribution, defined by the retention time and the width at the base of each corresponding chromatographic peak. In this concern, the analyst aims to reduce peak broadening, in order to increase the number of components that can be ideally

placed, side by side, in the chromatographic space at a suitable resolution. While retention times are related to the thermodynamic features of the analytical column, peak width is related to the efficiency of the analyte mass transport from stationary and mobile phase (and viceversa), and in relation to the kinetics of sorption and desorption processes. Chromatographically, column efficiency is described by the number of theoretical plates:

$$N = \left(\frac{t_R}{\sigma}\right)^2 = 16\left(\frac{t_R}{w_b}\right)^2 = 5.54\left(\frac{t_R}{w_h}\right)^2 \qquad \textit{eq 3.4}$$

Another term related to the number of theoretical plates is the height of theoretical plates, namely *H*:

$$H = \frac{L}{N} \qquad \textit{eq 3.5}$$

, where *L* is the length of the chromatographic column. *L* needs to be intended as divided into various volume units, where a complete equilibrium of the analyte between the two phases is reached. From these considerations, it's clear that narrow peaks produce a higher number of theoretical plates with respect to broader peaks.

Another step forward for the definition of band broadening was provided by Van Deemter, who identified three different effects that contribute to peak broadening. Peak broadening was expressed as the height of the theoretical plate (*H*), with the following equation

$$H = A + \frac{B}{\bar{u}} + (C_S + C_M)\,\bar{u} \qquad \textit{eq 3.6}$$

where the constant *A* (eddy diffusion) was described as the chromatographic band dispersion due to the gas flow irregularities in the column. The *B*-term (longitudinal molecular diffusion) represents the peak dispersion due to the diffusion processes occurring longitudinally inside the column, while the *C*-term (mass transfer) occurs in relation to a radial diffusion of the analytes. Since these terms are directly related to *H*, their value should be minimized to improve efficiency.

When Golay introduced open tubular capillary columns, a new equation was needed, since this type of modified column were different from the previous packed ones (A term). Golay proposed a new term to describe diffusion processes in the open tubular columns:

$$H = \frac{B}{\bar{u}} + (C_S + C_M)\,\bar{u} \qquad \textit{eq 3.7}$$

where B-term is the molecular diffusion, governed by the following equation:

$$B = 2D_G \qquad \textit{eq 3.8}$$

where D_G is the *diffusion coefficient* for the analyte in the carrier gas. As visible from Golay Equation, this term is divided by the linear velocity (ū). Thus, a high velocity will reduce the contribution of the molecular diffusion to the peak broadening, since the analyte will spend a reduced time in column.

As visible in Golay Equation, *C* term is divided into two terms: one related to the mass transfer in the stationary phase, C_S, and one for mass transfer in the mobile phase C_M. C_S term is described by the following formula:

$$C_S = \frac{2\ k\ d_f^2}{3(1+k)^2 D_S} \qquad \textit{eq 3.9}$$

Dealing with the ratio k /(1 + k)^2, large values will be related to very high solubility in the stationary phase. Although this ratio is strongly minimized at large values of k, a little decrease involves with k values >20. Since a very large value may involve in very long time analysis, k value near to 20 is the preferred solution. To reduce peak broadening for this term, film thickness should be small, while the diffusion coefficient large. Another term of the equation, D_S, is the diffusion coefficient of the solute in the stationary phase, while d_f is the film thickness of the liquid stationary phase. In this concern, minimization of the C_S -term can be achieved when mass transfer into and out the stationary liquid phase is as fast as possible.

C_M term is governed by the following equation:

$$C_M = \frac{(1+6k+11k^2)r_c^2}{24(1+k)^2 D_G} \qquad \textit{eq 3.10}$$

, where rc is the radius of the column. Briefly, the relative importance of the C terms in Golay equation is related to the film thickness and the column radius. In this concern, for thin films (< 0.2 μm), the *C*-term is controlled by mass transfer in the mobile phase. Differently, for thicker films (2-5 μm), it is controlled by mass transfer in the stationary phase, while for the intermediate films (0.2 to 2 μm) both terms must be considered.

Resolution

Another way to measure the efficiency of a chromatographic column is the Resolution (Rs). The formula describes the degree of two adjacent peaks, having retention factors k1 and k2:

$$Rs = \frac{\sqrt{N}}{4}\left(\frac{a-1}{a}\right)\left(\frac{k2}{k2+1}\right) \qquad eq\ 3.11$$

, where *Rs* is proportional to the square root of the number of theoretical plates *N*, and is influenced by both the selectivity α and the retention factor k. These three terms describes column efficiency, system selectivity and column retentivity. About the number of theoretical plates, if the column length is doubled, resolution factor increases of only 1.414. This finding explains how a considerable increase in resolution can be achieved only using very long columns. However, this solution can lead to very long time analysis, which is not a desirable consequence. About k, an increase in the retention factor (k) has a substantial effect on resolution, *Rs*, only for analytes with low k values (≤ 3). Dealing with selectivity, the choice of a more selective stationary phase is always useful, since resolution will benefit greatly. In this concern, selectivity has the greatest effect on resolution, thus it is mandatory to choose the right stationary phase in relation to the sample analysed. However, in the case of a complex mixture, selectivity will often provide an improved resolution for some solutes, and a poorer for other ones.

3.2 Multidimensional gas chromatography

The development of new highly performing chromatographic systems in separation sciences needs to be linked to the everlasting thirst of discovery of human beings, in this case of chromatographers. Dealing with monodimensional GC systems, the employment of capillary columns [Golay 1958] in replacement of packed ones led to a relevant increase in chromatographic efficiency for the analysis of real samples. Several advances were achieved also by the capability to hyphen to GC systems highly performing MS detectors, as time of flight analysers (ToF). However, the analysis of complex matrices still represented a primary issue, since a single chromatographic separation would not be able to provide a full characterization of overlapping components. In this concern, mass spectrometry can help to overcome co-elution issues by operating in selected ion monitoring (SIM) or by means of extracted ions mode. However, in the case of components having a very similar fragmentation pattern, overlappings are restrictive, since conventional MS detectors are not sophisticated enough to highlight clear differences. To these aims, advanced separation systems are required.

Multidimensional gas chromatographic systems [Bertsch 1999, Mondello 2002], or performed by heart cut (MDGC) or by comprehensive chromatography (GC x GC), filled this gaps, since the combination of two capillary columns was able to improve the resolution of key components prior to the detection. Separations in column chromatography are called multidimensional when

separations are consequently performed in two or more columns, directly coupled in series to the column when the first separation had place.

In this concern, the demand of multidimensional techniques is strictly linked to the need to increase the peak capacity (*n*) of a chromatographic system. Chromatographically, peak capacity is defined as the maximum number of components that can be placed, side by side, into the chromatographic space at a given resolution. The formula is shown below:

$$n = \frac{\sqrt{N}}{4R} \ln\left(\frac{t_2}{t_1}\right) + 1 \qquad \textit{eq 3.12}$$

defined for a retention window from t_1 to t_2, where peak capacity is directly proportional to the square root of efficiency (*N*). According to the *eq 3.5* about the relation between efficiency and the height of theoretical plates, it's clear how the employment of longer columns, in the case of GC runs, would be a suitable solution to increase the efficiency of a capillary column. Such a solution would allow an optimized separation of key components. In this concern, according to *eq 3.12*, if *R*=1, a 50m long column to develop 2 x 10^5 plates with a peak capacity of 260. However, as shown by Berger, a gas chromatographic profile of gasoline analysed on a 400m long capillary column (time analysis= 11 hours) still involves in several co-elutions, although it develops 1.3 x 10^6 plates with a peak capacity of 1000 [Berger 1996]. In this concern, the development of multidimensional gas chromatographic systems was required for two main aims. First, to guarantee a relevant increase in terms of peak capacity, and secondarily to reduce total time analysis for complex mixtures. However, the first term covers a primary importance. About this matter, chromatographic theory teaches us that a doubling in column length results in a small increase in the number of theoretical plates. Contrarily, what is really required in the coupling of GC columns is not a greater number of theoretical plates, but the complementary selectivity, guaranteed by the employment of a different stationary phase in the second dimension. The real improvement in terms of peak capacity in a MDGC system is related to the degree of orthogonality between the selectivity of the capillary columns in each dimension. This definition lays its basis in a critical paper published by Giddings in 1984, with the title "Two-Dimensional Separations: Concept and Promise". In relation to the development of 2D methods in the future, Giddings wrote: "any 2D technology must stand on the shoulders of 1D building blocks. Whereas the thrust of 1D research is to improve the building blocks, the thrust of of 2D research will be to find powerful and ingenious ways of combining building blocks". Through these sentences, Giddings highlighted how a 2D method needs the combination of building blocks, namely the combination of stationary phases of different selectivity [Giddings 1984]. From another point of view, the choice of the 2D

column must be accurate, since it must not worsen the separation of components already separated in the 1D profile.

Dealing with multidimensional systems in gas chromatography, two approaches can be distinguished. Multidimensional separations can be performed by transferring only specific regions from the first column to the second one, by means of the heart cut mode (MDGC); otherwise, all the sample can be transferred from the first to the second dimension by means of a modulator in comprehensive gas chromatography (GCxGC). In the following paragraphs, a brief description of GCxGC comprehensive approach is described, while a deeper discussion is provided for heart cut techniques.

3.2.1 Brief description of comprehensive GCxGC systems

Comprehensive GCxGC was first introduced by Liu and Philips in 1991 [Liu and Philips 1991]. In this paper, the authors reported a GC×GC separation of a mixture of standard compounds and of a sample of coal liquid by means of a dual-stage thermal desorption modulator (TDM). Separation was performed by combining a capillary PEG column of dimensions 21 m × 0.25 mm ID × 0.25 μm df as 1D, while the 2D was 1 m × 0.10 mm ID × 0.50 μm df column with a methyl silicone stationary phase. Since the first application, GCxGC demonstrated to be advantageous for quali-quantitative analysis with respect to MDGC, due to the capability to analyse the entire sample in a single chromatographic run. In a MDGC system, only selected regions are subjected to a further separation in the second dimension, while the remaining part is directed to the detector in the first dimension, or vented off. Differently, in a GCxGC analysis, all the matter is transferred from the 1D to the 2D. In terms of peak capacity, main differences thus involve between MDGC and GCxGC application. Operating by means of a heart cut transfer device (MDGC), the total number of peaks that can be placed in the separation space (nc), is the sum of that of the first and second dimensions, the latter multiplied by number (x) of heart-cuts [$nc_1 + (nc_2 \times x)$]. Differently, in GC×GC application, the total peak capacity equals to that of the first dimension multiplied with the second dimension ($nc_1 \times nc_2$).

In comprehensive analysis, the heart of the system is the transfer device between the two dimensions, called modulator. Modulator in GCxGC covers a primary importance, since it has to accumulate the analytes from the first dimension, refocus them, and release in narrow zones (down to 50msec peak width) in the second dimension. In this concern, the separation of components in the 2D must be completed before further analytes are injected in the 2D, to avoid overlap of peaks derived from different modulation cycles (wraparound). These findings explain how the second

column analysis needs to be much faster than the first one, thus leading to 2D separation time about 100 times more rapid than in the 1D.

3.2.2 Multidimensional gas chromatography (MDGC) performed in heart cut mode

Since the first application by Simmons and Snyder in 1958, where the authors reported a coupling of two 50m capillary columns using a pneumatically operated diaphragm six-port valve, several advances were done in the field of multidimensional gas chromatography [Simmons and Snyder 1958]. As reported by Tranchida in 2012, nowadays the transfer systems between the two columns can be classified in three groups: (I) in-line valve, (II) out-line valve and (III) valveless systems [Tranchida 2012]. For in-line valves, a valve interfaces the two columns in a direct manner; differently out-line valves are employed to regulate the direction of gas flow towards the column interface, while valveless systems are rarely used. Regardless of the type of system used, multidimensional gas chromatography, performed by means of a Deans Switch transfer device [Deans 1973], works by means of two different operational modes [Tranchida 2012, Marriott 2016, Nolvachai 2017]. In stand-by mode, all the analytes eluting from the 1D column are directed to the detector in the 1D. Differently, when the cut mode is activated, the stream of gas carrier leads the target analytes from the 1D to the 2D, to perform a complementary separation prior to the detection. As already highlighted in the previous section, this kind of system will allow a higher peak capacity, ever more for those sample having a wide concentration of analytes. However, increasing the amount of heart cut windows in the first dimension may complicate the separation of the previous separated compounds in the 2D. To these aims, the capability to operate with independent temperature programs may be beneficial to reduce this issue. In fact, MDGC separations can take place or by employing a single oven, or by means of multi oven systems. A very first application was demonstrated by Fenimore in 1973, where the secondary oven allowed to use a lower temperature in the second column [Fenimore 1973]. In this concern, two oven configuration allows to develop faster analysis, still providing higher resolution separations. By setting a secondary oven program temperature in the 2D, the analytes transferred from the 1D can be better re-focused, and thus orthogonally separated prior to the detection. Moreover, columns with a low thermal stability, as chiral or wax columns, can still be used in combination with methyl polysiloxane ones, by employing two independents temperature programs. A further way to improve the resolution performance of a twin-capillary system can be achieved by using an additional pressure source connected to the columns connection point.

A MDGC system, characterized by a microfluidic transfer device was proposed by Agilent Technologies [McCurry 2003, Quimby 2007]. As already highlighted, optimal conditions for

MDGC operations, namely stand-by, cut and backflush, are provided by employing an electronic pressure control. The interface system is composed of five ports: two of them are connected to the first and second column, while another one is linked to a restrictor, with the same flow resistance as the second dimension. This requisite is important, since the pressure drop along the first column needs to be constant during stand-by and cut. Otherwise, in cut mode the retention times will be shifted with respect to the previous st-by analysis, denying an efficient MDGC analysis. This restrictor is also connected to a detector to register the first-dimension separation. Figure 3.3 resumes the two operational modes, namely st-by (bypass) and cut (inject). During the st-by mode, the solenoid valve directs the auxiliary flow to the left part of the Deans switch, which is connected through a channel to the port of the secondary column. Herein, as visible in the Figure 3.3, the gas flow is divided in two parts. Whilst the first part is directed to the second column, the other part is mixed with the first-dimension flow and arrives at the restrictor. When the valve is activated, the flow is directed on the side of the transfer device connected to the restrictor. At this level, the gas flow is again split. In this case one part is directed to the restrictor, while the other part is mixed with the first-column flow and directed to the second column. The main disadvantage of this system is that the capillary linked to the stand-by detector needs to be characterized by the same flow resistance of the secondary column: it means that both the second column and the restrictor needs to be replaced when changing the configuration.

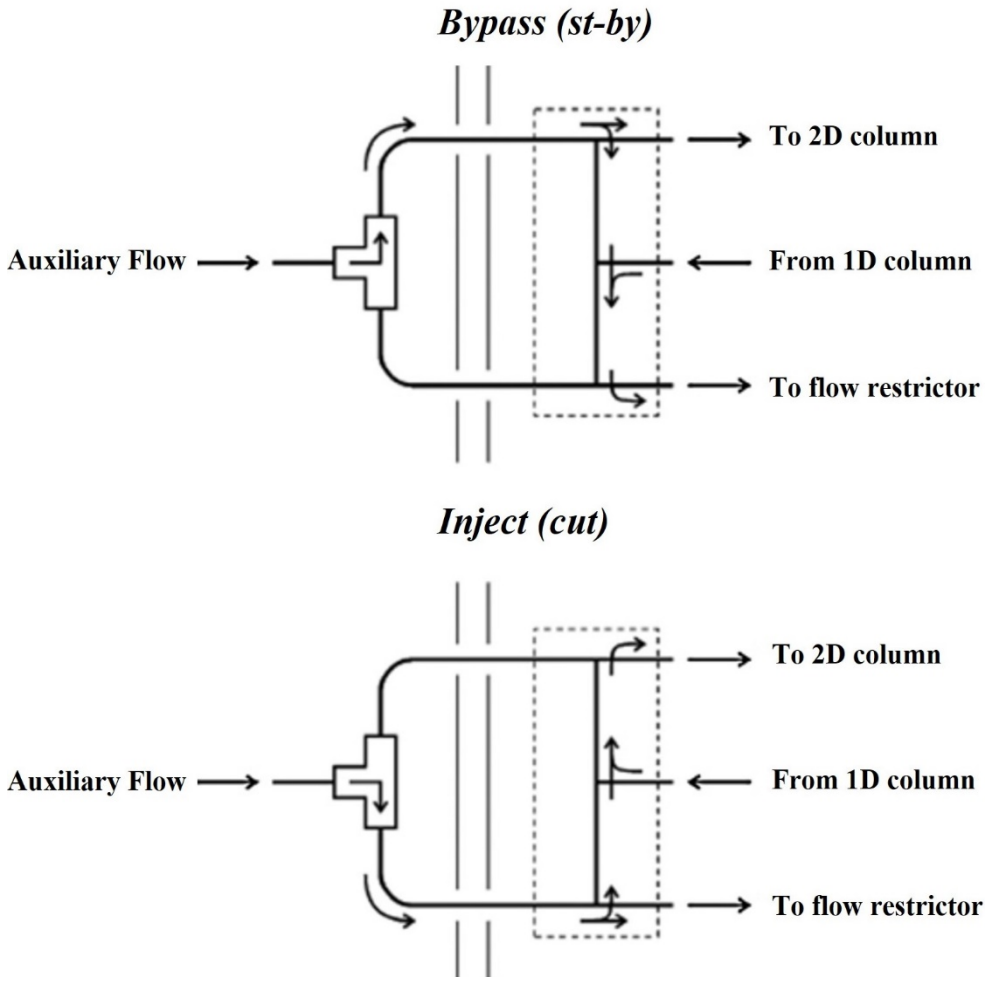

Figure 3.3 Scheme of the Agilent Deans switch operating in bypass (st-by) and inject (cut) modes

Few years later Gerstel commercialized another system based on the Agilent capillary flow technology [Sasamoto 2010], with the name "selectable 1D/2D GC-MS". In this system, the same mass spectrometer is able to perform both GC-MS and MDGC-MS. Since the same MS system is employed in stand-by and cut analysis, the peaks subjected to these separations appear in the same chromatogram. Although this system is surely interesting, it has a main drawback, related to the uncapability to perform multiple heart cuts, which have limited its diffusion.

A further efficient MDGC system based on Deans-switch transfer device was proposed by Shimadzu Corporation. In this system, 1st and 2nd column are placed in two different ovens and are connected by means of a thermally stable and chemically inert steel interface. This component is placed in the 1D oven, simultaneously connected to an auxiliary pressure system and to a 1D detector to perform stand-by analysis. As visible in Figure 3.4, the Deans-switch is composed of three different fused silica restrictors (R1, R2, R3), able to operate in a st-by (a) and a heart cut (b) mode. In both the operations, stand-by and cut, an auxiliary pressure system drives a constant gas pressure to the R3 and to a two-way solenoid valve. The latter is connected to the restrictor R2,

which can produce a pressure drop higher than that generated by R3. In this concern, in the stand-by mode the valve is closed, and the driving pressure force will obviously lead the analytes eluted from the 1D column to the detector in the first dimension. Differently, when the solenoid valve is opened, the analytes from the 1D are directed to the 2D one.

With respect to previous systems, this system is able to overcome limitations associated to multiple heart cut operations. Thanks to the configuration with three restrictors, no retention time shifts will happen during heart cut operations, as well as the fluctuations in terms of retention times after each run.

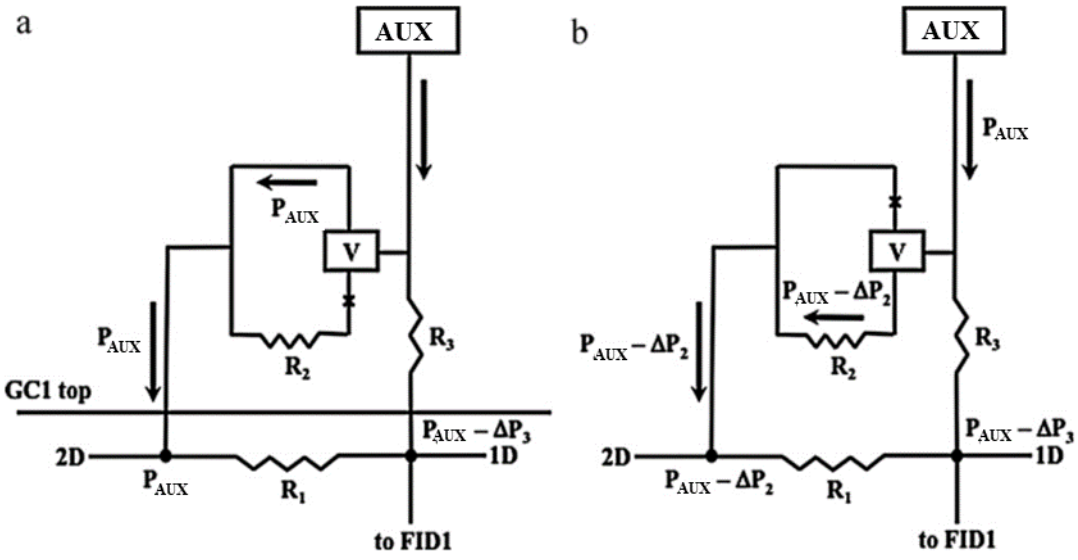

Figure 3.4 Scheme of the Shimadzu Deans Switch operating in st-by (a) and cut (b) modes

Dealing with MDGC application performed by means of the Shimadzu Deans Switch, several parameters need to be monitored to efficiently heart cut target retention windows. In a conventional condition, with the coupling of two full length columns having the same characteristics (30m, 0.25 x 0.25), injection pressure and auxiliary pressure cover a primary importance to perform a heart cut process with a recovery equal to 100%. Moreover, also temperature programme in both the 1D and 2D dimensions needs to be accurately optimized, as well as temperature rate. Otherwise, a no efficient transfer will take place since some components will remain in the first operating column (Recovery < 100%). This issue is very limiting for quali-quantitative aims but ever more in the case of the coupling to particular detection systems as IRMS, since it may produce unreliable data [Juchelka 1998]. In this concern, Figure 3.5 reports an example of a working method, to be optimized prior to perform such MDGC analysis. As visible in Figure 3.5(a), when the valve is closed, the auxiliary pressure leads to a pressure drop related to R3, driving the components eluted

from the 1D column to the 1D detector. In detail, the R3 generates a ΔP3 of 0.5 kPa, pushing the analytes from the 1D column to the 1D detector. In the cut mode a pressure driving force pushes the analytes coming from the 1D column to the 2D one. When the valve is opened, R2 can generate a pressure drop (128.8 kPa) higher than that generated by R3 (129.5 kPa). It's clear that such pressure conditions allow to drive the analytes from the 1D (129.5 kPa) to the second one (128.8 kPa).

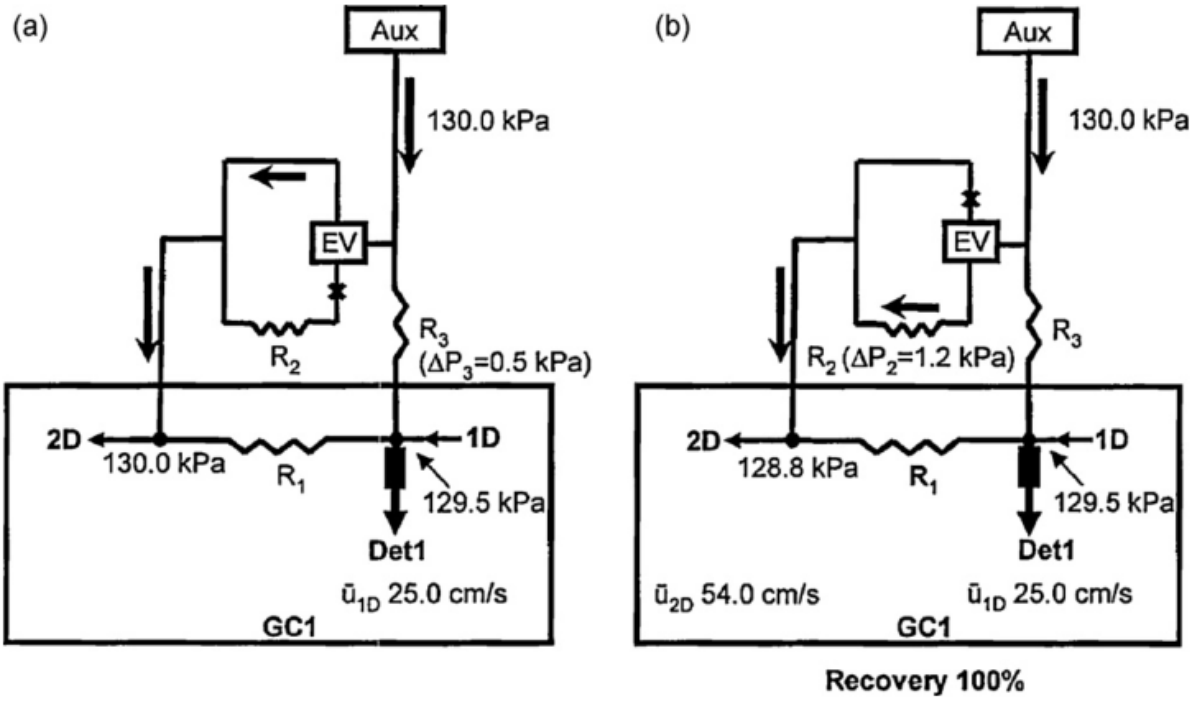

Figure 3.5 Explained scheme of the working operation for the Shimadzu Deans Switch

Another instrument based on the Deans switch transfer device was introduced in 1991 by Brechbühler, named moving capillary stream switching (MCSS). This system allow the diversion of the effluent from the 1D to the 2D by means of the movement of the 1D capillary inside an inverted dome, as reported in Figure 3.6. By means of the combination of a transmission rod and an electrically activated magnet, a longitudinal movement of the 1D capillary is achieved. In stand-by mode, the 1D capillary is positioned above the middle of dome to direct the effluent to the 1D detector. When solute transfer involves, the capillary is moved upwards to allow this transfer.

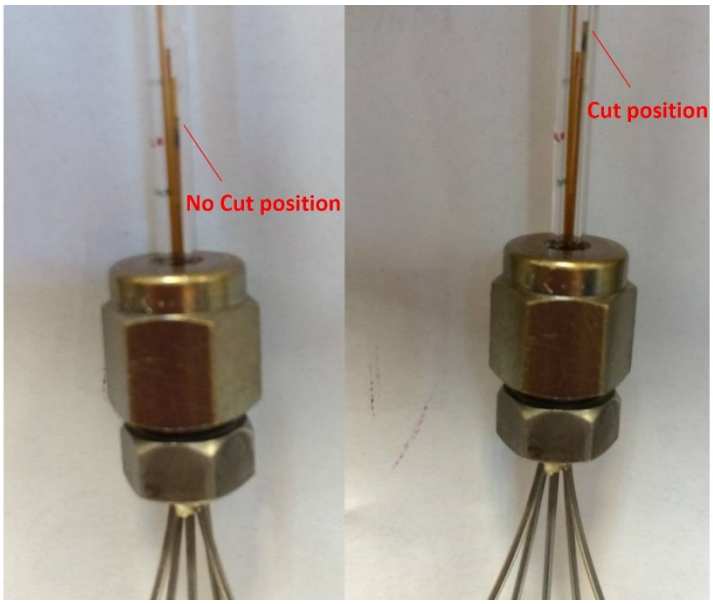

Figure 3.6 Scheme of the Brechbühler Deans Switch in the "no cut" and "cut" positions

As shown, MDGC systems based on Deans Switch transfer devices are surely one of the answers to increased peak capacity for the analysis of complex samples. In the next paragraph (3.2.4) and chapters (Chapter 4 and Chapter 6), a deep discussion will deal with their employment in the field of preparative gas chromatography, isotopic ratio mass spectrometry and enantio-selective gas chromatography.

3.2.3. Multidimensional preparative gas chromatography

Preparative gas chromatography (prep-GC) is an analytical technique able to guarantee the isolation of target components from a matrix, in order to collect them for various further application [Kim 2012]. In the case of the isolation of unknown components, the collection is usually followed by elucidation structural analysis, as mass spectrometry (MS) and nuclear magnetic resonance (NMR). Figure 3.7 shows a conventional prep-GC system.

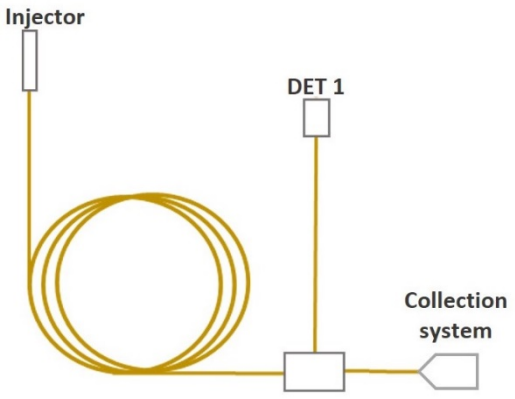

Figure 3.7 Scheme of a conventional monodimensional preparative gas chromatography

As visible, at the end of the chromatographic column the eluent can be directed or to the detector or to the collection system by a switching device. Typically, the eluent is first directed to the detector to identify the target chromatographic zone; after, in a successive analysis that zone will be collected. Dealing with separation system, the employment of packed column was usually preferred in the past. Since a higher amount of sample volume can be injected for run, thus a higher amount of target analytes can be collected. Conversely, packed columns suffer of renowned lower efficiency with respect to capillary columns. In the case of complex natural samples, this drawback can be really limiting. Due to the low efficiency, more than one component will be collected for each analysis, drastically complicating the successive identification step. Complementarily, while conventional capillary columns have a renowned higher efficiency, on the other hand the lower capacity allow to collect only few micrograms of target analyte for run. Moreover, the injection of high amount of sample leads to peak overloading which definitively compromise the efficiency of the columns. In this concern, wide bore capillary columns (0.53 mm I.D.) were the most suitable for preparative aims, since they can accommodate a larger amount of sample. However, as well as packed columns, they suffer of low efficiency in the case of the analysis of complex samples. To these aims, multidimensional gas chromatographic methods, by means of Deans switch transfer device, were developed over the years to overcome these limitations.

Eyres *et al*., in 2008 developed a new preparative MDGC system to allow a suitable collection of geraniol in a mixture of essential oils [Eyres 2008]. In this system, target components were heart cut to the 2D through a programmed sequence of trap/release events, achieved by the longitudinally modulated cryotrap (LMCS). By injecting a sample composed by lavender and peppermint essential oils, geraniol resulted co-eluted with other six components in the first column. Once developed the MDGC approach, at the end of the second column geraniol was efficiently transferred by means of the Deans switch and trapped with a high degree of purity.

A very step forward in preparative gas chromatography was done in 2012, when Sciarrone *et al*., developed a novel triple deans-switch multidimensional preparative gas chromatographic system [Sciarrone 2012, Sciarrone 2014], whose scheme is reported in Figure 3.8.

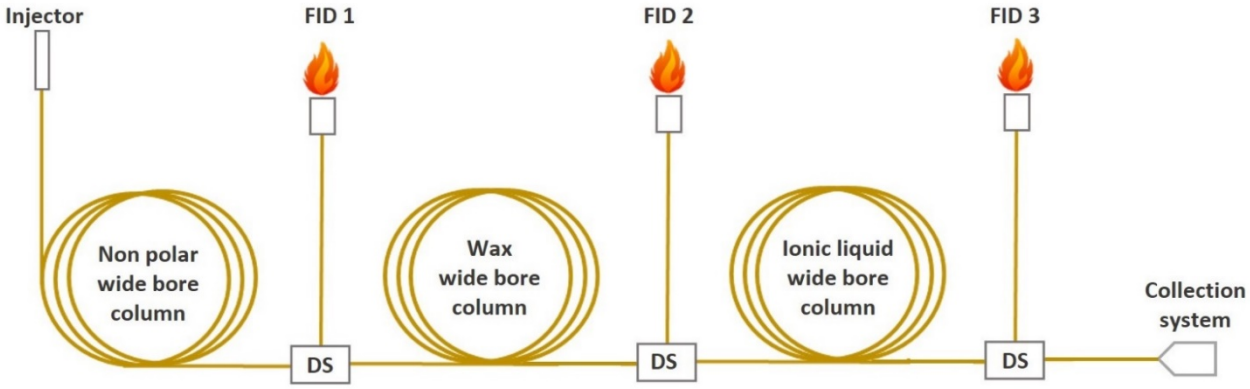

Figure 3.8 Scheme of the MDGC preparative system developed by Sciarrone *et al*. [Sciarrone 2012]

By means of the combination of three different stationary phases, namely apolar-wax-ionic liquid, the authors demonstrated the capability to isolate key target components with a very high degree of purity. In detail, the authors aimed to collect carotol from a complex essential oil, by comparing both monodimensional and multidimensional systems. By means of the monodimensional approach, carotol resulted still "contaminated" by the co-eluting peaks, with a reduced collection purity degree. On the other hand, the multidimensional approach, performed by combining 0.53 mm I.D columns, allowed to collect carotol with a purity > 99%, drastically reducing total time analysis. Consequently, 2.22 mg of carotol were efficiently collected in a total analysis time of 216 min.

In other application, MDGC prep system is coupled off-line to several elucidation structural systems, as NMR, MS, FTIR to identify unknown chemical components [De Grazia 2022], prior also to investigate its biological activity.

3.3 The coupling of gas chromatography to mass spectrometry (GC-MS)

As discussed in the previous paragraphs, gas chromatography separates components in a mixture in relation to their retention times, and thus accordingly to their physic-chemical features. Generally, routine GC detector as flame ionization detector (FID) produces a chromatogram, which is the result of the different electric signals registered at the elution time of each component from the chromatographic column. By these means, peak identification is limiting, since it depends only on retention time, which may greatly vary modifying GC conditions. Differently, when coupling gas chromatography to mass spectrometry (MS), each component will produce a typical mass fragmentation spectrum, providing new helpful information for identification. The chromatogram produced by the MS will be the sum of a series of mass spectra, related to the

components eluted from the GC column. In this paragraph, a brief description of mass spectrometry principles and the main mass analysers is provided.

From an historical point of view, mass spectrometry was introduced by Thomson, Aston and Dempster at the beginnings of twentieth century [Thomson 1897, Thomson 1907, Aston 1918, Dempster 1919].

Dealing with the coupling to GC, mass spectrometers ionizes, separates, and thus detects all the volatiles eluted from the chromatographic column. In this concern, Figure 3.9 shows a simple scheme of the main components of a MS.

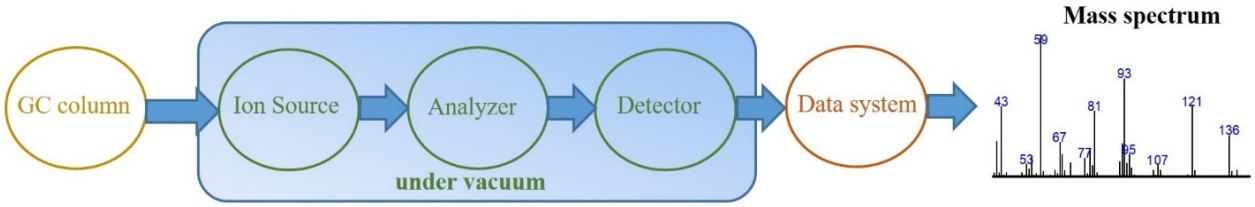

Figure 3.9 Schematic of the main components of a MS system (coupled to GC)

As visible, a MS is composed of an inlet system (in this case the GC column), which works under atmospheric conditions. Differently, ion source, mass analyser and detector operate under vacuum conditions (from 10^{-4} to 10^{-7} bar). Vacuum is necessary in order to guarantee the integrity of the molecules coming from the GC, as well as their reproducible ionization, run by run. These conditions ensure that, once the ion is produced in the ion source, it will move to the mass analyser without collision with other molecules. Dealing with the coupling to GC, a vacuum-sealed transfer line is needed: its temperature is normally higher than that of GC oven to avoid possible re-condensation phenomena. The most employed ionization mode in GC-MS application is surely the electron ionization (EI). Nowadays, EI is still the ionization technique of choice for the analysis of organic molecules having low-medium polarity and a molecular mass under 1000 Da. By applying an electron energy of about 70 eV, highly reproducible spectra are produced for each target component, performed on the same on or different types of instruments. This discover has carried out to the development of EI mass spectral databases, named libraries (National Institute of Standards and Technology NIST). Coming back to electron ionization process, in an EI source, a resistively heated metal filament, made of rhenium or tungsten, produces the beam of ionizing electrons. Electrons are thus accelerated towards an anode and collide with the gaseous molecules provoking their ionization. This process takes place by means of the ejection of an electron from the analyte, according to the following formula:

$$M + e^- \rightarrow M^{+\bullet} + 2e^-$$

where *M* represents the neutral molecule in the gas phase. Once the collision takes place, a radical cation, or an odd-electron (open-shell) ion is generated. Since only 20 eV are transferred to the neutral molecule for ionization, it's clear that the excess energy is responsible for other fragmentations starting from the radical cation, leading to the typical fragmentation pattern of each analyte.

After the ionization, molecules are led to mass analyser, which will separate the ions produced according to their mass to charge ratio (m/z).

Single quadrupole

Quadrupole mass analyser was first described by Paul and Steinwedel in 1953 [Paul and Steinwedel 1953]. A single quadrupole mass analyser is composed of four parallel hyperbolical rod electrodes, having a squared configuration [Campana 1980, Miller 1986, Dawson 1986]. A scheme is provided in Figure 3.10

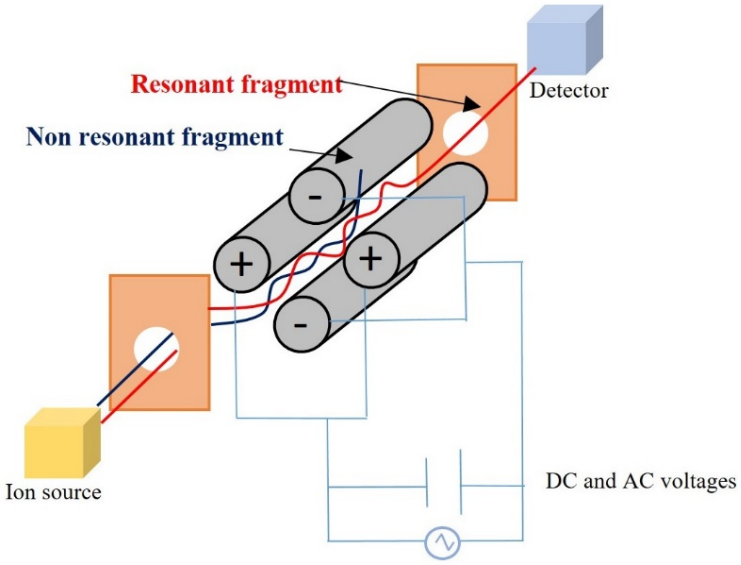

Figure 3.10 Schematic representation of single quadrupole mass analyser

Opposite rods are each maintained at the same potential (positive or negative), composed by a direct-current (DC) and an alternating current (AC). When the combination of a radiofrequency (RF) and DC is applied to the electrodes, a high frequency oscillating electric field is generated, able to separate ions once they cross the quadrupole. Opposite rods are connected electrically in pairs, and each pair will have the same potential with an opposite sign. Once a positive ion enters inside the quadrupole, it will be attracted towards the negative rods. When the potential changes,

the ion will modify its trajectory, avoiding to discharge against the negative rod. Typically, rod voltages are modified periodically, and attraction and repulsion forces will be alternated. In this concern, at specific values of DC and RF potentials, only target ions having a specific m/z range will have a stable trajectory and are able to be detected (red trace in Figure 3.4). Otherwise, they will collide in the rod with opposite sign (blue trace in Figure 3.4). In this concern, Mathieu equations describe the theory of ion travelling along the quadrupole [McLachlan 1947]. Quadrupole mass spectrometers (qMS) are by far the most employed analyser in GC-MS application. Since this device is a scan mass analyser, the operator can work both through untargeted (full scan mode) and targeted (SIM, selected ion monitoring) analysis.

Triple quadrupole mass spectrometry

Triple quadrupole is a linear combination of three quadrupoles. In this concern, only the first (q1) and the third quadrupoles (q3) are to be considered as mass analysers since they operate with a combination of a DC and a RF for mass selection. Differently, the second quadrupole (q2) is normally a hexapole or an octapole with a fixed voltage, and operates as a collision cell with ion focusing properties. By these means, the first quadrupole is set to transmit a specific m/z; the second quadrupole produces a fragmentation, while in the third quadrupole the ions produced are analysed. Generally, four types of scanning mode are used, namely the product ion scan, precursor ion scan, neutral loss scan and selected reaction monitoring as visible in Figure 3.11

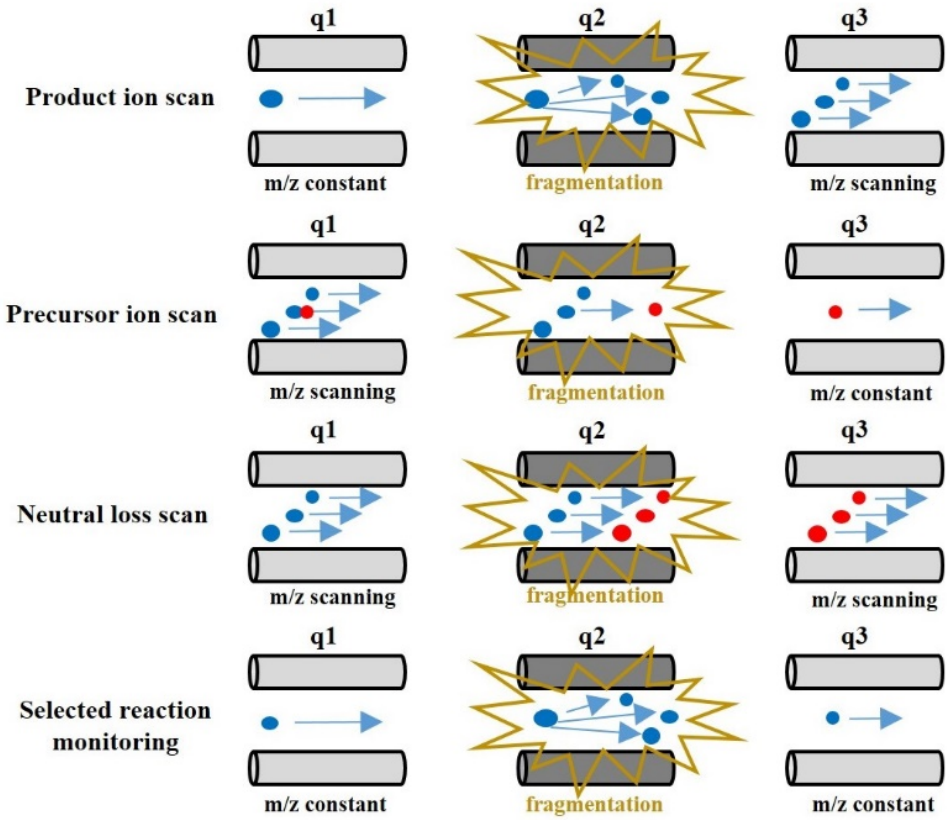

Figure 3.11 Schematic of the main operational modes of a triple quadrupole mass spectrometer

Product ion scan mode is carried out by setting the first mass analyser (MS1) to a specific m/z value, while performing a scan on a range of m/z value in the second mass analyser (MS2). This procedure is the most known MS/MS approach, and it is typically employed for structural elucidation aims. Contrarily, precursor ion scan is performed by scanning a mass range in MS1, while a target m/z is set for MS2. In the neutral loss scan mode, both the mass analysers operate with the same scan speed, while MS2 is shifted by a determined m/z value with respect to the first one. In selected reaction monitoring, target transitions of m/z values from a precursor to specific ions produced are monitored along the analysis. Since more transitions can be performed in an analysis, this approach is also called multiple reaction monitoring (MRM).

Magnetic sector (Isotope ratio mass spectrometry)

Magnetic sector are by far the preferred mass analyser for precise determination of isotope ratios. This mass analyser is superior to the quadrupole one for different reasons, as already discussed in the Chapter 1. Thanks to its operational mode, it can be set for multiple-collector analysis, providing high-quality peak shapes. These conditions are of primary importance for isotope ratio analysis, since a high precision and accuracy is required (Figure 3.12).

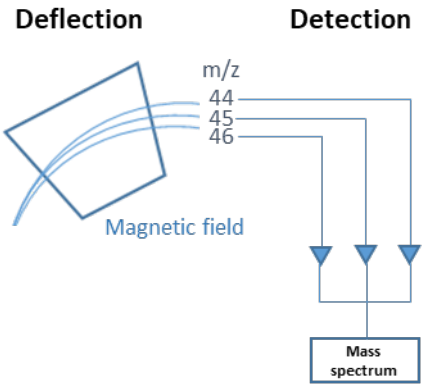

Figure 3.12 Scheme of the magnetic sector employed in an isotopic ratio mass spectrometer

As already discussed in the IRMS section, this type of mass spectrometer was developed by Alfred Nier, and is also called as "Nier type" [Nier 1940]. In this instrument, ion separation in mass analyser will depend on the different trajectory provided by the magnetic sector. Beams having lighter ions will bend at a smaller radius with respect to beams with heavier ions. After that, the current of each ion beam is then measured employing Faraday cups, each set at a specific m/z value. A deep discussion related to the coupling of IRMS to GC will be provided in the next Chapter.

References

Aston, F.W. A positive ray spectrograph. Philos. Mag. 38 (1919) 709.

Berger, T. A. 'Separation of a gasoline on an open tubular column with 1.3 million effective plates', Chromatographia 42 (1996) 63.

Bertsch, W. Two-dimensional gas chromatography. Concepts, instrumentation, and applications—part 1: fundamentals, conventional two-dimensional gas chromatography, selected applications. J. HighResolut. Chromatogr. 22 (1999) 647–65.

Campana, J. E., Elementary theory of quadrupole mass spectrometry, Int. J. Mass Spectrom. Ion Proc. 33 (1980) 101.

Dawson P.H. Quadrupole Mass Analyzers: Performance, Design and Some Recent Applications. Mass Spectrom Rev 5 (1986) 1–37

De Grazia, G., Cucinotta, L., Rotondo, A., Donato, P., Mondello, L., Sciarrone, D. Expanding the Knowledge Related to Flavors and Fragrances by Means of Three-Dimensional Preparative Gas Chromatography and Molecular Spectroscopy, Separations, 9:8 (2022) 202

Deans, D. R., Scott, I. Gas chromatographic columns with adjustable separation characteristics Anal Chem, 45:7 (1973) 1137-1141.

Dempster, A.J. A new method of positive ray analysis. Phys. Rev. 11 (1918) 316.

Eyres, G. T., Urban, S., Morrison, P. D., Dufour, J. P., Marriott, P. J. Method for small-molecule discovery based on microscale-preparative multidimensional gas chromatography isolation with nuclear magnetic resonance spectroscopy, Anal Chem. 80 (2008) 6293

Fenimore, D. C., Freeman R. R., Loy, P. R. 'Determination of 9 -tetrahydrocannabinol in blood by electron capture gas chromatography', Anal. Chem. 45 (1973) 2331–2335.

Giddings, J.C., Two-dimensional separations: concept and promise. Anal. Chem., 56:12 (1984) 1259

Golay, M. J. E. Gas Chromatography 1958 (Amsterdam Symposium), ed. D.H. Desty, Butterworth, London (1958) 36.

James A. T., Martin, A. J. P. Gas-liquid partition chromatography; the separation and micro-estimation of volatile fatty acids from formic acid to dodecanoic acid Biochem. J. 50 (1952) 679-690.

Juchelka, D., Beck, T., Dettmar, F., Mosandl. A., Multidimensional gas chromatography coupled on-line with isotope ratio mass spectrometry (MDGC-IRMS). J. High Resolut. Chromatogr. 21 (1998) 145

Kim, L., Marriott, P.J. Preparative gas chromatography, in: C.F. Poole (Editor), Gas Chromatography, Elsevier, Amsterdam, 2012, pp. 395–414.

McCurry, J.D., Quimby, B.D. Two-dimensional gas chromatography analysis of components in fuel and fuel additives using a simplified heart-cutting GC system, J. Chromatogr. Sci. 41 (2003) 524–527.

McLachlan. D.W., Theory and Applications of Mathieu Functions. Oxford, Clarendon Press (1947).

Miller, P. E., Bonner Denton, M., The quadrupole mass filter: basic operating concepts, J. Chem. Educ. 63 (1986) 617.

Mondello, L., Lewis, A. C., Bartle K.D. (Editors), Multidimensional chromatography, Wiley & Sons, Chichester, England, 2002.

Nier A.O. A mass spectrometer for routine isotope abundance measurements. Rev Sci Instrum 11:7 (1940) 212–6.

Nolvachai Y, Kulsing C, Marriott P.J. Multidimensional gas chromatography in food analysis. Trends Anal Chem 96 (2017) 124–137

Paul, W., Steinwedel, H. Notizen: Ein neues Massenspektrometer ohne Magnetfeld Z. Naturforsch. A. 8 (1953) 448.

Phillips, J.B., E.B. Ledford Thermal modulation: A chemical instrumentation component of potential value in improving portability Field Anal. Chem. Technol. 1 (1996) 23.

Quimby, B., McCurry, J., Norman, W. Capillary Flow Technology for Gas Chromatography: Reinvigorating a Mature Analytical Discipline LC GC The Peak April (2007) 7-15

Sasamoto, K., Ochiai, N. Selectable one-dimensional or two-dimensional gas chromatography–mass spectrometry with simultaneous olfactometry or element-specific detection J Chromatogr A 1217 (2010) 2903-2910

Schomburg, G., Husmanm, H., Hubinger, E., Konig, W.A. Multidimensional capillary gas chromatography – enantiomeric separations of selected cuts using a chiral second column, J. High Resolut. Chromatogr. 7 (1984) 404-410.

Sciarrone D., Ragonese C., Carnovale C., Piperno A., Dugo P., Dugo G., Mondello L. Evaluation of tea tree oil quality and ascaridole: a deep study by means of chiral and multi heartcuts multidimensional gas chromatography system coupled to mass spectrometry detection. J Chromatogr A 1217 (2010) 6422–6427.

Sciarrone, D., Pantò, S., Ragonese, C., Tranchida, P.Q., Dugo, P., Mondello, L. Increasing the isolated quantities and purities of volatile compounds by using a triple Deans-switch multidimensional preparative gas chromatographic system with an apolar-wax-ionic liquid stationary-phase combination, Anal. Chem. 84 (2012) 7092–7098.

Sciarrone, D., Pantò, S., Tranchida, P.Q., Dugo, P., Mondello, L. Rapid isolation of high solute amounts using an online four-dimensional preparative system: normal phase-liquid chromatography coupled to methyl siloxane–ionic liquid–wax phase gas chromatography, Anal. Chem. 86 (2014) 4295–4301.

Sharif, KM, Chin, ST, Kulsing, C, Marriott, PJ The microfluidic Deans switch: 50 years of progress, innovationand application Trends in Analytical Chemistry 82 (2016) 35–54

Thomson, J.J. XL. Cathode rays. Philos. Mag. 44 (1897) 293.

Thomson, J.J. XLVII. On rays of positive electricity. Philos. Mag. 13 (1907) 561.

Tranchida, P.Q., Sciarrone, D., Dugo, P., Mondello, L. Heart-cutting multidimensional gas chromatography: A review of recent evolution, applications, and future prospects, Anal. Chim. Acta 716 (2012) 66– 75.

Chapter 4

The coupling of monodimensional and multidimensional gas chromatography to isotopic ratio mass spectrometry

4.1 Gas chromatography coupled to isotopic ratio mass spectrometry (GC-C-IRMS)

The very first study relative to the compound specific isotopic analysis is attributed to Sano, related to an application about ^{13}C-labeled methyl benzoate, and its metabolites in human urine [Sano 1976]. In this research, the authors coupled a gas chromatograph to a mass spectrometer by means of a combustion interface, which was able to produce CO_2. The first term used by Sano for this application was "mass fragmentography", and only in 1978 was substituted by Matthew and Hayes, who introduced the term "isotope ratio monitoring GC/MS" [Matthew and Hayes 1978]. After that, Barrie in 1984 developed a dual collector system, which represented the very first gas chromatograph coupled to combustion chamber and to isotope ratio mass spectrometry (GC-C-IRMS). However, only from 1990 GC-C-IRMS has become commercially available [Meier Augestein 1999], experiencing several advances along the years. In general, the instrumental configuration of GC-C-IRMS combined the high precision of IRMS with the high purification effect of GC separation, reducing laborious sample clean-up procedures. The main components of a GC-C-IRMS system are shown in Figure 4.1.

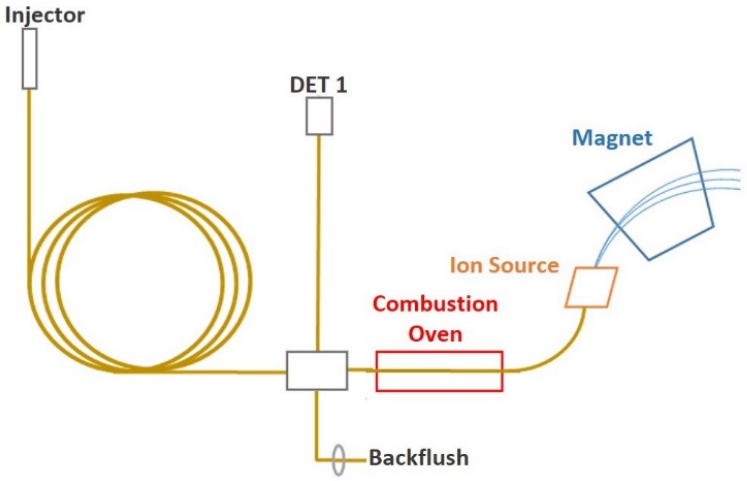

Figure 4.1 Typical instrument configuration of a GC-C-IRMS system

Briefly, the analytes separated in the GC column are directed to the combustion tube to produce the required gases prior to IRMS detection. Dealing with $\delta^{13}C$ values determinations, the combustion interface is provided with a source of O_2, in order to guarantee the formation of CO_2 and H_2O from the organic matter analysed. Generally, this reagent is composed of CuO, with Pt as catalyst, able to produce O_2. However, to preserve the integrity of the catalyst, the solvent from the GC run needs to be diverted far from the furnace. Generally, the end of the 1D capillary column, as shown in the Figure 4.1, is both connected to the combustion interface, and or to a backflush system or a valve, to deflect the flux of solvent peak. In this concern, the valve is both able to push the solvent peak to the backflush, and the analytes to the combustion chamber when required. In some cases, the flux may be also directed to another detector. Dealing with carbon isotopic application, after the combustion process, all the organic matter is converted to CO_2 and H_2O. However, water must be removed after combustion. Otherwise, it may interfere in the detection of CO_2 since it can produce HCO_2^+, interfering with the analysis of the fragment 45 (related to ^{13}C contribute). To overcome this limitation, the analyte stream is passed through a semi-permeable membrane as Nafion. At this level, a dry helium counter flow is used to remove the water. Along the process, the flow rate of the analytes is monitored by an open split, to provide a stable flow rate to the IRMS. After the ionization, CO_2 ions are deflected by a magnetic sector (section 3.3), and finally detected by Faraday cups. In the case of carbon isotopic analysis, Faraday cups are set to detect 44, 45, 46 fragments of CO_2.

When developing a new method in GC-C-IRMS, much care must be paid to avoid isotopic fractionation, since it may lead to unreliable results [Sessions 2006]. For this discussion, the term isotopic fractionation is only related to isotopic shifts associated to chromatographic factors as

injection, separation, and peak resolution. Starting from the injection, isotopic fractionation may involve in the case of no-quantitative transfer from the injector. Such an issue did not influence on-column injections at all, since all the matter is directly injected into the column. Contrarily, in the case of split/splitless injections, it may be limiting since part of the organic matter is diverted. However, in literature no relevant shifts in terms of isotopic ratios were reported for splitless methods, and by applying programmable-temperature vaporizations (PTV). When using split/splitless injectors in split mode, part of the vaporized matter is vented, while only a specific fraction is sent to the column: in these conditions, isotopic fractionation may easily involve. However, literature studies by Wang and Li research groups' have not found isotopic fractionation when operating with different split ratios [Wang 2001, Li 2001]. In this concern, Zwank *et al*. compared on-column, splitless, and split (50:1) methods for volatiles, highlighting how all the methods are suitable for IRMS application [Zwank 2003]. Beside liquid injection, also other injections technique, as solid phase microextraction (SPME), were evaluated. In this concern, Harris highlighted how both SPME and purge and trap procedure are reliable methods for IRMS measurements, once optimized injection conditions [Harris 1999].

Whilst the description of injection methods highlighted how no critical fractionation processes typically involve, on the other hand peak separation represents a critical matter. The need of a baseline resolution for each target volatile detected by the IRMS is a cornerstone of the coupling with gas chromatography. In the case of co-elutions between key components, unreliable results will be detected. This issue is so much limiting that, often, different type of analysis (consisting of different injection volumes) are needed to fully determine the $\delta^{13}C$ of key volatiles in a sample [Schipilliti 2011]. In other cases, this issue has been often underestimated in literature, although it can provide wrong isotopic results. Briefly, this matter lays its basis in the detection of the CO_2 peak from the IRMS. As already shown in Figure 4.1, after the GC run the analytes are all converted to CO_2, prior to the detection of the isotopomers $^{44}CO_2$ and $^{45}CO_2$. However, as reported by several research works, these species elute at different times leading to a no homogeneous distribution along an entire peak of CO_2. This behaviour was called as "chromatographic isotopic effect", since it involves when coupling a chromatographic system to IRMS. In this concern, Figure 4.2 shows how the mass $^{45}CO_2$ (green peak) elutes 180ms earlier than mass $^{44}CO_2$ (blue peak).

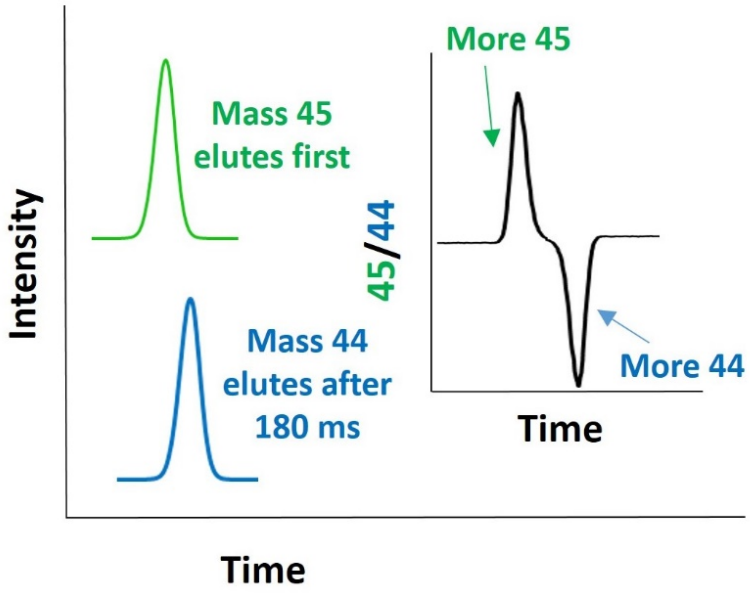

Figure 4.2 Gas chromatographic isotopic effect of CO_2 along a GC-C-IRMS analysis

If plotting this distribution in a graph, defined as *S* shape [Mosandl 1995], it is clear how the ratio $^{45/44}$ will be more affected by the mass $^{45}CO_2$ in the initial part of the peak, while the tail will be more influenced by the mass $^{44}CO_2$. Dealing with HPLC-IRMS, other research groups highlighted the opposite behaviour, since mass $^{44}CO_2$ elutes earlier than mass $^{45}CO_2$. Investigating on the reasons about chromatographic isotopic effect, Matucha described how this uneven distribution might be related to different retentive forces between the column and CO_2 species [Matucha 1991]. In any cases, due to the uneven distribution of CO_2 species along the peak, an overlap between two target components results critical for the detection of their $\delta^{13}C$ values. In order to overcome these issues, some attempts were done by employing a mathematical deconvolution to resolve coeluting peaks [Goodman 1995], but these systems are not still incorporated into commercial software. Moreover, in the case of co-elutions of more than two components, this approach is not able to provide a right response. For these reasons, the employment of multidimensional gas chromatography can represent the solution to increase the peak capacity prior to the detection, as described in the next paragraph.

4.2 Multidimensional gas chromatography coupled to isotopic ratio mass spectrometry (MDGC-C-IRMS)

When dealing with complex samples as flavours or environmental mixtures, sample preparation often includes several steps in order to isolate the key components, whose isotopic determination is required. This procedure is carried out to simplify the gas chromatographic profile prior to the IRMS detection. Otherwise, the presence of very crowded zones along the chromatogram may

lead to co-elutions, compromising the reliability of the method. In this concern, with the aim to overcome complicated separation steps, and to reduce total time analysis, multidimensional gas chromatography was considered as a suitable way to purify target components.

The coupling of MDGC to IRMS had its 30th birthday this year, starting from the very first application by Nitz in 1992 [Nitz 1992]. As already reported in the MDGC chapter, the coupling of two columns having different selectivity is the key concept of a multidimensional separation. In the field of multidimensional techniques coupled to IRMS, the employment of MDGC based on heart cut systems [Nitz 1992, Sewenig 2005, Greule 2008, Brailsford 2012, Casilli 2016, Ponsin 2017, Sciarrone 2018, Putz 2018] has covered a higher importance with respect to comprehensive GCxGC techniques over the years. Whilst for quali-quantitative aims comprehensive GCxGC is surely more suitable than MDGC, also due to the increased peak capacity, differently, for compound specific isotopic analysis, the sophisticated system configuration complicated its diffusion. In 2008 Tobias *et al*., developed a prototypal comprehensive GCxGC-IRMS system [Tobias 2008]. According to comprehensive gas chromatography, the authors coupled two different capillary columns (in terms of length, internal diameter, stationary phase film) by means of a longitudinally modulated cryogenic system. Dealing with acquisition rate, IRMS resistors were necessarily modified (acquisition rate =25 Hz) in order to enable a fast response for the very sharp peaks provided by GCxGC separation, as well as the combustion tube. However, due also to the complexity of the system, only two publications were carried out in this direction by the same research group [Tobias 2008, Tobias 2011]. In general, the selection of specific target components, performable by means of Deans Switch transfer devices, is more suitable to the definition of compound specific isotopic analysis. The chromatographic separation with the MDGC system allows the analysis of many components from complex matrices, as well as of minor components in the presence of large amounts of main compounds. Since only selected components are transferred, this operation does not overload the main column, which is directly connected with the combustion oven. Since less matter is directed to the combustion, this feature also allows a longer life for combustion tubes. Finally, with respect to comprehensive gas chromatography, heart-cut MDGC doesn't require highly specialized analysts in order to develop efficient methods. However, in spite of the evident advantages related to an increased resolution power provided by MDGC, this system is not routinely hyphenated to an IRMS detection (all the research works published are carried out on prototypes). Indeed, searching on scientific search engines in October 2022, very few works have been published coupling a MDGC system to IRMS. Specifically, by searching on Scopus the key words "GC" and "IRMS", more than 1200 results are found; differently, by searching "MDGC" and "IRMS" less than 20.

However, the issue associated to insufficient resolution assumes great importance for IRMS detection, with respect to common MS systems. Such a limitation is of primary importance, since co-elutions involve in unreliable isotopic results. Dealing with the first MDGC-C-IRMS prototype, the system proposed by Nitz consists of a double oven equipped with capillary columns having complementary selectivity; the transfer device was based on a Deans switch system, operating in heart cut mode [Nitz 1992]. The author compared the performance of a monodimensional GC-C-IRMS with a multidimensional C-IRMS. In general, the $\delta^{13}C$ values obtained by both configurations were very similar each other for baseline separated peaks (Table 4.1). Instead, many differences were found for components co-eluted in the monodimensional approach. In detail, Nitz highlighted how ethyl 2-methylbutyrate and cis-3-hexen-1-ol could not be satisfactorily separated from co-eluting substances to the extent that the determination of the isotope ratio was not possible [Nitz 1992]. Only by means of a MDGC system, a reliable determination of the $\delta^{13}C$ values was achieved. Whilst the $\delta^{13}C$ of ethyl 2-methylbutyrate was undetectable with a monodimensional approach, on the other hand with a MDGC approach its $\delta^{13}C$ value was equal to -27.20‰. Similarly, cis-3-hexen-1-ol registered a difference of two point of $\delta^{13}C$, between monodimensional (-32.95‰) and multidimensional approach (-34.99‰).

Number	**Component**	**GC-C-IRMS separation**	**$\delta^{13}C$ GC-C-IRMS**	**$\delta^{13}C$ MDGC-C-IRMS**
1	Ethyl 2-methylbutyrate	Co-eluted	-	-27.20
2	Trans-2-Hexenal	separated	-29.23	-29.71
3	1-hexanol	Co-eluted	-30.91	-32.49
4	Cis-3-hexen-1-ol	Co-eluted	-32.95	-34.99
5	Trans-2-hexen-1-ol	separated	-31.09	-31.12

Table 4.1 $\delta^{13}C$ values comparison between monodimensional and multidimensional approaches (all the standard deviations were under 0.5 ‰)

In 1998, Juchelka *et al*., investigated in depth the potentiality of a MDGC system coupled to IRMS detection [Juchelka 1998]. The author evaluated the response of an IRMS system comparing bulk EA-IRMS, GC-C-IRMS and MDGC-C-IRMS analysis. As already highlighted by Nitz, in the case of baseline resolved components, no differences are expected in terms of $\delta^{13}C$ values. From a gas chromatographic point of view, Juchelka *et al*., highlighted the need of specific cut windows for

the transfer of each target component [Juchelka 1998]. As visible in Figure 4.3, target component (Peak 2) in a MDGC analysis must be entirely transferred from the 1D to the 2D, in relation to the retention time in the previous stand-by analysis.

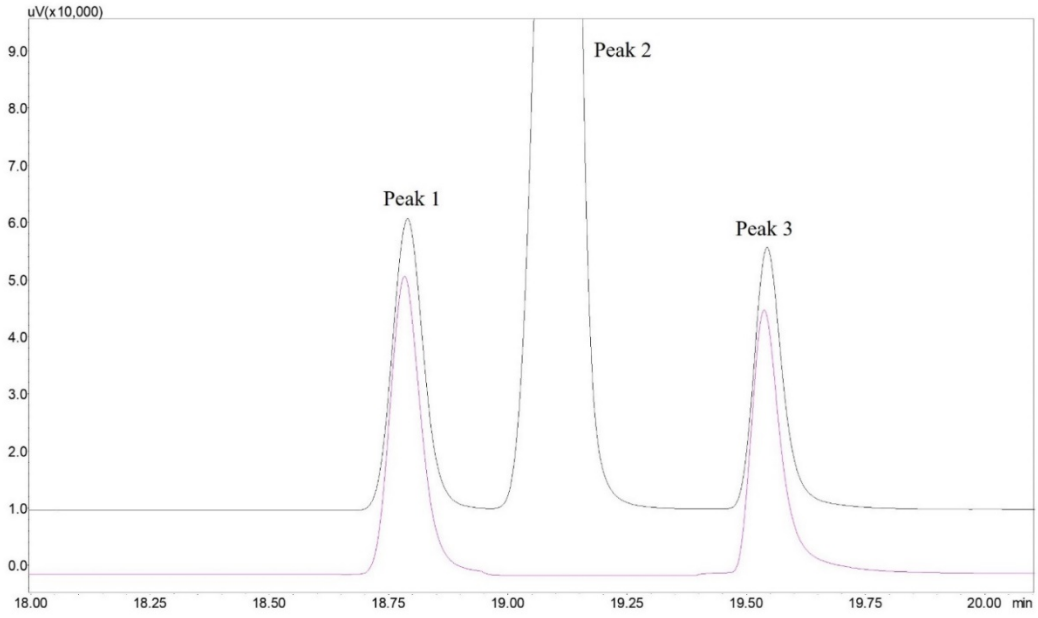

Figure 4.3 Data comparison between 1D st-by analysis (black trace) and 1D cut one (pink trace)

Otherwise, in the case of premature or delayed cuts, more positive or more negative $\delta^{13}C$ values will be obtained with respect to conditions of complete cuts, as visible in Table 4.2.

$\delta^{13}C$ (‰)	5-nonanone	menthol	γ-decalactone
Complete cuts	-27.84	-26.61	-30.05
Premature cuts	-3.58	-14.70	-13.09
Delayed cuts	-57.06	-71.60	-91.28

Table 4.2 $\delta^{13}C$ values comparison among complete cuts, premature cuts and delayed cuts

In the case of anti-doping analysis, GC-C-IRMS is considered one of the preferred techniques to unveil the presence of synthetic hormones in urine. However, several procedures, including liquid-liquid extraction, solid phase extraction and high pressure liquid chromatography (HPLC) clean up, are needed before the injection of the target hormones for GC-C-IRMS analysis. To these aims, Brailsford *et al*., and Casilli *et al*., developed efficient MDGC-C-IRMS systems, able to eliminate the HPLC step, reducing total time analysis [Brailsford 2012, Casilli 2016].

Moving to the field of flavour and fragrances, Sciarrone *et al*., developed a new MDGC-C-IRMS/qMS system [Sciarrone 2018] for the analysis of truffles and truffle based food products (Figure 4.4).

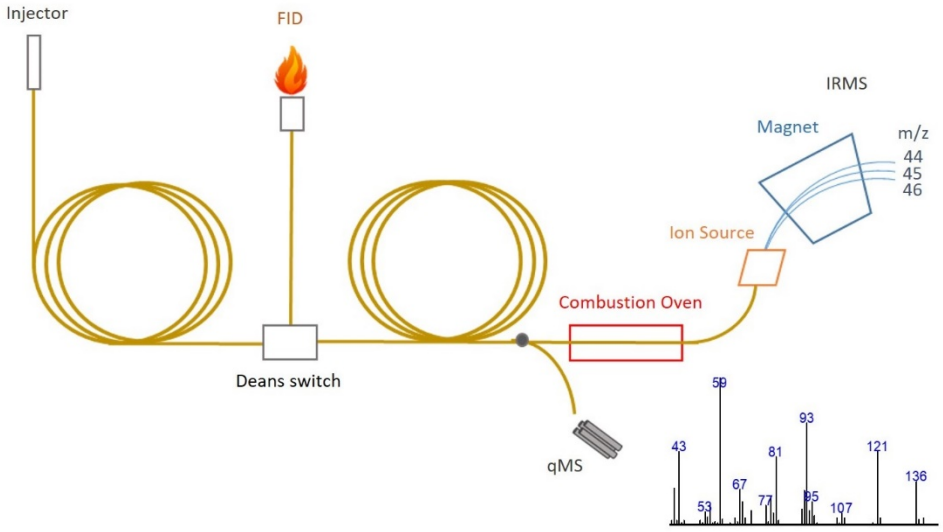

Figure 4.4 Scheme of the MDGC-C-IRMS prototype developed by Sciarrone [Sciarrone 2018]

The system consisted of two GC ovens, equipped with apolar (1D) and ionic liquid stationary phases (2D), and interfaced by means of Deans switch transfer device. In stand-by mode all the analytes were directed to the FID in the 1D, to select a proper cut window to transfer bismethylthiomethane for the 2D detection. With respect to other systems, the flux from the 2D column was split to the IRMS and to a single quadruple MS (qMS). The presence of the qMS allowed to confirm the identity of the peaks transferred from the 1D to the 2D, by comparing MS fragmentation spectra with those recorded in MS spectral fragmentation libraries. Extra-column band broadening has been greatly reduced thanks to the optimization of the microcombustion furnace and to the elimination of the heart-split valve, not necessary in a multidimensional configuration.

The next chapter will deal with a deep comparison between monodimensional and multidimensional C-IRMS systems, and the critical errors in case of co-elutions, in order to highlight even more the need of MDGC systems for the analysis of complex samples.

References

Brailsford, A.D., Gavrilovìc, I., Ansell, R.J., Cowan, D.A., Kicman, A.T., Two-dimensional gas chromatography with heart-cutting for isotope ratio mass spectrometry analysis of steroids in doping control, Drug Test. Anal. 4:12 (2012) 962–969

Casilli, A., Piper, T., Azamor de Oliveira, F., Costa Padilha, M., Pereira, H.M., Thevis, M., de Aquino Neto, F.R., Optimization of an online heart-cutting multidimensional gas chromatography clean- up step for isotopic ratio mass spectrometry and simultaneous quadrupole mass spectrometry measurements of endogenous anabolic steroid in urine, Drug Test. Anal. 8 (2016) 1204–1211

Goodman, K. J., Brenna, J. T. High-precision gas chromatography-combustion isotope ratio mass spectrometry at low signal levels, J. Chromatogr. A 689 (1995) 63 – 68.

Greule, M., Mosandl A. Heptan-2-ol and trans-linalool oxide (fur.) as inherent indicators of natural blackberry flavour using enantioselective and multielement-MDGC-IRMS analysis. Eur Food Res Technol 226:5 (1995) 1001–6.

Harris, S. A., Whiticar, M. J., Eek, M. K. Molecular and isotopic analysis of oils by solid phase microextraction of gasoline range hydrocarbons Org. Geochem. 30 (1999) 721 – 737

Juchelka, D., Beck, T., Dettmar, F., Mosandl. A., Multidimensional gas chromatography coupled on-line with isotope ratio mass spectrometry (MDGC-IRMS). J. High Resolut. Chromatogr. 21 (1998) 145

Li, M., Huang, Y., Obermajer, M., Jiang, C., Snowdon, L.R., Fowler, M.G. Hydrogen isotopic compositions of individual alkanes as a new approach to petroleum correlation: case studies from the Western Canada Sedimentary Basin. Org. Geochem. 32 (2001) 1387–1399.

Matthews, D.E., Hayes, J.M. Isotope-ratio-monitoring gas chromatography-mass spectrometry. Anal Chem 50:11 (1978) 1465–73

Matucha M, Jockisch W, Verner P, Anders G. Isotope effect in gas—liquid chromatography of labelled compounds. J Chromatogr A. 588:1-2 (1991) 251-258

Meier-Augenstein W. The chromatographic side of isotope ratio mass spectrometry – pitfalls and answers. LC.GC. Mag Liquid Gas Chromatogr 15 (1997) 244–253.

Mosandl A. Enantioselective capillary gas chromatography and stable isotope ratio mass spectrometry in the authenticity control of flavors and essential oils. Food Rev Int 11:4 (1995) 597–664.

Nitz, S., Weinreich, B., Drawert, F., Multidimensional Gas Chromatography - Isotope Ratio Mass Spectrometry (MDGC-IRMS). Part A: System Description and Technical Requirements, J. High Resolut. Chromatog. 15:6 (1992) 387-391.

Ponsin, V., Buscheck, E.T., Hunkeler, D.J., Heart-cutting two-dimensional gas chromatography–isotope ratio mass spectrometry analysis of monoaromatic hydrocarbons in complex groundwater and gas-phase samples, J. Chromatogr. A 1492 (2017) 117–128

Putz, M., Piper, T., Casilli, A., de Aquino Neto, F. R., Pigozzo, F., Thevis, M., Development and validation of a multidimensional gas chromatography/combustion/isotope ratio mass spectrometry-based test method for analyzing urinary steroids in doping controls, Anal. Chim. Acta 1030 (2018) 105–114

Sano M, Yotsui Y, Abe H, Sasaki S. A new technique for the detection of metabolites labelled by the isotope 13 C using mass fragmentography. Biomed Mass Spectrom 3:1 (1976) 1–3

Schipilliti L, Dugo G, Santi L, Dugo P, Mondello L. Authentication of bergamot essential oil by gas chromatography-combustion-isotope ratio mass spectrometer (GC-C-IRMS). J Essent Oil Res 23:2 (2011) 60–71.

Sciarrone, D., Schepis, A., Zoccali, M., Donato, P., Vita, F., Creti, D., Alpi, A., Mondello, L., Multidimensional gas chromatography coupled to combustion- isotope ratio mass spectrometry/quadrupole

ms with a low-bleed ionic liquid secondary column for the authentication of truffles and products containing truffle, Anal. Chem. 90 (2018) 6610–6617

Sessions, A.L. Isotope-ratio detection for gas chromatography, J. Sep. Sci. 29 (2006) 1946–1961

Sewenig, S., Bullinger, D., Hener, U., Mosandl, A. Comprehensive authentication of (E)-α(β)-ionone from raspberries, using constant flow MDGC-C/P-IRMS and enantio-MDGC-MS. J Agric Food Chem 53:4 (2005) 838–844.

Tobias, H.J., Sacks, G.L., Zhang, Y., Brenna, J.T. Comprehensive two-dimensional gas chromatography combustion isotope ratio mass spectrometry. Anal Chem 80:22 (2008) 8613–8621

Tobias, H.J., Zhang, Y., Auchus, R.J., Brenna, J.T. Detection of Synthetic Testosterone Use by Novel Comprehensive Two-Dimensional Gas Chromatography Combustion-Isotope Ratio Mass Spectrometry, Anal. Chem. 83 (2011) 7158–7165.

Wang, Y., Huang, Y. Hydrogen isotope fractionation of low molecular weight n-alkanes during progressive vaporization, Org. Geochem. 2001, 32, 991–998.

Zwank, L., Berg, M., Schmidt, T. C., Haderlein, S. B. Compound-specific carbon isotope analysis of volatile organic compounds in the low-microgram per liter range Anal. Chem. 2003, 75, 5575 – 5583.

Chapter 5

Overcoming the lack of reliability associated to monodimensional gas chromatography coupled to isotopic ratio mass spectrometry data by heart-cut two-dimensional gas chromatography

5.1 Introduction

Since the earliest stages of its development, gas chromatography coupled to combustion isotopic ratio mass spectrometry (GC-C-IRMS) has proven to be much suitable to assess the authenticity of natural samples, based on the isotope ratio measurement of different elements of key volatile compounds. To this regard, GC-C-IRMS has been the workhorse in different fields, including environmental, geochemistry, drugs, food and beverage, and flavour and fragrance [Meier Augenstein 1999]. The investigation of key elements, mainly carbon ($^{13}C/^{12}C$), hydrogen (D/H), and nitrogen ($^{15}N/^{14}N$), allowed in many cases to highlight fraudulent practices across a wide range of food, beverages and natural ingredients [Camin 2016]. Among the latter, essential oils have been extensively studied as key components of high economic value in cosmetics and in the food and beverage industry, whose composition and market price may vary greatly, depending on the geographical origin. The increasing demand for "premium quality" products has led to fraudulent actions, aiming to imitate the composition of natural essential oils, mainly in terms of their major volatile constituents. Different techniques have been applied to ascertain the genuineness of essential oils successfully, by the thorough investigation of both the volatile and non-volatile fractions [Cacciola 2017, Do 2015]. However, nowadays more sophisticated adulteration approaches are hardly detected, by these means. GC-MS and GC-FID have been employed successfully to detect the presence of foreign compounds in essential oils, revealing adulterations based on the addition of cheaper oils. Likewise, the presence of synthetic compounds remained undetectable, until investigation of the enantiomeric distribution became feasible [Schmidt 2016]. Soon after the introduction of capillary GC columns equipped with chiral selectors, enantio-selective (Es) GC [Gil Av 1970] has been exploited to unveil fraudulent

additions, through the evaluation of the enantiomeric excess of specific key compounds; later on, multidimensional Es-GC was also implemented by Schomburg *et al.* [Schomburg 1984]. Chiral components in vegetable oils from different sources are characterized by distinctive enantiomeric ratios, as related to the biosynthetic pathway and plant metabolism. Consequently, their addition can be easily revealed down to certain percentages, if reference data are available for the genuine samples. Chiral approaches allowed to easily detect the addition of synthetic compounds such as limonene, linalool and linalyl acetate as racemic mixtures, resulting in final enantiomeric ratios different from those of the original oil [Bonaccorsi 2011]. In this context, extensive work has been carried out by Dugo's research group, who reported the use of different approaches, including GC-FID, GC-MS, Es-GC [Bonaccorsi 2011, Dugo 2012, Bonaccorsi 2012, Schipilliti 2012, Dugo 2010] and GC coupled to combustion-isotope ratio MS [Dugo 2012, Bonaccorsi 2012, Schipilliti 2012], for the analysis of oil volatile fraction. Aiming to make it more and more difficult to highlight the fraudulent addition of chiral compounds from different origins, these components are selected from natural sources with enantiomeric distribution identical or similar to that of the genuine oil. Several chiral compounds extracted from natural sources are available on the market, such as linalool from ho oil, coriander oil or lavandin oil, and linalyl acetate from lavandula [Do 2015]. In these cases, more sophisticated analytical tools are required to give evidence of the characteristic parameters related to the plant origin. The measurement of the $\delta^{13}C$ isotopic value of the volatile fraction by means of GC-C-IRMS is a valid method to assess sample genuineness, delivering highly precise measurements of the major sample components (± 0.01‰–0.2‰) [Meier Augenstein 1999]. Yet, a number of specific problems strictly linked to the operational mode of this technique have severely limited its spreading. Even if data related to GC-C-IRMS are available in literature since the late 70', the feasibility of this approach has been seriously hindered by an insufficient separation of the analytes, originated by the system dead volumes associated to the combustion step. This has in turn resulted in low reliability of the GC-C-IRMS data obtained from unresolved peaks. Unlike other MS approaches where neighbouring compounds, although coeluted, can be still identified by exploiting deconvolution, extracted-ion or tandem-MS approaches, in IRMS detection a partial peak integration would compromise the reliability of the measurement, for the well-known chromatographic isotope effect of CO_2 [Meier Augenstein 1999, Brenna 1997]. A complete separation is thus mandatory since, differently from the cited MS techniques, the $\delta^{13}C$ measurement is thereby achieved after conversion of all organic components to CO_2. To this purpose, the coupling of two (or more) stationary phases, characterized by different selectivities, affords increased separation capabilities for unresolved peaks. In heart-cut two-dimensional GC (HC-MDGC), selected fractions are transferred from a first to a second full-length

column by means of a Deans switch device, whereas in the comprehensive mode only a short column segment is used [Tranchida 2012]. Dealing with HC-MDGC, it is noteworthy that, to the best of our knowledge, very few papers have reported the use of multidimensional separation coupled to IRMS [Nitz 1992, Juchelka 1998, Nara 2006, Brailsford 2012, Casilli 2016, Ponsin 2017, Putz 2018, Sciarrone 2018]. This gives evidence that most research is still being conducted using one-dimensional chromatography. Moreover, most of these works reported the use of MDGC techniques as a mean to accelerate the sample purification procedure and increase the automation of the IRMS processes [Brailsford 2012, Casilli 2016, Putz 2018], while among the others, little insight was made into the causes of wrong $^{13}C/^{12}C$ ratio measurements resulting from peak coelution. The importance of applying a multidimensional separation to enhance the accuracy and precision of isotopic measurements has been highlighted in a limited number of studies [Nitz 1992, Nara 2006, Ponsin 2017, Sciarrone 2018].

This work aims to urge IRMS practitioners to carefully evaluate the reliability of $\delta^{13}C$ data obtained by means of monodimensional GC-C-IRMS, given the likelihood for a few critical issues. Although the detrimental influence of peak co-elutions is well known, this problem appears to have been often underestimated, so far. Hereby, a set of essential oils were selected as model samples, to provide a critical comparison of the reliability of $\delta^{13}C$ data obtained by means of monodimensional GC-C-IRMS, *vs.* MDGC-C-IRMS. In the latter, a Deans switch system already reported in various application by our group [Mondello 2008, Pantò 2015] was employed, for the coupling to a secondary separation column, consisting of polyethylene glycol. Finally, a medium-polarity ionic liquid phase was exploited as secondary column in the MDGC system, with the aim to investigate the influence of the column bleeding on the $\delta^{13}C$ data for late eluted components, thanks to the higher thermal stability with respect to the polyethylene glycol column.

5.2 Materials and methods

5.2.1 Samples and sample preparation

Cold-pressed bergamot essential oil was kindly provided by Capua S.r.l. (Italy), while helichrysum, myrtus and rose essential oil samples were purchased in a local store (Messina, Italy). All the samples were diluted in hexane (1:10, *v/v*) prior to injection into the GC system. C_7-C_{30} *n*-alkane and C_4-C_{24} fatty acid methyl ester mix, used for the calculation of linear retention index (LRI) values were kindly provided by Merck Life Science (Darmstadt, Germany). Indiana mix and iodomethane (Indiana University, Bloomington, IN) were used for the calibration of the $\delta^{13}C$ value of the CO_2 reference gas.

5.2.2 Monodimensional GC-C-IRMS/qMS

The GC-C-IRMS/MS system consisted of an AOC-20i autosampler, a GC2010 Plus gas chromatographer (Shimadzu Europa, Duisburg, Germany), directly connected via a zero dead-volume tee-union to a QP2010 Ultra quadrupole mass spectrometer (Shimadzu Europa, Duisburg, Germany) and to a VisION IRMS system by means of a GC V furnace system (Elementar Analysensysteme GmbH, Langenselbold, Germany) maintained at 850 °C. A split/splitless injector was kept at 280 °C, with a split ratio of 50:1. A capillary SLB-5ms column, 30 m × 0.25 mm i.d. × 0.25 μm d_f (Merck Life Science, Darmstadt, Germany) was operated at a constant flow rate of carrier gas (helium) of 1 mL/min. The GC oven temperature was ramped as follows: 50 °C to 220 °C at 3 °C/min, and then to 300 °C at 20 °C/min. The gas stream from the GC column outlet was splitted through a zero dead-volume tee-union (Valco) to the combustion chamber and afterwards to the IRMS and to the qMS system in the ratio 10:1, via a 0.85 m × 0.25 mm i.d. and a 1.5 m × 0.1 mm i.d. uncoated column, respectively. The qMS ion source and interface temperature were maintained at 200 °C and 250 °C, respectively, and a mass range of 40-400 *m/z* was monitored at 10 Hz of an acquisition speed. GCMS data were acquired by the GCMS solution software ver. 4 (Shimadzu Europa, Duisburg, Germany). The separated compounds were identified by searching their qMS spectra against the FFNSC 4.0 mass spectral library database (Shimadzu Europa, Duisburg, Germany), using a double filter based on the spectral similarity results and Linear Retention Index (LRI) values. The VisION IRMS (Elementar Analysensysteme GmbH, Langenselbold, Germany) was a bench top 5 kV system equipped with an integrated gas delivery monitoring system. The combustion chamber was equipped with a high performing silicon carbide tube furnace for the quantitative, fractionation-free conversion of the delivered compounds to pure gases (CO_2 and H_2O). The CO_2 produced by combustion of each component was transferred to the IRMS, while the water produced was removed through a nafion membrane. The following settings were applied to the VisION system: acceleration voltage, 3789.907 V; trap current, 600.000 μA; magnet current, 3700.000 mA. IRMS data were handled by the IonOS stable isotope data processing software ver. 4.4.3.9348 (Elementar Analysensysteme GmbH, Langenselbold, Germany).

5.2.3 Multidimensional GC-C-IRMS/qMS

The MDGC-C-IRMS/qMS prototype configuration was the same adopted for a previous research from our group [Sciarrone 2018]. Two GC-2010 Plus gas chromatographs (defined as GC1 and GC2) were connected by means of a heated transfer line (Shimadzu Europa, Duisburg, Germany). GC1 was equipped with a Deans-switch (DS) transfer device, connected to an APC unit, which

supplied the same carrier gas (He) (Shimadzu Europa, Duisburg, Germany) allowing to divert the first column eluent to the FID or to the second column in GC2. The split/splitless injector was maintained at 280 °C, with a split ratio of 10:1. A capillary SLB-5ms column, 30 m × 0.25 mm i.d. × 0.25 μm d_f (Merck Life Science, Darmstadt, Germany) was operated at a constant flow rate of carrier gas (helium) at 2.4 mL/min: a pressure programme was used from 185 to 330.0 kPa at 1.71 kPa/min. GC1 oven temperature was ramped as follows: 50 °C to 220 °C at 3 °C/min, and then to 300 °C at 20 °C/min. The FID (330 °C; H_2 flow, 40.0 mL/ min; air flow rate, 400 mL/min; sampling rate, 80 ms equal to 12.5 Hz) was connected to the DS device via a 0.25 m × 0.18 mm i.d. stainless steel uncoated column and used to monitor the first column eluent. GC2 was equipped alternatively with a SUPELCOWAX 10 column, 30 m × 0.25 mm i.d. × 0.25 μm d_f or a SLB-IL60i column, 30 m × 0.25 mm i.d. × 0.20 μm d_f (Merck Life Science, Darmstadt, Germany), operated under the following temperature program: 50 °C (hold for 10 min) to 240 °C at 3 °C/min. GC2 was connected on one side to the DS device while on the other side a T-union was used to split the effluent to the qMS and C-IRMS systems (as in the monodimensional applications). A pressure program was applied to the APC unit to maintain the carrier gas flow rate constant also in the second column (1 mL/min): 140 kPa to 189 kPa at 1.35 kPa/min, and to a final pressure of 265 kPa at 6.61 kPa/min. The qMS and C-IRMS conditions were the same as in the monodimensional configuration. Apart for the IRMS, all data were acquired by the MDGC solution control software package (Shimadzu Europa, Duisburg, Germany) allowing for setting up the DS device parameters and to monitor both the GC1 (FID) and GC2 (qMS), simultaneously.

5.3 Results and Discussion

Reliability of the data obtained in the presence of coeluted components was evaluated, for different samples, and the extent to which such co-elutions affected the measured $\delta^{13}C$ values was assessed. Apart from the insufficient separation resulting from the sample complexity, several specific problems were taken into account, severely hampering the usefulness of this technique. Although the coupling of IRMS to GC by means of a combustion furnace was readily recognized as a powerful approach toward the assessment of sample genuineness, yet this technique has traditionally suffered from several limitations/drawbacks inherent to the characteristics of the single techniques employed. Possible sources of potential errors may be envisaged in natural isotopic abundances, chromatographic effects, and issues related to analytes conversion to CO_2 prior to IRMS measurement.

5.3.1 Natural isotopic abundances

Attention must be paid in GC-C-IRMS applications, especially when dealing with natural samples, which are often characterized by a medium to high complexity and, moreover, by the presence of compounds in a wide concentration range. The sample amount to be injected should be carefully chosen trying to compromise between the desired sensitivity and the column capacity, i.e., trying to attain good sensitivity for the trace components, while at the same time avoiding overloading the chromatographic column with respect to the most abundant sample constituents. In this concern, it is furthermore crucial not to introduce insufficient quantities of analytes, in view of the reduced sensitivity of the technique. In fact, much higher detection limits than those observed with other MS techniques are encountered in IRMS, due to an approximately 100 times lower natural relative abundance of ^{13}C compared to that of ^{12}C. To this concern, a low chromatographic efficiency caused by dead volumes in the system, resulting in a lower signal-to-noise ratio, will affect the sensitivity of IRMS to even a higher extent, in comparison with other detection approaches.

5.3.2 Chromatographic effects

In the case of carbon isotopes measurement, a significant variation is observed in the ratio between ^{13}C and ^{12}C along the entire chromatographic peak, where higher amounts of ^{13}C and ^{12}C can be found in the first and in the last part of the peak, respectively. These differences are caused by the fact that species which are richest in the heavier isotope result in stronger C-C bond, and thus tend to elute in the first part (front) of a peak, while the peak tail will contain molecules with higher amounts of the lighter isotope having weaker C-C bond. Furthermore, the background ion current can influence the determination of the correct isotope ratio values significantly, especially for low concentrated components (low signal-to-noise ratio). Under ideal conditions, acceptable standard deviation values of ± 0.1‰ for signals of sufficient intensity are typical, increasing to about ± 0.5‰ for signals close to 0.5-1 nA intensity [Ricci 1994]. It is therefore evident that, especially in the presence of analytes at small amounts, the precision of the measurements can be much affected by fluctuations above the accepted value of ± 0.5‰. This could lead to difficulties in discriminating between the same analytes of different origin, often characterized by small differences in the isotope ratio values measured.

5.3.3 Analytes conversion to CO_2

From the IRMS standpoint, on-line combustion of the analytes to CO_2 is necessary before reaching the mass spectrometer, for measurement of the isotope ratio between *m/z* 44, relative to $^{12}CO_2$, and

m/z 45 of $^{13}CO_2$. This step eliminates any qualitative information about the species from which the CO_2 is generated. It will be impossible to assess the origin of CO_2 produced by combustion of two or more compounds which are not (or not completely) separated by the chromatography, resulting in the incorrect evaluation of the isotope ratio. Specifically, three cases may occur: if the coelution affects the front of the peak, a depletion of the ^{13}C value will be observed, due to its higher concentration in this area, causing the measurement of a more negative value. In the opposite situation, i.e. for coelution occurring at the peak tail, a depletion of ^{12}C will result in the measurement of more positive values. A third case can arise if the peak of interest is completely coeluted: such an occurrence will be not evidenced, unless CO_2 ratio differentiation is used, with consequent impossibility of rectifying the isotope ratio value. Because of the foregoing, a complete separation of the peak before its conversion to CO_2 and its complete integration, from base-to-base level, is mandatory requirement to avoid errors arising from chromatographic isotope fractionation [Meier Augenstein 1999, Brenna 1997, Ricci 1994].

5.3.4 Column bleed

When high-boiling compounds are investigated, attention must be paid to the presence of column bleed because of stationary phase release at the higher temperatures. While apolar stationary phases are characterized by high thermal stability and low bleed, more polar stationary phases suffer from lower thermal stability, and this often leads to a pronounced bleeding effect. In this situation, the additional CO_2 produced by the combustion of the stationary phase will affect the $\delta^{13}C$ data measured, especially for low-concentrated components. Nowadays, low-bleed stationary phases based on room temperature ionic liquids (RTILs) are available, characterized by polarity comparable to that of polyethylene glycol (SLB-IL60i) phases, but with a different selectivity. These columns thus represent a viable separation alternative, in cases where additional resolution is required [Ragonese 2011, Anderson 2005].

5.3.5 Monodimensional vs MDGC-C-IRMS analysis

Essential oil samples of bergamot (*Citrus bergamia* Risso & Poiteau), helichrysum (*Helichrysum italicum* (Roth) G. Don), myrtus (*Myrtus communis* L.) and rose oil (*Rosa damascena* Mill.) were analysed in monodimensional and multidimensional conditions. Given the lack of identification capability in IRMS detection, due to the conversion of the organic molecules to CO_2, the GC effluent was splitted between the IRMS and a qMS detector. In monodimensional applications, identification was achieved using a commercial MS database and applying a double filter, consisting of minimum spectral similarity and a LRI tolerance window. The GCMS software

automatically calculated LRIs for the compounds of interest referring to C_7-C_{30} alkanes homologous series analysed under the same chromatographic conditions.

In multidimensional separations, since MS detection was available only after the second dimension, in order to correctly identify and then to determine a cut window for each component of interest, LRI values were calculated according to the ^{1}D stand-by analysis (FID) retention times after the injection of a homologous alkane series. Heart-cuts windows corresponding to +/- 5 LRI units were then selected for each component of interest. In fact, since an apolar stationary phase was exploited as first dimension GC column, it is well known that a high repeatability of +/- 5 LRI units must be expected for each component on this stationary phase [Ragonese 2011]. According to the different peak widths, the LRI units (cut windows) were enlarged to fit the wider chromatographic bands. After the ^{2}D separation, the qMS spectra acquired were first filtered according to a minimum spectral similarity of 90% within the MS database, and afterwards selected because of the LRI values, according to the ^{1}D separation.

In a first step, all the samples were subjected to conventional GC-C-IRMS analyses. The need to use a combustion furnace introduces dead volumes into the system, affecting the chromatographic separation negatively; to this concern particular precautions need to be taken, to minimize these phenomena. In the system here described the use of a high-performance silicon carbide tubular furnace with a small internal diameter allowed to limit the loss of efficiency as well as to preserve the chromatographic resolution. The high efficiency separation of a bergamot essential oil sample (see Figure 5.1) showed no significant peak broadening in the resulting GC-C-IRMS chromatogram.

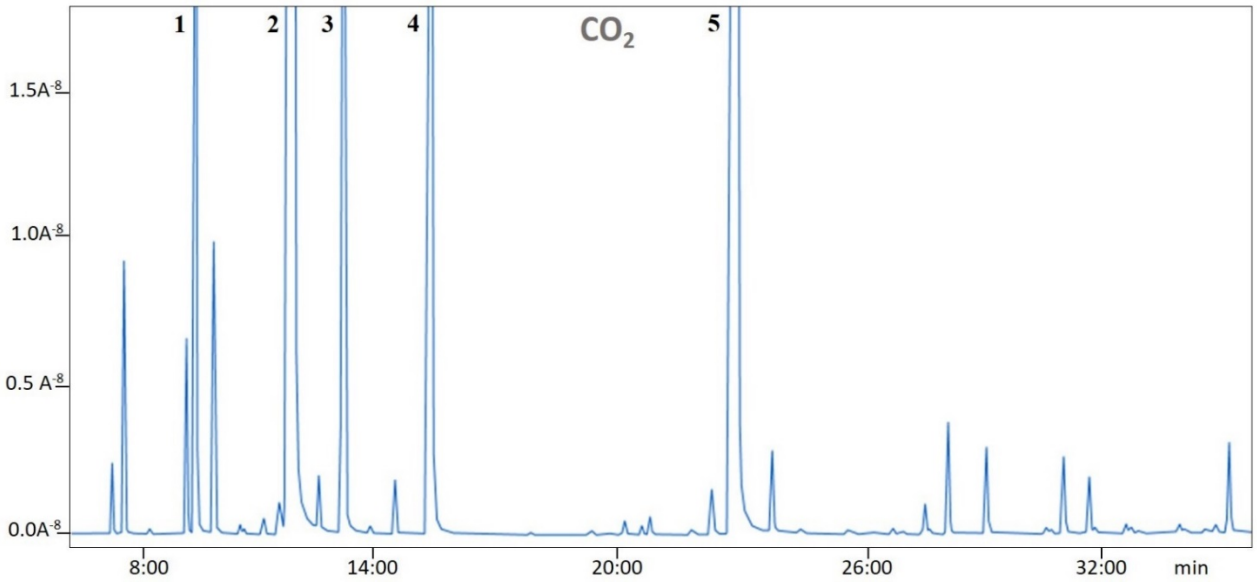

Figure 5.1 Monodimensional GC-C-IRMS chromatogram of a bergamot essential oil sample. For peak ID, refer to Table 5.1.

In this case, even if the composition of the bergamot essential oil includes a high number of components, their almost homogenous distribution along the chromatographic space allows in most cases for a satisfactory separation to be achieved by a monodimensional approach. The absence of significant chromatographic co-elutions, which in turn would affect the accurate estimation of the $\delta^{13}C$ values of the sample components, is reflected in the data listed in Table 5.1.

ID	*Target compound*	*GC-C-IRMS*		*MDGC-C-IRMS*	
		$\delta^{13}C$	**Std. dev**	**$\delta^{13}C$**	**Std. dev**
1	β-Pinene	-29.21	0.21	-29.14	0.20
2	Limonene	-29.00	0.20	-28.94	0.13
3	γ-Terpinene	-30.60	0.12	-31.12	0.11
4	Linalool	-28.70	0.10	-28.97	0.10
5	Linalyl acetate	-29.26	0.24	-29.02	0.12

Table 5.1 Comparison of the $\delta^{13}C$ data obtained for the main terpene constituents of a bergamot essential oil sample, analysed by conventional GC-C-IRMS and by MDGC-C-IRMS (average of three replicates and standard deviations).

A nice correspondence was thus evidenced between the $\delta^{13}C$ values measured after monodimensional GC separation and those obtained after multidimensional separation of the bergamot oil components. While the effectiveness of a conventional GC separation is evident in such situations, on the other hand, unpredictable sources of variations in the chromatographic profile make the employment of multidimensional GC separation highly recommendable. Variations of peak relative amounts may be observed in samples obtained in different harvesting periods, and this could generate unexpected coelutions. Similarly, the formation of oxidation products may occur, leading to additional peak components in the samples, depending on the different storage conditions and sample ageing. The latter would ultimately affect reliability of the $\delta^{13}C$ values measured for the sample components. In other critical separations chosen as case studies, different elution regions of the monodimensional chromatograms were selected for a deeper study under multidimensional conditions. For a summary of the results from data comparison later discussed, the reader is referred to Table 5.2.

Sample	*ID*	*Target compound*	*GC-C-IRMS*		*MDGC-C-IRMS*	
			^{1}D LRI	**δ^{13}C**	**^{2}D LRI$_{FAMEs}$**	**δ^{13}C**
***Myrtus Communis* L.** (Figure 1)	1	α-Terpineol	1195	-27.22	1099	-31.24
	2	Myrtenol	1202	-43.52	1191	-30.21
***Helichrysum italicum* Roth** (Figure 2)	1	Limonene	1030	-32.29	608	-32.36
	2	α-Copaene	1375	-30.20	898	-31.30
	3	Geranyl acetate	1380	-37.33	1159	-33.34
	4	β-Caryophyllene	1424	-31.08	996	-30.81
	5	*trans*-α-Bergamotene	1432	-11.07	985	-33.23
	6	trimethyl-dec-en-dione	1434	-41.92	1289	-29.89
	7	Selina-4,11-diene	1476	-27.39	1076	-30.22
	8	γ-Curcumene	1480	-29.75	1090	-30.04
	9	α-Curcumene	1482	-37.92	1173	-33.20
***Rosa Damascena* Mill.** (Figure 3)	1	Limonene	1030	-27.72	608	-28.55
	2	Eucalyptol	1032	-32.78	614	-29.60
	3	Nerol	1229	n.d.	1189	-26.28
	4	Citronellol	1232	-27.02	1166	-27.24
	5	Geraniol	1255	-24.83	1232	-25.15

Table 5.2 Comparison of the δ^{13}C data obtained for selected constituents of *Myrthus Communis* L., *Helichrysum italicum* Roth and *Rosa Damascena* Mill essential oil samples, analysed by conventional GC-C-IRMS and by MDGC-C-IRMS. Linear retention indices are reported, relative to an apolar (5%) stationary phase for the monodimensional application, and to a polar (wax) stationary phase, used as secondary column in the multidimensional applications (n.d.: not detected).

The first critical case investigated was myrtus (*Myrtus communis* L.) essential oil (Figure 5.2). As in the case of bergamot essential oil, a high number of components were present, but in this sample, the resolution capability of monodimensional GC was insufficient*, e.g.* in the case of α-terpineol (peak 1) and myrtenol (peak 2), as can be clearly seen in Figure 5.2A.

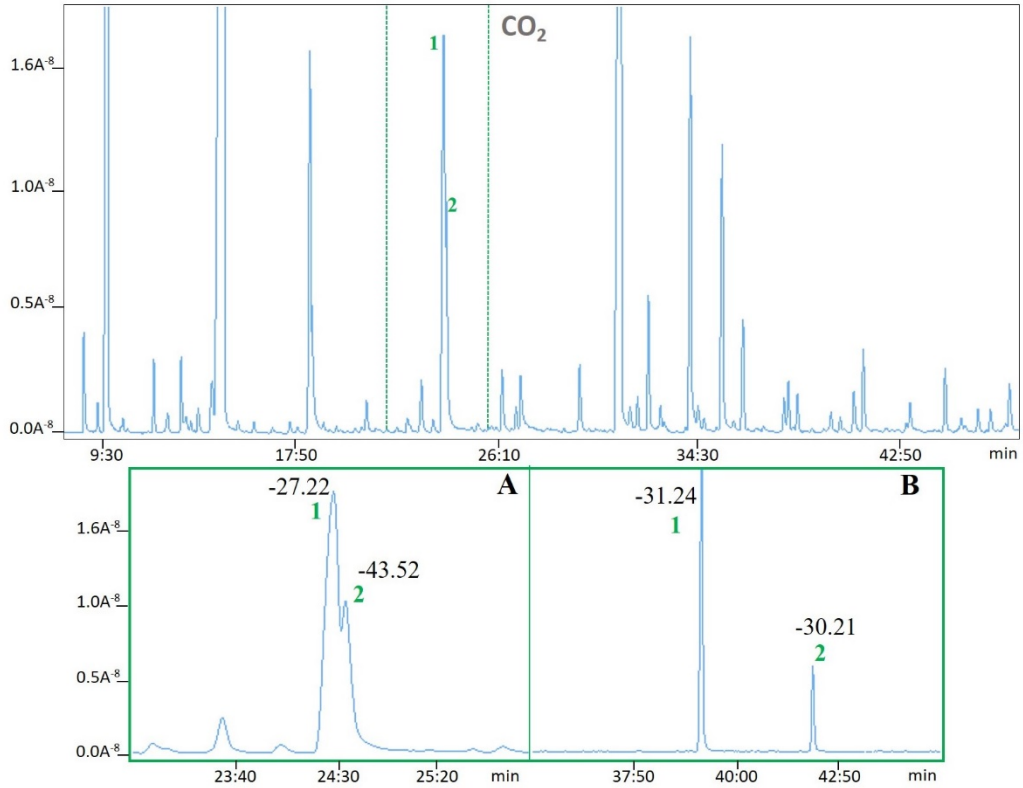

Figure 5.2 *Myrtus Communis* L. essential oil GC-C-IRMS chromatogram (upper trace) with zoomed regions showing monodimensional (A) and multidimensional GC separation (B) of two compounds. Peak IDs: (1) α-terpineol, (2) myrtenol.

These two compounds were characterized by slight differences in LRIs on the first dimension (apolar) column (1195 *vs* 1202), resulting in an insufficient chromatographic resolution. Comparing the $\delta^{13}C$ values measured after a conventional GC approach with those obtained after multidimensional GC separation (Figure 5.2B) (see Table 5.2), a significant shift of the isotope values measured was observed for both peaks, related to the incomplete separation achieved in a monodimensional GC separation. In the MDGC approach, the use of a more polar stationary phase as the second separation dimension afforded additional selectivity, as it was predictable from the LRI values known for polar phases. As for the latter, LRI values are generally calculated against a fatty acid methyl ester homologue series (FAMEs), in place of the *n*-alkane mixture used for apolar stationary phases. The higher difference in LRI_{FAMEs} on the secondary column (*viz*, 1099 *vs* 1191) finally led to the baseline resolution of the two compounds. As a consequence, the $\delta^{13}C$ value measured for α-terpineol changed from -27.22‰ in monodimensional GC to -31.24‰ in multidimensional GC, while for myrtenol the same values were -43.52‰ and -30.21‰, respectively (see Table 5.2). A second critical case investigated was Helichrysum (*Helichrysum italicum* Roth) essential oil. The overall sample composition was mainly represented by

oxygenated monoterpenes (≈ 50%) and sesquiterpenes (≈ 15%), eluting in a limited chromatographic space. As showed in Figure 5.3, different critical couples resulted from the monodimensional GC-C-IRMS separation.

As for limonene (peak 1: Figure 5.3 - IA), since it eluted in the early part of the chromatogram where few terpenes were present, it was sufficiently separated in the monodimensional approach, and its $\delta^{13}C$ value (-32.29‰) was practically the same to the one measured in multidimensional conditions (Figure 5.3 - IB), where a $\delta^{13}C$ value of -32.36‰ was obtained. On the contrary, moving further in the chromatogram to the busiest zone, it is clear that different co-elutions arose.

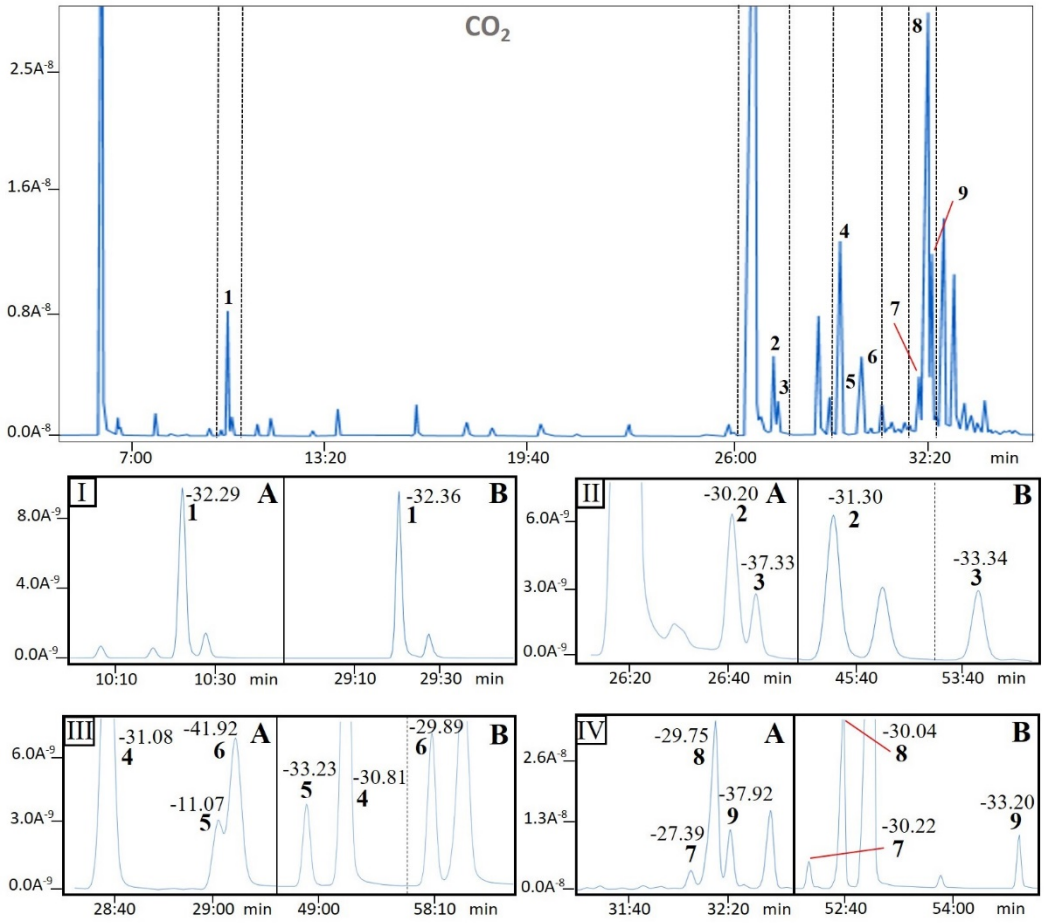

Figure 5.3 *Helichrysum italicum* (Roth) G. Don essential oil GC-C-IRMS chromatogram (centre trace) with zoomed regions showing monodimensional separation (A) and the same zone separated by multidimensional GC (B). Peak IDs: (1) limonene, (2) α-copaene, (3) geranyl acetate, (4) β-caryophyllene, (5) *trans*-α-bergamotene, (6) trimethyl-dec-en-dione, (7) selinadiene, (8) γ-curcumene, (9) α-curcumene.

As predictable, for all the compounds investigated in this crowded part of the chromatogram, a multidimensional approach was highly beneficial in terms of separation, affording much higher

resolution compared to the monodimensional analysis. Although the separation between α-copaene (peak 2) and geranyl acetate (peak 3) obtained by monodimensional GC (Figure 5.3 - IIA) apparently was not affected by a significant coelution, yet the comparison of their $\delta^{13}C$ values with those achieved by multidimensional GC (Figure 5.3 – IIB) showed shifted values, according to the mechanisms discussed earlier. In fact, the $\delta^{13}C$ value for α-copaene was slightly more positive (-30.20‰ *vs* -31.30‰) because of the coelution occurring at the right end of the peak. However, the variation was rather small, probably due to the lower amount of the compound eluted as the next peak. The situation was exactly the opposite for geranyl acetate, for which an important $\delta^{13}C$ value shift was measured, when comparing the monodimensional and multidimensional approaches, *viz*. -37.33‰ *vs* -33.34‰. In this case, a significantly more negative $\delta^{13}C$ value was obtained in monodimensional GC, since the left-end of the peak was affected by coelution with a higher amount of compound from the previous peak. A comparison of the $\delta^{13}C$ values obtained for β-caryophyllene (peak 4), eluted as a pure peak in both approaches (Figure 5.3 – IIIA and B), showed very similar values (-31.08‰ *vs* -30.81‰). Likewise, an important coelution occurred in the monodimensional GC separation between *trans*-α-bergamotene (peak 5, LRI 1432) and trimethyl-dec-en-dione (peak 6, LRI 1434), with strong variations attained for $\delta^{13}C$ values of the coeluted peaks, accordingly. An undoubtedly highly positive $\delta^{13}C$ value of -11.07‰ was measured for *trans*-α-bergamotene, with respect to a $\delta^{13}C$ value of -33.23‰ after baseline separation by MDGC (Figure 3 – IIIA and B). The same coelution generated an opposite result for trimethyl-dec-en-dione, whose $\delta^{13}C$ values changed from -41.92‰ when partially co-eluted, to -29.89‰ when completely separated by MDGC, as a result of the different selectivity of the polar column (LRI_{FAMEs} differing by around 300 units, *viz*. 985 *vs* 1289). A further example illustrated for this sample regards selinadiene (peak 7), γ-curcumene (peak 8) and α-curcumene (peak 9). Also in these cases, the $\delta^{13}C$ values measured after monodimensional GC (Figure 2 - IVA) were different with respect to those obtained by MDGC measurements (Figure 5.3 - IVB), as a result of the isotopic effect discussed earlier arising from incomplete peak separations. In fact, only few LRI units spaced the three components on the apolar column, namely 4 LRI units between selinadiene and γ-curcumene (1476 *vs* 1480), and 2 LRI units between γ-curcumene and α-curcumene (1480 *vs* 1482). The coupling of a polar secondary column in MDGC resulted in improved separation and increased LRI_{FAMEs} differential, namely 14 LRI units between selina-4, 11-diene and γ-curcumene (1076 *vs* 1090), and 83 LRI_{FAMEs} units between γ-curcumene and α-curcumene (1090 *vs* 1173). The respective $\delta^{13}C$ values in monodimensional and MDGC were as follows: -27.39‰ *vs* -30.22‰ for selina-4, 11-diene, -29.75‰ *vs* -30.04‰ for γ-curcumene (the highest abundant

component, and thus the less affected by other interferences), and -37.92‰ *vs* -33.20‰ for α-curcumene.

Another sample investigated was *Rosa damascena* Mill. essential oil, illustrated in Figure 5.4. The first critical pair is represented by limonene and eucalyptol, which on the apolar column are closely eluted peaks as reflected in their similar LRIs, *viz*. 1030 and 1032. Depending on the relative amount of each component in a given sample, these two terpenes may be coeluted; such evidence usually occurs in Citrus essential oils. In the Rosa oil, even if only a tiny coelution was observed for these two components, shifted values were again observed when comparing the $\delta^{13}C$ measurements: limonene (peak 1, Figure 5.4 - IA) $\delta^{13}C$ value was slightly more positive in monodimensional GC (-27.72‰) with respect to MDGC (Figure 5.4 - IB) (-28.55‰). Likewise, an important variation was observed for eucalyptol (peak 2), with a more negative value in monodimensional GC, due to the coelution of the left-end of the peak with a higher concentrated component (-32.78‰ vs -29.60‰). The most important case to be highlighted is related to nerol (peak 3) and citronellol (peak 4), a similar situation to the limonene-eucalyptol case, with an LRI difference of only three units on an apolar phase (1229 *vs* 1232).

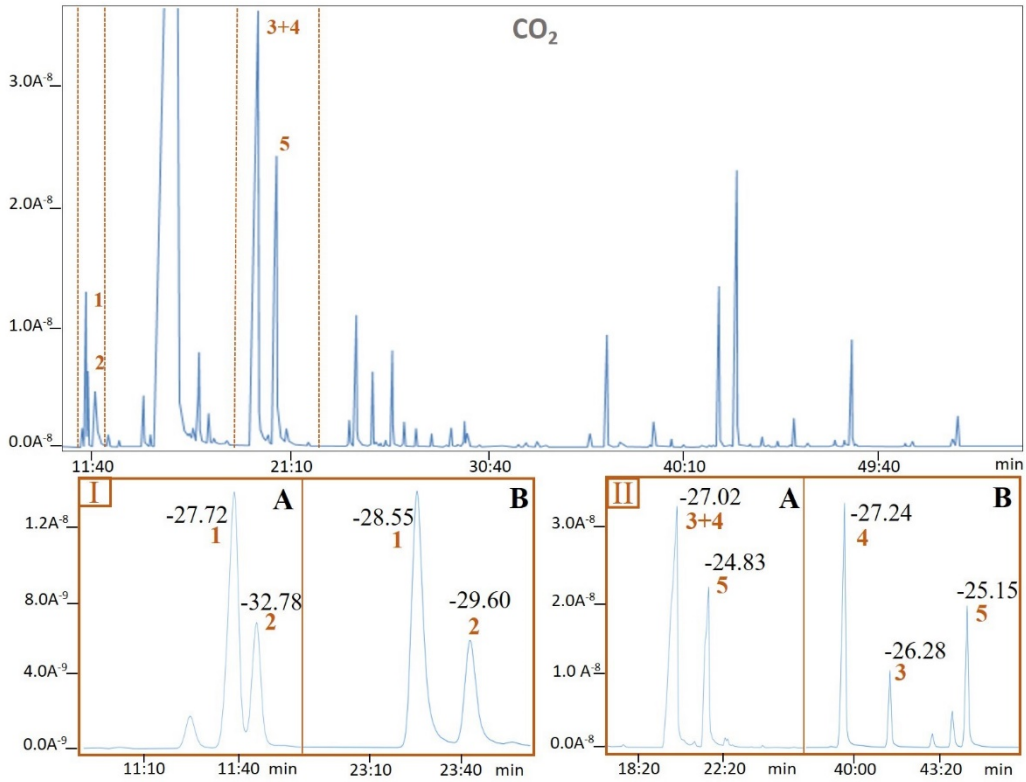

Figure 5.4 *Rosa damascena* Mill. essential oil GC-C-IRMS chromatogram (centre trace) with zoomed regions showing mono (A) and relative separation after multidimensional GC (B). Peak IDs: (1) limonene, (2) eucalyptol, (3) nerol, (4) citronellol, (5) geraniol.

Differently from the previous case where low concentrated components were investigated (> 1%), citronellol represents one of the major sample components (≈ 10%), and this resulted in the complete coelution with the close-eluted nerol peak; a $\delta^{13}C$ value of -27.02‰ was obtained (Figure 5.4 - IIA). Such a value would be regarded as a correct estimation, being compatible with C_3 plants $\delta^{13}C$ values, since the shape of the peak did not suggest the presence of a coelution, and moreover no qualitative information was available, due to the oxidation of all the components to CO_2. Thus, this can be regarded as the worst situation to be faced when dealing with a GC-C-IRMS investigation, in which the analyst is prone to a wrong estimation of the $\delta^{13}C$ values, caused by the limitations of the monodimensional GC approach.

The potential and usefulness of a multidimensional GC-C-IRMS approach is more evident in such situations. As showed in Figure 5.4 - IIB, nerol and citronellol were baseline separated by MDGC with an inverted elution order with respect to the ^1D apolar phase, with LRI_{FAMEs} of 1189 and 1166 on the polar secondary column, respectively. As for their $\delta^{13}C$ value measurements, a value of -27.24‰ was obtained for citronellol, the major sample component, much similar to the value of -27.02‰ attained in monodimensional GC. Likewise, a value of -26.28‰ was obtained for nerol, being purified only after separation on the ^2D column. Also, for the next eluted peak geraniol (peak 5), the MDGC approach allowed for more accurate measurement of the $\delta^{13}C$ value, namely -25.15‰ *vs* -24.83‰ (MDGC *vs* monodimensional GC). A last case involved the investigation of a higher boiling point analyte, namely nootkatone. Due to the higher eluting temperature, when a medium polarity stationary phase is employed as secondary column in a multidimensional column set, the $\delta^{13}C$ measurement would be affected by the stationary phase release, an effect commonly known as column bleed, causing an increased base line noise. The consequent production of CO_2, due to the combustion step, then generates a possible source of error for the evaluation of components eluting in this retention zone. Room temperature ionic liquids (RTILs) have been recently introduced as GC stationary phases, characterized by higher thermal stability compared to stationary phases with same polarity degree [Ragonese 2011, Anderson 2005]. Aiming to evaluate the influence of column bleed, an ionic liquid-based stationary phase (SLB-IL60i) with a similar polarity degree was exploited as an alternative to the polyethylene glycol secondary column. Figure 5.5 shows the superimposed chromatograms relative to the ^2D elution of the nootkatone peak. A remarkable bleeding effect is evident for the polyethylene glycol column, while with the SLB-IL60i an almost flat baseline was observed. Concerning the $\delta^{13}C$ measurement, a more negative value was obtained when using the polyethylene glycol column, with respect to that achieved on the ionic liquid stationary phase (-33.64‰ *vs* -32.80‰). Such a result suggests an influence of the different noise level present during the combustion of

nootkatone before IRMS detection. In the light of this evidences, the use of a low-bleed column is advisable for compounds which are eluted at high temperatures from a medium-polarity stationary phase.

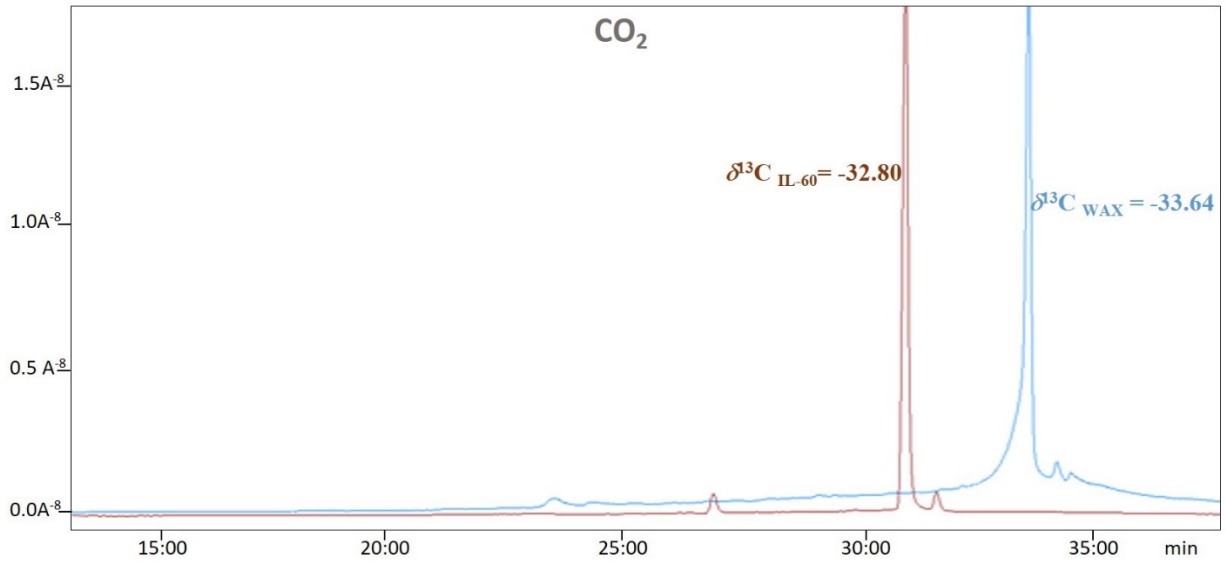

Figure 5.5 Elution of nootkatone on polyethylene glycole (blue trace) and ionic liquid (brown trace) stationary phase used as secondary columns in MDGC-C-IRMS experiments. Bleeding observed at >200 °C column temperature.

5.4 Conclusions

The present research highlighted the common limitations to be faced when dealing with the isotopic ratio evaluation of volatile components separated by gas chromatography. The sample complexity plays a fundamental role in GC-C-IRMS, but unlike what is common in other techniques, where the concept of complexity is commonly associated to a high number of components in a sample, in this technique complexity is rather linked to the presence of highly crowded areas of the chromatogram, rather than to the number of components. In general, any type of co-elution should be avoided since no correction factors can be applied. Insufficient selectivity rather than column overloading effects can lead to incomplete separation, with consequent incorrect measurement of the isotope ratio of the analytes. In addition to cases in which clear co-elutions are known, for which the advantage of using the multidimensional technique is evident, also unpredictable co-elutions may occur, occasionally generated by oxidative compounds or by compounds added for fraudulent practices. In this context, multidimensional chromatography appears to be of fundamental importance to prevent the aforementioned problems and finally aiming to guarantee accurate results. As with other techniques for which an MDGC approach has

made it possible to overcome separation problems (such as GC-FID or enantio-GC), or to simplify the work required of a mass spectrometer, also in GC-C-IRMS it is evident that multidimensional separations play a pivotal and essential role. While, in the past, this technique could have appeared complex and at the exclusive use of highly specialized personnel, nowadays, thanks to software automation of the heart-cut devices, and their wide diffusion in research and quality control laboratories, there is no reason for any IRMS analysis to be left exposed to any of the risks described, when coupled to monodimensional GC separation.

References

Anderson, J.L., Armstrong, D.W. Immobilized ionic liquids as high-selectivity/high-temperature/high-stability gas chromatography stationary phases, Anal. Chem. 77 (2005) 6453-6462.

Bonaccorsi, I., Sciarrone, D., Cotroneo, A., Mondello, L., Dugo, P., Dugo, G. Enantiomeric distribution of key volatile components in Citrus essential oils, RBF 21:5 (2011) 841-849.

Bonaccorsi, I., Sciarrone, D., Schipilliti, L., Dugo, P., Mondello, L., Dugo, G. Multidimensional Enantio Gas Chromatography/Mass Spectrometry and Gas Chromatography-Combustion-Isotopic Ratio Mass Spectrometry for the Authenticity Assessment of Lime Essential Oils (C. aurantifolia Swingle and C. latifolia Tanaka), J. Chromatogr. A 1226 (2012) 87-95.

Brailsford, A.D., Gavrilovìc, I., Ansell, R.J., Cowan, D.A., Kicman, A.T., Two-dimensional gas chromatography with heart-cutting for isotope ratio mass spectrometry analysis of steroids in doping control, Drug Test. Anal. 4:12 (2012) 962–969

Brenna, J.T., Corso, T.N., Tobias, H.J., Caimi, R.J. High-Precision Continuous-Flow Isotope Ratio Mass Spectrometry, Mass Spectrom. Rev. 16 (1997) 227–258

Cacciola, F., Donato, P., Sciarrone, D., Dugo, P., Mondello, L. Comprehensive Liquid Chromatography and Other Liquid-Based Comprehensive Techniques Coupled to Mass Spectrometry in Food Analysis, Anal. Chem. 89 (2017) 414-429.

Camin, F., Bontempo, L., Perini, M., Piasentier, E. Stable Isotope Ratio Analysis for Assessing the Authenticity of Food of Animal Origin, Compr. Rev. Food Sci. Food Saf. 15:5 (2016) 868−77.

Casilli, A., Piper, T., Azamor de Oliveira, F., Costa Padilha, M., Pereira, H.M., Thevis, M., de Aquino Neto, F.R., Optimization of an online heart-cutting multidimensional gas chromatography clean- up step for isotopic ratio mass spectrometry and simultaneous quadrupole mass spectrometry measurements of endogenous anabolic steroid in urine, Drug Test. Anal. 8 (2016) 1204–1211

Do, T.K.T., Hadji-Minaglou, F., Antoniotti, S., Fernandez, X. Authenticity of essential oils, Trends Anal. Chem. 66 (2015) 146–157.

Dugo, G., Bonaccorsi, I., Sciarrone, D., Schipilliti, L., Russo, M., Cotroneo, A., Dugo, P., Mondello, L., Raymo, V. Characterization of cold-pressed and processed bergamot oils by using GC-FID, GC-MS, GC-C-IRMS, enantio-GC, MDGC, HPLC and HPLC-MS-IT-TOF, J. Essent. Oil Res. 24:2 (2012) 93-117.

Dugo, P., Ragonese, C., Russo, M., Sciarrone, D., Santi, L., Cotroneo, A., Mondello, L. Sicilian Lemon Oil: Composition of Volatile and Oxygen Heterocyclic Fractions and Enantiomeric Distribution of Volatile Components, J. Sep. Sci. 33 (2010) 3374-3385.

Gil-Av, E., Korman R. Z., Weinstein, S. Gas chromatographic determination of the configuration of alanine and serine in staphylococcal cell walls, Biochim. Biophys. Acta, 211 (1970) 101.

Meier-Augenstein W. The chromatographic side of isotope ratio mass spectrometry – pitfalls and answers. LC.GC. Mag Liquid Gas Chromatogr 15 (1997) 244–253.

Mondello, L., Casilli, A., Tranchida, P. Q., Sciarrone, D., Dugo, P., Dugo, G. Analysis of Allergens in Fragrances by using Multiple Heart-cut Multidimensional Gas Chromatography-Mass Spectrometry, LC-GC Europe 21:3 (2008) 130-137.

Nara, H., Nakagawa, F., Yoshida, N. Development of two-dimensional gas chromatography/ isotope ratio mass spectrometry for the stable carbon isotopic analysis of C2 –C5 non-methane hydrocarbons emitted from biomass burning, Rapid Commun. Mass Spectrom. 20 (2006) 241–247.

Nitz, S., Weinreich, B., Drawert, F., Multidimensional Gas Chromatography - Isotope Ratio Mass Spectrometry (MDGC-IRMS). Part A: System Description and Technical Requirements, J. High Resolut. Chromatog. 15:6 (1992) 387-391.

Pantò, S., Sciarrone, D., Maimone, M., Ragonese, C., Giofrè, S., Donato, P., Farnetti, S., Mondello, L. Performance evaluation of a versatile multidimensional chromatographic preparative system based on three-dimensional gas chromatography and liquid chromatography–two-dimensional gas chromatography for the collection of volatile constituents, J. Chromatogr. A 1417 (2015) 96–103

Ponsin, V., Buscheck, E.T., Hunkeler, D.J., Heart-cutting two-dimensional gas chromatography–isotope ratio mass spectrometry analysis of monoaromatic hydrocarbons in complex groundwater and gas-phase samples, J. Chromatogr. A 1492 (2017) 117–128

Putz, M., Piper, T., Casilli, A., de Aquino Neto, F. R., Pigozzo, F., Thevis, M., Development and validation of a multidimensional gas chromatography/combustion/isotope ratio mass spectrometry-based test method for analyzing urinary steroids in doping controls, Anal. Chim. Acta 1030 (2018) 105–114

Ragonese, C., Sciarrone, D., Dugo, P., Dugo, G., Mondello, L. Evaluation of a Medium-Polarity Ionic Liquid Stationary Phase in the Analysis of Flavor and Fragrance Compounds, Anal. Chem. 83 (2011) 7947-7954.

Ricci, M.P., Merritt, D.A., Freeman, K.H., Hayes, J.M. Acquisition and processing of data for isotope-ratio-monitoring mass spectrometry, Org. Geochem. 21 (1994) 561–571.

Schipilliti, L., Bonaccorsi, I., Sciarrone, D., Dugo, L., Mondello, L., Dugo, G. Determination of petitgrain oils landmark parameters by using gas chromatography–combustion–isotope ratio mass spectrometry and enantioselective multidimensional gas chromatography, Anal. Bioanal. Chem. 405 (2-3) (2012) 679-690.

Schmidt, E., Wanner, J. Adulteration of essential oils, in: Handbook of essential oils Ed. By K. Husnu Can Baser and Gerhard Buchbauer, CRC Press, Taylor & Francis Group, 2016, pp. 727-728

Schomburg, G., Husmanm, H., Hubinger, E., Konig, W.A. Multidimensional capillary gas chromatography – enantiomeric separations of selected cuts using a chiral second column, J. High Resolut. Chromatogr. 7 (1984) 404-410.

Sciarrone, D., Schepis, A., Zoccali, M., Donato, P., Vita, F., Creti, D., Alpi, A., Mondello, L., Multidimensional gas chromatography coupled to combustion- isotope ratio mass spectrometry/quadrupole ms with a low-bleed ionic liquid secondary column for the authentication of truffles and products containing truffle, Anal. Chem. 90 (2018) 6610–6617

Tranchida, P.Q., Sciarrone, D., Dugo, P., Mondello, L. Heart-cutting multidimensional gas chromatography: A review of recent evolution, applications, and future prospects, Anal. Chim. Acta 716 (2012) 66– 75.

Chapter 6

Enantio-selective gas chromatography as a suitable tool for authenticity assessment

6.1 Enantio-selective gas chromatography: application and multidimensional gas chromatographic approaches (Es-MDGC)

Gil-Av in 1966 provided the very first separation of enantiomers in a gas chromatographic column [Gil-Av 1966]. In the successive 35 years, as reported in a review by Schurig, more than 20000 separations of enantiomers were reported, involving more than 5000 chiral stationary phases, and culminating in more than 2000 publications [Schurig 2001]. Such an interest on chiral components is strictly related to the different behaviour of enantiomers when interacting with living beings. From a pharmaceutical point of view, chiral drugs can be characterized also by very different pharmacological activity, since they may register sometimes also opposite behaviours. One of the striking case was related to thalidomide, since the (R)-enantiomer had sedative action, while its (S)-form was teratogenic [Mellin 1962]. This report shocked the scientific community, leading to a more attention for the use of chiral mixtures in medicine field. Consequently, the interest on stereochemistry grew considerably, aimed to guarantee a proper separation of bioactive chiral compounds. Dealing with the chiral GC stationary phases, pioneer works in the field were carried out by Armstrong *et al*. (1990), Li *et al*. (1990), and Schurig and Novotny (1988), with the employment of α, β, γ derivatised cyclodextrins (CDs) [Armstrong 1990, Li 1990, Schurig 1988]. Accordingly, as reviewed by Bicchi *et al*., CDs are by far the most employed chiral selectors in the separation of volatile chiral components [Bicchi 1999]. Due to the high enantio-selectivity and reproducibility of CDs, their use is a common application for chiral recognition. This procedure enables the operators to analyse a high number of chiral components reliably.

Moving to an olfactory point of view, Ohloff demonstrated how differences between enantiomers involve also from an odour perceptive point of view. In this concern, the dextrorotatory form of citronellol was described to have a typical citronella odour, while the levorotatory form was responsible of a geranium type odour [Rienacker 1961]. Other clear differences in odour perception are resumed in Table 6.1.

Compounds	*Odour description*
Linalool	(+) sweet, petitigrain (-) woody lavender
Carvone	(+) caraway (-) spearmint
Menthol	(+) sweet, fresh, minty (-) dusty, less minty
Limonene	(+) orange (-) turpentine
Nootkatone	(+) grapefruit (-) woody

Table 6.1 Varying odour description in relation to the target stereoisomer

Beside the differences in odour quality, enantiomers can show also different odour sensations, as well as different odour intensity (odour threshold).

In the field of flavour and fragrances, the determination of enantiomeric excesses has covered a primary importance for the analysis of valuable natural matrices. Whilst it has been very useful to investigate the biochemical pathways of a specific sample, on the other hand it was able to provide key information in terms of authenticity assessment. Koenig *et al*., evaluated the applicability of Es-GC with modified CD for the authenticity of essential oils having high economic value; the authors deduced that this technique is highly effective when enantiomerically pure constituents are present in natural oils [Koenig 1997]. Otherwise, this technique is not adequate in the case of naturally varying enantiomeric composition.

Dealing with Citrus essential oils, research group of Dugo G. *et al*., extensively described the typical enantiomeric ratios of chiral terpenes in a large variety of fruits. Figure 6.1 shows the two enantiomers of limonene, whose enantiomeric excess is towards the dextrorotatory form in citrus products.

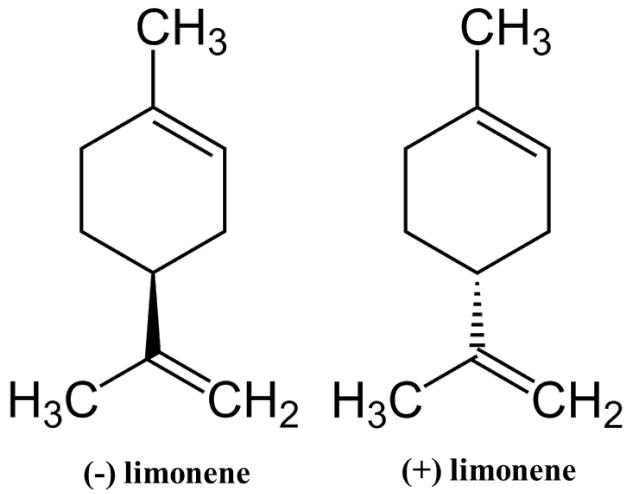

Figure 6.1 Levorotatory (-) and dextrotatory (+) form of limonene

One of the clearest examples about the paramount importance of chiral GC is surely bergamot essential oil. In this case, chiral recognition is by far the most suitable technique for authenticity assessment, since limonene, linalool and linalyl acetate have a typical enantiomeric excess (always higher than 97%) in cold pressed products. Differently, their ratio changes considering distilled products (see linalool enantiomeric ratios in Table 6.2), allowing an efficient recognition by these means.

Compounds	*Cold Pressed range*	*Distilled*
Limonene (-)	1.4-2.7	1.5
Limonene (+)	98.6-97.3	98.5
Linalool (-)	99.3-99.7	61.9
Linalool (+)	0.7-0.3	38.1
Linalyl acetate (-)	99.1-99.8	>99.0
Linalyl acetate (+)	0.9-0.2	<1.0

Table 6.2 Typical enantiomeric ranges of cold pressed bergamot essential oil compared with distilled products

However, chiral recognition may be sometimes limiting by employing monodimensional Es-GC approaches, even more in the case of complex mixtures. In these cases, a higher probability of peak overlaps occur, reducing the reliability of the enantiomeric ratio determined. In this concern, sample clean-up may be considered a good compromise, in order to guarantee a reliable stereo-differentiation of the enantiomers. Pre-separation techniques may include high performance thin-

layer chromatography (HPTLC), as well as high performance liquid chromatography, offline coupled to enantio-GC. By these means, enantiomeric ratios can be reliably measured by isolating target molecules offline, net to an increased total time analysis. Otherwise, more advanced analytical approaches can be performed by means of multidimensional gas chromatographic (MDGC) techniques. As already demonstrated in the previous chapters, the increased peak capacity of a MDGC approach allows a higher separation performance with respect to monodimensional methods. As well as for isotopic ratio mass spectrometer detection, the capability to choice selected chiral components is of paramount importance, since it reduces the probability of peak overlappings in the second dimension.

6.2 The coupling of enantio-selective gas chromatography to isotopic ratio mass spectrometry

As already discussed, in the case of naturally varying enantiomeric ratios, chiral recognition should be combined with other analytical approaches. Mosandl in 1995 published the following review "Enantioselective capillary gas chromatography and stable isotope ratio mass spectrometry in the authenticity control of flavors and essential oils", demonstrating the complementarity of chiral recognition and isotope ratio mass spectrometry for authenticity assessment [Mosandl 1995]. In detail, Mosandl stated how "enantioselectivity and isotope discrimination, during biosynthesis may both serve as endogenetic parameters in the authenticity control of natural flavour and fragrance compounds". In this concern, several research works were carried out in literature by means of multi analytical approaches, including Es-GC and GC-C-IRMS, in order to provide a thorough investigation of natural premium matrices. Dealing with citrus essential oils, Schipilliti *et al*. evaluated both chiral and isotopic data for a thorough investigation of bergamot, lemon and mandarin essential oils [Schipilliti 2011, Schipilliti 2012, Dugo 2012]. In this field, whilst chiral data was useful to distinguish between cold-pressed and distilled products, IRMS signature was of paramount importance to provide a better distinction in terms of geographical origin. Due to the complementary capability of both the techniques to investigate in depth the biochemical pathways of the plant, Mosandl firstly proposed a simultaneous detection by means of an on-line enantio-GC coupled to IRMS for the analysis of γ-decalactone enantiomers. This coupling allows combining the information related to the enantiomeric excess of target components, as well as the measurement of their isotopic ratio. Moreover, since chiral separation allows separating enantiomers each other, the isotopic ratio mass spectrometer will be able to measure the specific isotopic value of each target enantiomer separated. The following chapters (Chapter 7, 8, 9) will deeply investigate the potentiality of this combined approach, from the authenticity assessment of

Cannabis sativa L. essential oils (Chapter 7) to the chiral isotopic fractionation discovered in lemon essential oils (Chapter 9).

References

Armstrong, D.W., Li, W.Y., and Chang C.D. 1990. Polar-liquid, derivatized cyclodextrin stationary phases for the capillary gas chromatography separation of enantiomers. Anal. Chem. 62:914–923

Bicchi, C., D'Amato, A., Rubiolo, P. Cyclodextrin derivatives as chiral selectors for direct gas chromatographic separation of enantiomers in the essential oil, aroma and flavour fields. J. Chromatogr. A 843 (1999) 99–121

Brenna, E., Fuganti, C., Serra, S. Enantioselective perception of chiral odorants. Tetrahedron: Asymmetry 14 (2003) 1–42

Dugo, G., Bonaccorsi, I., Sciarrone, D., Schipilliti, L., Russo, M., Cotroneo, A., Dugo, P., Mondello, L., Raymo, V. Characterization of cold-pressed and processed bergamot oils by using GC-FID, GC-MS, GC-C-IRMS, enantio-GC, MDGC, HPLC and HPLC-MS-IT-TOF J. Essent. Oil Res. 24:2 (2012) 93-117

Gil-Av, E., Feibush, B., Charles-Sigler, R. Separation of enantiomers by gas liquid chromatography with an optically active stationary phase. Tetrahedron Lett. (1966) 1009

Koenig, W.A., Fricke, C., Saritas, Y., Momeni, B., Hohenfeld, G. Adulteration or Natural Variability? Enantioselective Gas Chromatography in Purity Control of Essential Oils. J. Resolut. Chromatogr. 20 (1997) 55.

Li, W.Y., Jin, H.L., and Armstrong, D.W. 1990. 2,6-Di-O-pentyl-3-O-trifluoroacetyl cyclodextrin liquid stationary phases for capillary gas chromatographic separation of enantiomers. J. Chromatogr. 509:303–324

Mellin G.W., Katzenstein M. The saga of thalidomide. Neuropathy to embryopathy, with case reports of congenital anomalies. The New England Journal of medicine Volume 267, Pages 1184-1192 (1962)

Mosandl, A. and A. Kustermann, Stereoisomere Aromastoffe. XXX: HRGC-Analyse chiraler γ-Lactone aus Getränken und Fruchtzubereitungen, Z. Lebensm. Unters. Forsch., 189, 212-215 (1989)

Mosandl A. Enantioselective capillary gas chromatography and stable isotope ratio mass spectrometry in the authenticity control of flavors and essential oils. Food Rev Int 11:4 (1995) 597–664.

Rienacker, R., Ohloff, G. Optisch aktives β-Citronellol aus (+) - oder (−)-Pinan. Angewandt Chemie 73:7 (1961) 240-250

Schipilliti, L., Dugo, G., Santi, L., Dugo, P., Mondello, L. Authentication of Bergamot Essential Oil by Gas Chromatography-Combustion-Isotope Ratio Mass Spectrometer (GC-C-IRMS) J. Essent. Oil Res. 23:2 (2011) 60-71

Schipilliti, L., Dugo, P., Bonaccorsi, I., Mondello, L. Authenticity control on lemon essential oils employing Gas Chromatography–Combustion-Isotope Ratio Mass Spectrometry (GC–C-IRMS), Food Chem. 131 (2012) 1523-1530

Schmarr, H.G., Mosandl, A., Grob, K. Stereoisomeric Flavour Compounds. XXXVIII: Direct chirospecific analysis of 7-lactones using on-line coupled HPLC-HRGC with a chiral separation column, Chromatographia, 29, 125-130 (1990)

Schomburg, G., Husmanm, H., Hubinger, E., Konig, W.A. Multidimensional capillary gas chromatography – enantiomeric separations of selected cuts using a chiral second column, J. High Resolut. Chromatogr. 7 (1984) 404-410.

Schurig, V. Separation of enantiomers by gas chromatography J. Chromatogr. A, 906 (2001) 275-299

Schurig, V., and Novotny, H. 1988. Separation of enantiomers on diluted permethylated β-cyclodextrin by high- resolution gas chromatography. J. Chromatogr. 441:155–163.

Chapter 7

Simultaneous evaluation of the enantiomeric and carbon isotopic ratios of Cannabis sativa L. essential oils by multidimensional gas chromatography

7.1 Introduction

Cannabis is an herbal annual plant, for which research has long been limited because of legal restrictions across the twentieth and the beginning of the twenty-first century, due to its renowned psychotropic activity and the related illicit use. From a normative point of view, the cultivation has been promoted in Europe only in the last decade, specifically for those varieties, e.g., Cannabis sativa L., with content in tetrahydrocannabinol < 0.2% (https:// eur- lex. europa. eu/ LexUr iServ/ LexUr iServ. do? uri= OJ:L: 2013: 347: 0608: 0670: IT: PDF). As a consequence of the increased scientific interest, nowadays, hemp market and the linked manufactures are ever spreading. Among the products derived from Cannabis sativa L., the essential oil obtained by the inflorescences is one of the most distinctive, due to the harmonious balance between the main monoterpene and sesquiterpene components along with their oxygenated derivatives [Sommano 2020]. Cannabis chemical composition may vary in relation to the inflorescence being fresh or dry [Sommano 2020], its variety, and the extraction methodology used. In the last decades, steam distillation or hydro-distillation [Ternelli 2020] has been the most used technique for oil extraction, as well as the innovative microwave-assisted hydro-distillation (MADH) apparatus [Fiorini 2020, Micalizzi 2021]. In MADH extraction of the hemp inflorescences, the final yield can be maximized by finely tuning some instrumental parameters, i.e., microwave power and time program [Micalizzi 2021]. Alongside genuine oils obtained from the inflorescences, also reconstituted oils obtained by natural or synthetic sources are nowadays more and more present on the market. Most of them are declared to contain the typical hemp terpene compounds, such as α-pinene, myrcene, and (E)-β-caryophyllene, aiming to emulate the flavor and other properties of natural cannabis oils. Yet, no reference data are reported in the literature about the chemical composition of these oils. In this regard, gas chromatography coupled to flame ionization detector (GC-FID) and to mass spectrometry (GC–MS) are well-suited techniques for investigation of the qualitative and

quantitative composition in terms of volatile components. However, there is no chance to highlight the differences with respect to extracted genuine oils, by these means. The employment of more sophisticated analytical techniques is needed to tackle such a task. Enantio-selective gas chromatography (Es-GC) has historically played a key role in the authenticity assessment of natural essential oils, proving to be one of the most effective analytical approaches for this purpose [Mondello 2010]. In fact, chiral compounds show typical enantiomeric ratios in natural samples, being the metabolites of specific biochemical pathways of the plant of origin. Thus, the presence of unusual enantiomeric ratios for a given sample has often allowed unveiling fraudulent additions, by comparison to genuine reference values, using monodimensional and multidimensional GC [Dugo 2010, Mondello 2008, Bonaccorsi 2011]. Conversely, nowadays, key chiral components can be selected by natural sources having identical or similar enantiomeric ratios with respect to the sample investigated [Do 2015], thereby reducing the possibility to detect any differences deriving from adulterations. In such cases, additional analytical techniques are needed to highlight further typical traits of the plant of origin. Gas chromatography coupled to isotope ratio mass spectrometry (GC-C-IRMS) is equally broadly recognized as a suitable technique to assess the origin and genuineness of a sample. A GC-C-IRMS method can provide crucial information about the natural, synthetic, or biosynthetic origin of specific compounds in a sample, allowing in many cases to unveil fraudulent practices. Since the distribution of carbon stable isotopes strictly depends on the photosynthetic carbon metabolism and the geographic origin of the plant, the evaluation of the $\delta^{13}C$ values of key volatile compounds represents a powerful tool for genuineness assessment [Sciarrone 2018, Zhang 2012, Reay 2019]. It is straightforward that a combined approach consisting of Es-GC-C-IRMS would allow for the simultaneous evaluation of both chiral and $\delta^{13}C$ values, thus enabling to detect fraudulent additions to genuine oil samples. The coupling of chiral separation and IRMS detection was first demonstrated by Mosandl *et al*. [Mosandl 1990] for the differentiation of biotechnological and synthetic γ-decalactone, and later by few more authors [Silfer 1991, Mosandl 1995, Reichert 2000, Badea 2015]. Although representing a powerful tool for authenticity assessment, this approach suffers from important drawbacks, which have greatly limited its widespread diffusion. When dealing with medium-to-high complex samples, incomplete separation of the compounds of interest may occur, due to insufficient chromatographic resolution. Within crowded zones across a chromatogram, co-elutions would in turn result in wrong evaluation of the enantiomeric and isotopic ratios. Chiral compounds can be resolved into their enantiomers on a suitable stationary phase, and in the presence of further co-elutions, the enantiomeric ratios can be still calculated by extracting specific m/z ions. On the other hand, this problem would negatively affect the $\delta^{13}C$ value evaluation, due to the uneven

distribution of carbon isotopes (^{12}C and ^{13}C) along the CO_2 peak [Matucha 1991, Cucinotta 2021]. A slightly different retention is observable for the same molecules containing different amounts of the two isotopes. In fact, different van der Waals dispersion forces during solute/ stationary interaction cause an enrichment in the heavier isotope of the initial part of the peak, while the lighter isotope will be more represented in the final part. Thus, shifted isotopic values will be observed with respect to those of a pure peak [Matucha 1991, Cucinotta 2021], depending on which part of the peak is co-eluted. If the co-elution affects the front of the peak, a more negative δ^{13}C value will be observed; on the contrary, a more positive δ^{13}C value will be measured if the tail of the peak of interest is affected by co-elution. In the case of a complete co-elution, no MS "tricks" can be adopted, due to the conversion of the peak components to CO_2. In this case, evidence of such a situation would be only obtained by checking the CO_2 ratio differentiation [Cucinotta 2021]. Multidimensional gas chromatography exploited in the heart-cut mode (HC-MDGC) may represent the technique of choice for this task, thanks to the higher peak resolution afforded by the coupling of two full-length columns with different selectivity [Tranchida 2012]. In the literature, only few works have employed an MDGC system before the IRMS detection, and among these, only one deals with the detection of enantiomers [Reichert 2000]. Whereas cannabinoids extracted from marijuana samples have been investigated by means of compound-specific IRMS [Muccio 2012], no data are available relative to the terpene fraction. In this research, an Es-MDGC system coupled to IRMS via a combustion chamber (C-IRMS), and to a quadrupole mass spectrometer (qMS), was developed. An apolar column was used as the first dimension (1D) and a chiral cyclodextrine- based stationary phase as the second dimension (2D), to evaluate the enantiomeric and isotopic ratios of well- separated target terpenes in cannabis oils, for the first time. A MAHD method, earlier described by Micalizzi *et al*. [Micalizzi 2021], was adopted to obtain in-house genuine oils from the fresh and dried inflorescences of different cannabis varieties. In parallel, commercial oils declared as reconstituted or natural were analyzed, and the results were compared to those obtained for the genuine samples extracted in-house. To the best of our knowledge, this is the first time that δ^{13}C values are provided for the terpene fraction of Cannabis sativa L. essential oil samples. The data gathered from analysis of the different sample varieties were used to establish the characteristic enantiomeric and isotopic ranges of Cannabis sativa L. essential oil.

7.2 Experimental section

7.2.1 Monodimensional GC-C-IRMS/qMS conditions

The system consisted of a GC2010 Plus gas chromatographer equipped with an AOC-20i autosampler (ShimadzuEuropa, Duisburg, Germany). The instrument was directly connected via a zero dead-volume tee-union to a QP2010 Ultra quadrupole mass spectrometer (Shimadzu Europa) and to a VisION IRMS system, preceded by a GC V furnace system (Elementar Analysensysteme GmbH, Langenselbold, Germany) operated at 850 °C. A split/splitless injector was maintained at 280 °C, at a split ratio 10:1. The same GC-C- IRMS/qMS system configuration was used exploiting two different stationary phases, alternatively:

– A MEGA-DEX ASX 1 column, 25 m × 0.25 mm I.D. × 0.25 μm df (MEGA, Milano, Italy), was used as chiral stationary phase, ramped from 50 to 220 °C at 2 °C/min.

– A capillary SLB-5 ms column, 30 m × 0.25 mm I.D. × 0.25 μm df (Merck Life Science, Darmstadt, Germany), was used as apolar stationary phase, ramped from 50 to 280 °C at 3 °C/min.

The columns were operated at a constant flow rate of carrier gas (helium) of 1 mL/min. A pressure program was applied to the injector during the analyses, on the basis of the total resistance (column + retention gaps). For the chiral column, the program pressure started from 74 kPa, at 1.63 kPa/min, to 126 kPa. For the apolar column, the pressure was ramped from 85 to 165 kPa at 1.04 kPa/min. The column effluent was diverted to the IRMS system via a 0.85 m × 0.32 mm I.D. uncoated column, located inside a combustion chamber, and in parallel to the qMS system via a 2 m × 0.1 mm I.D. uncoated column. The qMS ion source and interface temperature was maintained at 200 °C; a mass range 40–400 m/z was monitored at an acquisition speed of 10 Hz. GCMS data were acquired by the GCMS solution software ver. 4 (Shimadzu Europa). Compound identification was carried by using the FFNSC 4.0 mass spectral library database (Shimadzu Europa), exploiting a double-filter approach based on spectral similarities and Linear Retention Index (LRI) values. The VisION IRMS was a bench-top 5-kV system equipped with an integrated gas delivery monitoring system. The combustion chamber was equipped with a high-performing silicon carbide tube furnace for the quantitative, fractionation-free conversion of the delivered compounds to pure gases (CO_2 and H_2O). The CO_2 produced by the combustion of each compound was transferred to the IRMS, while the H_2O produced was removed through a nafion membrane. The system was designed with reduced dead volumes to maintain the chromatographic resolution at the IRMS. The following settings were applied to the VisION system: acceleration voltage, 3795 V; trap current, 600 mA; magnet current, 3700 mA. An electron-impact ionization (EI) gas

source, a variable field, stigmatically focused electromagnet for beam separation and multi-channel Faraday collectors for beam detection were used. IRMS data were collected by IonOS stable isotope data processing software ver. 4.5 (Elementar Analysensysteme GmbH). The apex track integration method was exploited to automatically find the correct starting and finishing points of the peaks.

7.2.2 Multidimensional GC-C-IRMS/qMS conditions

The MDGC-C-IRMS/qMS prototype consisted of an AOC- 20i autosampler and two GC-2010 Plus gas chromatographers (defined as GC1 and GC2), connected by means of a heated transfer line (Shimadzu Europa). GC1 was equipped with a split/splitless injector, a flame ionization detector (FID), and a Deans-switch (DS) transfer device. GC1 was connected to an advanced pressure control unit (APC), which supplied the same carrier gas (He) (Shimadzu Europa) allowing to divert the first column eluent to the FID or to the second column in the GC2. The latter was hyphenated in parallel to a QP2010 Ultra quadrupole mass spectrometer (Shimadzu Europa) and to a VisION IRMS system by means of a GC V furnace system (Elementar Analysensysteme GmbH) maintained at 850 °C. The split/ splitless injector was maintained at 280 °C, at a split ratio 10:1. A constant helium flow of 1.0 mL/min was delivered to the 1D column, an SLB-5 ms 30 m × 0.25 mm I.D. × 0.25 μm df (Merck Life Science, Darmstadt, Germany). A pressure program was used, from 185 kPa (7 min) to 247 kPa (5 min) at 1.89 kPa/min, to 300 kPa at 1.89 kPa/min, and finally to 330 kPa at 9.48 kPa/min. The GC1 oven was ramped as follows: 50 °C (7 min) to 227 °C at 3 °C/min with an isotherm at 150 °C (5 min), finally to 280 °C at 15 °C/min. The FID was connected to the DS device via a 0.25 m × 0.18 mm i.d. stainless steel uncoated column and used to monitor the 1 D eluent. FID conditions were as follows: 330 °C; H_2 flow, 40.0 mL/min; air flow rate, 400 mL/min; sampling rate, 80 ms equal to 12.5 Hz. GC2 was equipped with a MEGA- DEX ASX 1 chiral column 25 m × 0.25 mm I.D. × 0.25 μm df (MEGA, Milano, Italy), and the temperature was ramped as follows: 40 °C (22 min) to 76 °C (5 min) at 2 °C/min, to 145 °C at 3 °C/min, and finally to 195 °C at 8 °C/min. The 2D column was connected at one side to the DS device and at the other side to a zero dead-volume tee-union (Valco). A pressure program was applied to the APC device to maintain a constant carrier flow also in the 2 D column (≈1 mL/min): 140 kPa (22 min) to 165 kPa (5 min), to a final pressure of 210 kPa at 1.39 kPa/min. An auxiliary He line (sample line He), automatically controlled through a second channel of the APC unit, was used in the furnace to allow a proper control over the open split conditions for the IRMS. Also in this case, the APC was operated in constant flow mode, to maintain the open split in a steady state. MS and IRMS conditions were the same used in the monodimensional approach. All the MDGC

analyses were carried out at least in triplicate and the standard deviations for IRMS measurements were found to be < 0.5 ‰.

7.2.3 Sample, sample preparation and standards

Fifteen samples of dry hemp inflorescences belonging to Futura 75, Kompolti, Felina 32, Tisza, and CS (Carmagnola Selezionata) varieties and one sample of fresh hemp inflorescences of Futura 75, registered in the EU Plant variety database (https:// ec. europa. eu/ food/ plant/ plant_ propagation_material/ plant_ variety_ catalogues_ databases/ search/ public/ index. cfm? event= Searc hVari ety& ctl_ type= A& species_ id= 240& variety_ name= & listed_ in= 0& show_ current=on& show_ deleted), were provided by the Canapar group (Ragusa, Italy). Nineteen commercial hemp oil samples, 16 reconstituted and 3 declared as naturals, were purchased from local stores. All the samples were diluted 1:10 in n-hexane before GC analysis.

Six-hundred milliliters of ultrapure water was added to 200 g of inflorescence, and the biomass was uniformly mixed. The resulting mixture was placed inside a 2-L ETHOS-X glass reactor and then into a Milestone "Ethos X" extractor (Milestones, Sorisole, Italy). The extraction was carried out under previously optimized conditions [Micalizzi 2021], and the essential oils were collected from the distillation system.

A C_7-C_{30} n-alkane mix was used for the calculation of Linear Retention Index (LRI) values. In order to calibrate the measured $\delta^{13}C$ values to the VPDB scale, the CO_2 reference gas was calibrated using four reference compounds, namely iodomethane ($\delta^{13}C$ value − 54.59‰) and three alkanes from the Indiana mix A7: hexadecane ($\delta^{13}C$ value: − 26.15‰), octadecane ($\delta^{13}C$ value: − 32.70‰), and eicosane ($\delta^{13}C$ value: − 40.91‰) (Indiana University, Bloomington, IN).

7.3 Results and Discussion

7.3.1 Extraction of the cannabis oil samples by MAHD

Extraction by MAHD was applied to sixteen genuine samples consisting of fresh and dry hemp inflorescences. By the employment of a microwave-assisted system, heat was applied to the soaked biomass to facilitate the break of the oileferous glands and the release of essential oil. By this method, the first drops of essential oil fell after about 5 min of distillation at 1200 W, at a temperature around 94 °C. The samples selected for extraction are listed in Table 7.1. One sample was obtained by fresh hemps of Futura 75 (sample 1), while the dry samples belonged to different varieties: 9 of Futura 75 (samples 2–10), 2 of Felina 32 (samples 11–12), 1 of Tisza (sample 13), 2 of Kompolti (samples 14–15), and 1 of CS (Carmagnola Selezionata) (sample 16).

Unfortunately, the high cost and the difficulties in retrieving genuine plant material have limited the number of oil samples included in this research. This represents a common issue for studies focused on ascertaining the genuineness ranges, since natural samples are required to assess the characteristic $\delta^{13}C$ values and enantiomeric ratios. The limited size of samples available prevented from obtaining statistically significant results, on the differences among the distinct Cannabis sativa varieties. Nonetheless, the data gathered from analysis of the essential oil samples were used to establish the characteristic ranges of the enantiomeric and isotopic ratios of Cannabis sativa L.

Samples	Varieties	Fresh or dry	Origin
1	Futura 75	Fresh	Italy
2	Futura 75	Dry	Italy
3	Futura 75	Dry	Italy
4	Futura 75	Dry	Italy
5	Futura 75	Dry	Italy
6	Futura 75	Dry	Italy
7	Futura 75	Dry	Italy
8	Futura 75	Dry	Italy
9	Futura 75	Dry	Italy
10	Futura 75	Dry	Croatia
11	Felina 32	Dry	Italy
12	Felina 32	Dry	Italy
13	Tisza	Dry	Italy
14	Kompolti	Dry	Italy
15	Kompolti	Dry	Italy
16	Carmagnola Selezionata	Dry	Italy

Table 7.1 Cannabis varieties selected for essential oil extraction from hemp inflorescences

7.3.2 Monodimensional Es-GC-C-IRMS/qMS analysis

Es-GC-C-IRMS/qMS analyses were initially carried out to determine both the enantiomeric and isotopic ratios of the genuine cannabis oils. To this purpose, a chiral MEGA-DEX ASX-1 stationary phase proved to be effective for the separation of the target enantiomers before the IRMS determination. Still a number of issues arose in the monodimensional GC analysis of some genuine cannabis oils, for the separation of the main chiral terpenes. This is shown in Fig. 7.1A for a Futura

75 essential oil. As can be easily noticed, although α-pinene and β-pinene enantiomers were efficiently separated by Es-GC-C-IRMS/qMS, co-elutions occurred with other achiral components. In the case of (+)-α-pinene, present in higher amount with respect to heptanal, the partial peak overlapping might have a limited influence on the peak area evaluation. Thus, it would not affect the enantiomeric ratio assessment and the $\delta^{13}C$ value evaluation [Cucinotta 2021]. Otherwise, the co-elution occurring between (+)-β-pinene and another major compound (e.g., myrcene) introduced a critical issue. The incomplete separation in fact hindered accurate evaluation of both the enantiomeric and isotopic ratios. Concerning the enantiomeric ratio evaluation, the use of simultaneous qMS detection would allow resolving the chromatographic co-elution by monitoring the extracted m/z ions of the compounds of interest. Unfortunately, the EI spectra of monoterpene compounds will be characterized by the same fragmentation pattern and show nearly identical fragment ions, thus precluding the use of this approach. From the IRMS standpoint, a similar approach cannot be envisaged. All the organic matter must be converted to CO_2 before the $\delta^{13}C$ value determination, with a consequent loss of any analyte structural information [Matucha 1991]. Therefore, the occurrence of a co-elution involving the right part (tail) of the peak, as for the case of (+)-β-pinene, is expected to cause a relevant positive shift of the $\delta^{13}C$ value. The latter is due to the depletion of the $^{44}CO_2$ fragment, related to a lower amount of β-pinene molecules containing 12 C. Figure 7.1B shows a further co-elution occurred in a Futura 75 oil, involving the (-)-limonene enantiomer and (E)-β-ocimene. Being the latter a higher abundant compound, a wrong estimation of the $\delta^{13}C$ value should be expected, unlike the case of (+)-α-pinene discussed above. Moving forward in the chromatogram, further critical cases may be observed in the sesquiterpene elution zone of a Kompolti sample (Fig. 7.1C). Selina-3,7(11)-diene and selina-4(15),7(11)-diene compounds were successfully separated into their enantiomers; nevertheless, the late eluting enantiomer of selina-4(15),7(11)-diene and the first eluting enantiomer of selina-3,7(11)-diene overlap with germacrene B peak. Likewise, unreliable results may be predicted in this case, notably a more positive $\delta^{13}C$ value for selina-4(15),7(11)-diene and a more negative $\delta^{13}C$ value for selina-3,7(11)-diene, with respect to the true values.

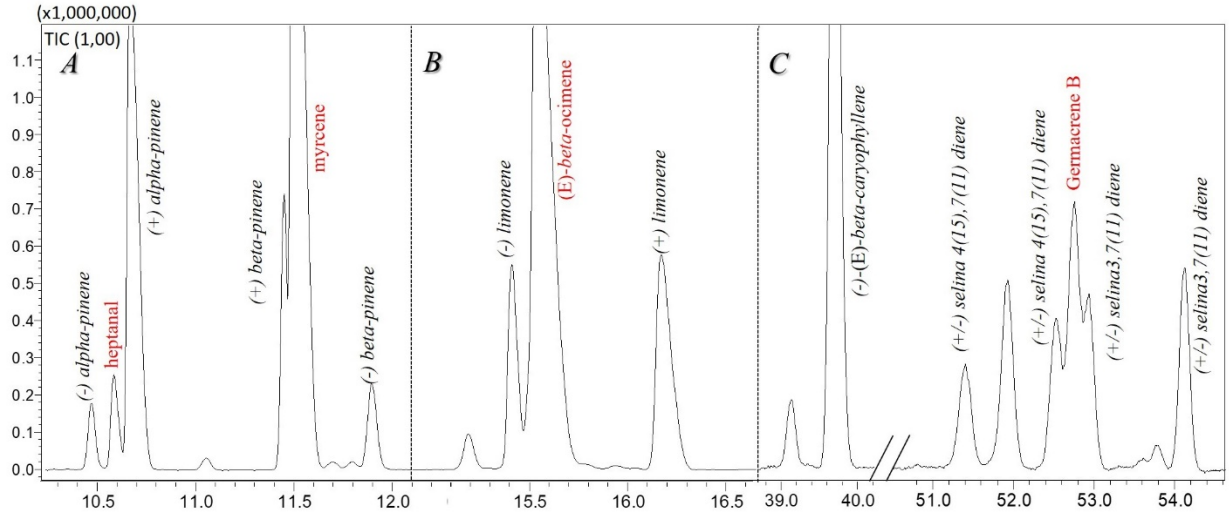

Figure 7.1. Es-GC-C-IRMS/qMS analysis showing the co-elutions of (+)-α-pinene and (+)-β-pinene peaks (A) and (-)-limonene peak (B) in a Futura 75 essential oil, and the enantiomers of selina diene isomers in a Kompolti essential oil (C)

7.3.3 Monodimensional GC-C-IRMS/qMS analysis

Inaccurate results were also obtained by GC-C-IRMS/qMS analysis performed on the apolar column. As can be seen in Fig. 7.2, co-elutions affected the target oil compounds eluting in the monoterpene and sesquiterpene zone. Figure 2A shows a partial co-elution involving limonene and eucalyptol in a Futura 75 sample. Due to their similar LRIs on an apolar stationary phase (1030 and 1032 respectively), a partial overlap occurred, again generating unreliable results for the $\delta^{13}C$ values. Figure 7.2B shows the critical case of selina-4(15),7(11)-diene, identified by exploiting double-filter search based on mass spectral similarity (> 90%) and LRI (± 5 units window). Due to its Gaussian shape, it would have been regarded as a pure peak, at first sight. Yet, a deeper insight into the MS spectrum along the peak highlighted the presence of co-eluted (E)-α-bisabolene in the peak tail. These components are characterized by the same LRI value of 1540 on the column employed, as reported in the FFNSC 4.0 database. Figure 7.2C shows how this co-elution can be resolved by monitoring the extracted ions from the MS total ion current (TIC) (lower trace) and by 45/44 CO_2 ratio differentiation at the IRMS (upper trace). In detail, m/z 93 and m/z 105 were extracted from the TIC, being the base peaks for (E)-α-bisabolene and for selina-4(15),7(11)-diene, respectively. The higher amount of the m/z 93 ion in the tail of the peak clearly suggested the presence of (E)-*α*-bisabolene, as further confirmed by the unusual 45/44 CO_2 ratio differentiation reported in the upper profile. On this basis, the need to implement a multidimensional approach emerged clearly, to increase the separation capability.

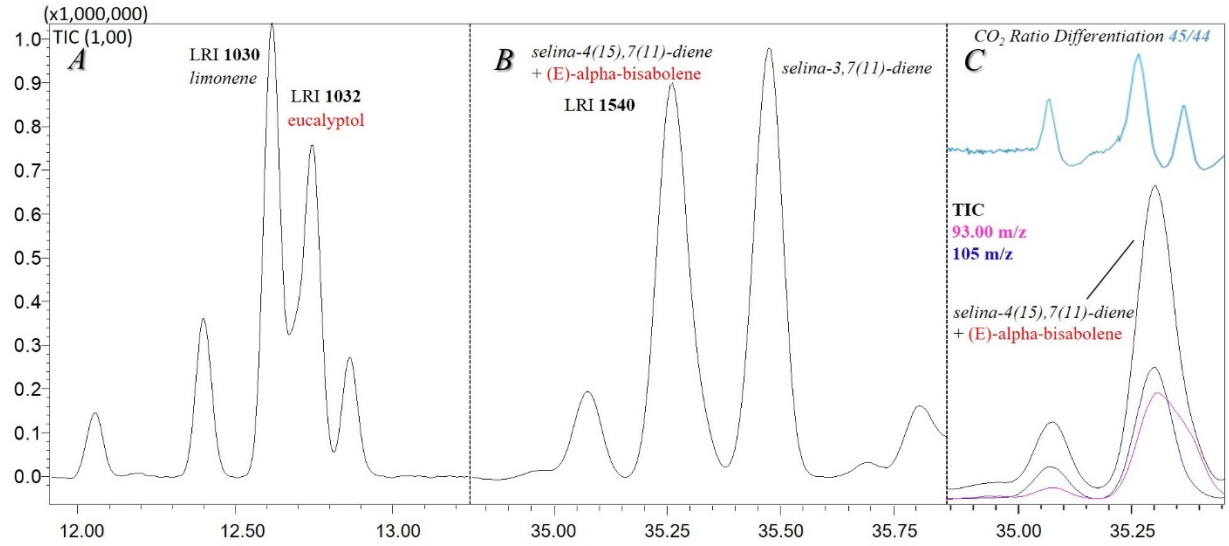

Figure 7.2. GC-C-IRMS/qMS analysis showing the co-elutions of limonene and eucalyptol peaks (A) and selina-4(15), 7(11)-diene, and (E)-α-bisabolene peaks (B) in a Futura 75 essential oil. 45/44 CO 2 ratio differentiation (IRMS: upper trace) and extracted ion chromatogram (qMS: lower traces) of selina-4(15),7(11)-diene peak (C)

7.3.4 Es-MDGC-C-IRMS/qMS approach

Selection of the peaks of interest after 1 D stand-by analysis:

An MDGC method was implemented as front-end separation, before simultaneous qMS and IRMS detection. This, in order to overcome the separation issues discussed in the "Monodimensional GC-C-IRMS/qMS analysis" section. In detail, an apolar SLB-5 ms column was employed as 1D column and a chiral MEGA-DEX ASX-1 as 2D. The first step of any HC-MDGC analysis involves the identification of the peaks of interest after a 1D analysis performed in the stand-by mode (no heart-cuts selected). Since no qualitative information was available after the 1D detector (FID), the identity of each peak of interest was confirmed on the basis of the elution order in monodimensional GC–MS on the same stationary phase. The experimental LRIs of the peaks calculated for a 1D stand-by analysis were matched to the theoretical values, allowing for a ± 10 units tolerance [Bicchi 1999]. Cannabis oil samples and a C_7–C_{30} alkane homologous series were analysed under the same conditions and the experimental LRIs were calculated by the following formula:

$$LRIx = 100n + 100\ (t\ Rx - t\ Rn)/\ (tR\ n + 1 - t\ R\ n)$$

where n and t R n are the carbon number and retention time of the alkane eluted before the peak of interest, and t R n + 1 is the retention time of the alkane eluted after the peak of interest.

The oil samples were separated by MDGC prior to measurement of the $\delta^{13}C$ values and enantiomeric ratios of the peaks of interest. Figure 7.3 shows the 1D FID chromatogram of a cannabis essential oil acquired in the stand-by mode on the apolar (5%) column (black trace). Among the main chiral terpenes, a total of nine compounds were selected for the heart-cut: α-pinene, β-pinene, limonene, linalool, α-terpineol, (E)-β-caryophyllene, selina-4(15), 7(11)-diene and selina-3,7(11)-diene, and β-caryophyllene oxide. Minor chiral components, namely camphene, borneol, fenchyl alcohol, and (E)-nerolidol, were not taken into consideration due to their low amount in the oils. As shown in Table 7.2, the experimental LRI values (LRI exp), calculated on the 1D apolar column, ranged within ± 5 units with respect to the theoretical data (LRI theor).

Peak no.	Compound	LRI theor	LRI exp
1	α-pinene	933	935
2	β-pinene	978	980
3	Limonene	1030	1032
4	Linalool	1101	1103
5	α-terpineol	1195	1200
6	β-caryophyllene	1424	1427
7	Selina-4(15),7(11)-diene	1540	1544
8	Selina-3,7(11)-diene	1546	1550
9	β-caryophyllene-oxide	1587	1591

Table 7.2. The theoretical and experimental LRI values calculated for a 1D stand-by analysis of a Kompolti oil (apolar 1 D column). LRI theor are reported in the FFNSC 4.0 mass spectral database for the same stationary phase (SLB-5 ms)

A heart-cut window was then selected, for each compound to be transferred to the second chiral column in the "cut" mode (pink trace in Figure 7.3).

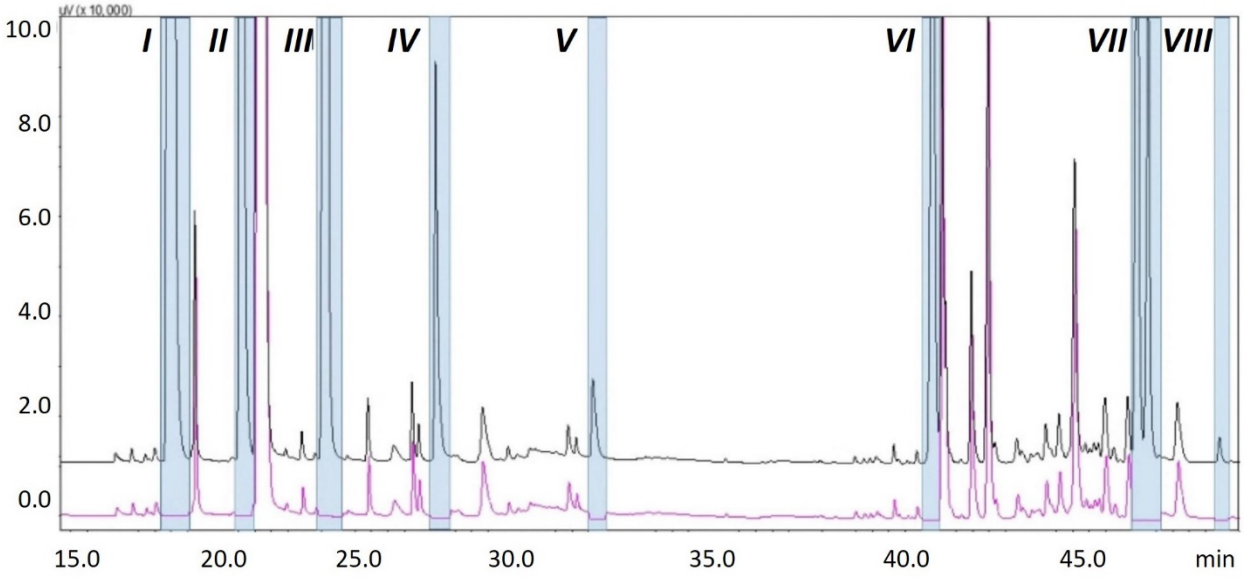

Figure 7.3. 1D stand-by (black chromatogram) and cut (pink chromatogram) FID analysis of a Cannabis sativa L. essential oil. Cut windows: I: α-pinene, II: β-pinene, III: limonene, IV: linalool, V: α-terpineol, VI: (E)-β-caryophyllene, VII: selina-4(15),7(11)-diene and selina-3,7(11)-diene, VIII: β-caryophyllene oxide

The combination of two chromatographic separation mechanisms provided substantial benefits over the monodimensional approach. First, a satisfactory separation was achieved for all the enantiomeric compounds transferred from 1D. Furthermore, all the co-elutions occurring with other (achiral) sample components were prevented. The gain in separation attained by MDGC can be appreciated in Fig. 7.4, showing different zoomed zones of the chromatogram.

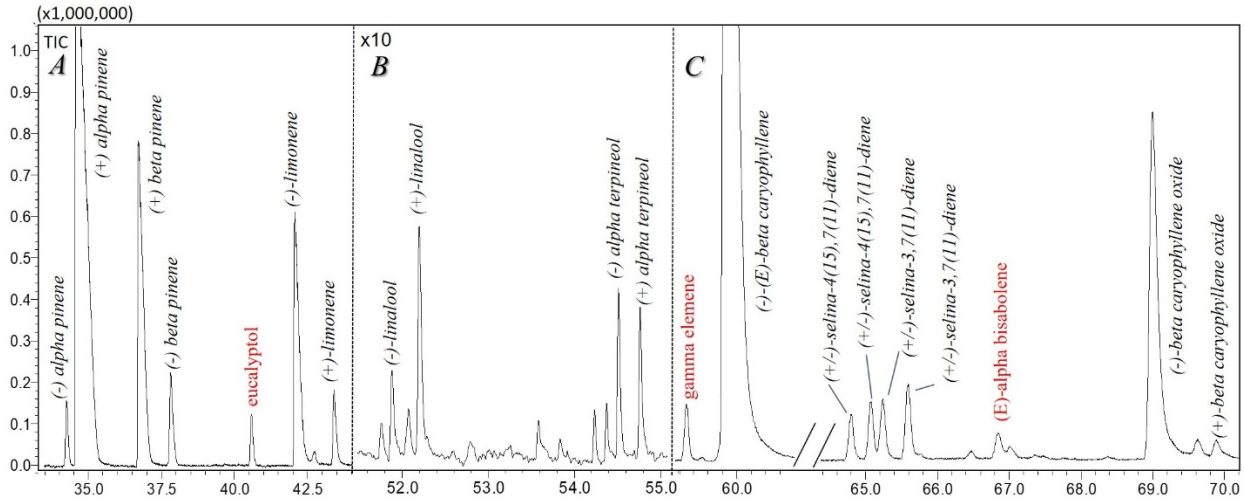

Figure 7.4. MDGC separation of the target monoterpenes in a Futura 75 (A) and a Felina 32 (B) essential oil sample and of the target sesquiterpenes in a Futura 75 essential oil sample (C)

In detail, α-pinene, β-pinene, and limonene enantiomers show up as separated peaks in Fig. 7.4A, whereas in the corresponding Es-GC-C-IRMS/qMS analysis important co- elutions occurred with heptanal, myrcene, (E)-β-ocimene, and eucalyptol. Figure 7.4B shows the separation obtained for linalool and α-terpineol enantiomers. Figure 7.4C shows the (E)-β-caryophyllene peak separated from γ-elemene. Noticeably, these compounds fully co-eluted on the apolar 1 D column due to the very close LRI values (1424 vs 1432) and to the high amount of caryophyllene in the sample. Moreover, the separation of the four enantiomers of selina diene isomers is evident in the same chromatogram, free from overlapping with germacrene B and (E)-α-bisabolene peaks. Separation on a single chiral column had resulted in co-elution of selina-4(15),7(11)-diene with germacrene B, as illustrated in Fig. 7.1. Likewise, monodimensional analysis on the apolar column has led to the co-elution with (E)-α-bisabolene, as illustrated in Fig. 7.2. After MDGC separation, only a minor co-elution was observed between the second eluting selina-4(15),7(11)-diene peak and the first eluting peak of selina-3,7(11)-diene enantiomers. Unfortunately, no data are available about theelution order of these enantiomers on the chiral stationary phase used. Finally, the separation of (E)-β-caryophylleneoxide enantiomers could be appreciated only in the dried hemp inflorescence samples. This compound is in fact generated as a result of the oxidation occurring upon drying of the plant material [Micalizzi 2021]. The enantiomeric ratios and $\delta^{13}C$ values obtained within a single analysis for all the sample components are reported in Table 7.3 and Table 7.4. Differences were found in the qualitative and quantitative composition in monoterpenes and sesquiterpene, according to the type of inflorescence and the variety itself. Moreover, characteristic enantiomeric ratios and $\delta^{13}C$ values were observed for the target compounds in all the sixteen genuine oils. The enantiomeric ratios of all the natural samples were in good agreement with the literature data [Micalizzi 2021], although in this research a higher number of samples were investigated. A marked preponderance was observed in all the hemp varieties of (+)-α-pinene (93.4–97.1%), (+)-β-pinene (78.6–88.0%), and (-)-β-caryophyllene oxide (91.7–98.9%). Similarly but to a lesser extent, (+)-linalool was predominant in all the varieties investigated (57.8–74.9%). In contrast, a similar trend could not be identified for limonene and α-terpineol enantiomers, whose enantiomeric ratios greatly varied in the samples. A racemic behavior was observed for selina diene isomers, with only a slight predominance of the late eluted enantiomers for both the 4(15) and 3(11) isomers. In this case, however, the elution order of the two enantiomers is unknown. Concerning the (E)-β-caryophyllene enantiomers, the occurrence of the levorotatory form at nearly 100% is widely reported, and the data obtained hereby were in accordance with this literature finding [Micalizzi 2021]. Dealing with isotopic distribution, differences were observed in terms of $\delta^{13}C$ values among the specific varieties, as reported in Table 7.4. The $\delta^{13}C$ values of pure

enantiomer peaks could be determined, after the 2D separation obtained on the chiral stationary phase. However, for low concentrated components and depending on the enantiomeric ratio, in few cases, only one enantiomer could be measured. A linearity test automatically performed by the system showed consistent $\delta^{13}C$ values in the response interval above 0.5 nA; thus, signals below this threshold were discarded. According to the few data available in the literature, no significant $\delta^{13}C$ value differences are to be expected within enantiomers of the same molecule [Mosandl 1990, Mosandl 1995, Reichert 2000]. In general, more negative $\delta^{13}C$ values were found for samples 13–16 (Tisza, Kompolti, and Carmagnola Selezionata) with respect to samples 1–10 (Futura 75) and 11–12 (Felina 32). Among Futura 75 samples, different values were observed between oils of different origin, namely from Italy (samples 1–9) and Croatia (sample 10), as can be appreciated in Figure 7.5A.

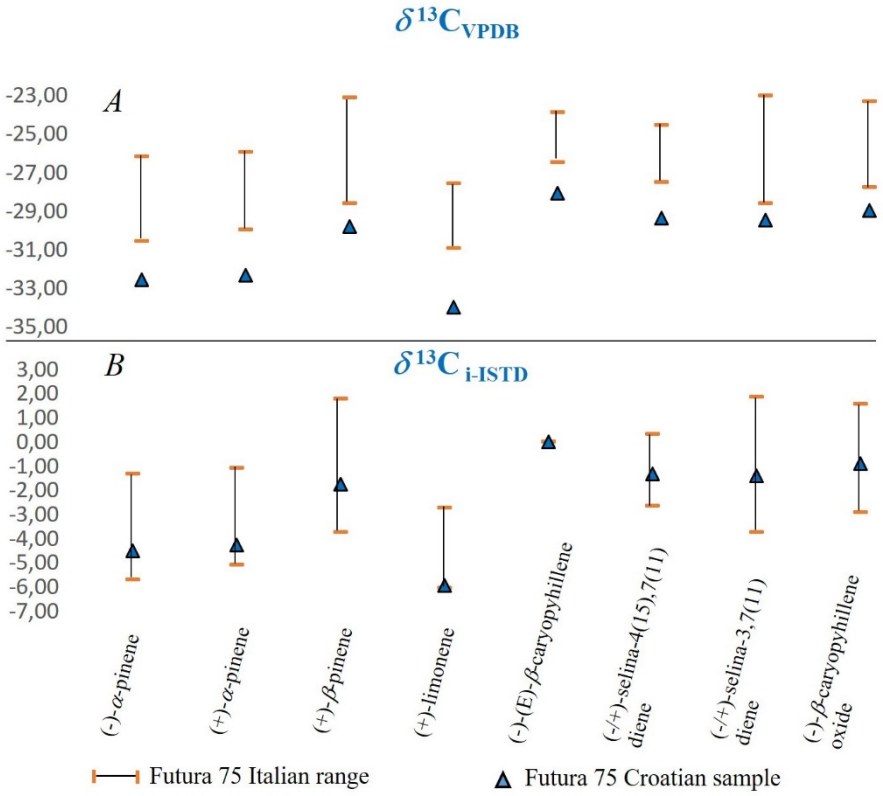

Figure 5 (A) Comparison between the $\delta^{13}C$ values range of Italian Futura 75 (samples 1–9) and Croatian Futura 75 (sample 10). (B) Results obtained by the use of (-)-(E)-β-caryophyllene reference compound (i-ISTD)

Specifically, sample 10 showed more negative $\delta^{13}C$ values with respect to samples 1–9. Given the genuineness of the Croatian oil, one of the terpene components was used as reference, to avoid the isotopic discrimination due to the geographical origin [Mosandl 1995]. (-)- (E)-β-Caryophyllene was chosen as isotopic internal standard (i-ISTD), being one of the characteristic compound in

cannabis essential oil and biogenetically related to the other compounds investigated. The i-ISTD approach allowed us to ascertain the genuineness of all the Futura samples, regardless of their origin (Fig. 7.5B). In the case of the two selina diene isomers, the small co-elution occurring between the second eluted enantiomer of the 4(15), 7(11) isomer and the first eluted enantiomer of the 3,7(11) isomer was negligible to the aim of enantiomeric ratio evaluation. Yet, such a small lack of separation significantly affected the evaluation of δ^{13}C values in all the samples analyzed. A representative example is illustrated by the δ^{13}C values measured for Futura 75 oil (sample 10). Among the four peaks corresponding to the distinct enantiomers of selina diene isomers, baseline separation was achieved only for the first (4(15),7(11)) and the fourth (3,7(11)) peaks. Thus, it could be assumed that accurate δ^{13}C values were determined for these two compounds. On the other hand, being the second and third peaks co-eluted to a very small extent, no significant δ^{13}C value differences should be expected with respect to their relative enantiomer δ^{13}C values, according to Mosandl *et al*. [Mosandl 1995]. Conversely, a more positive δ^{13}C value was measured for the second eluted enantiomer with respect to the first eluted enantiomer of selina diene 4(15),7(11), viz., − 27.2‰ vs − 29.3‰. The same discrepancy, but with an opposite trend, was observed for the first eluted selina diene 3,7(11) enantiomer, with a more negative δ^{13}C value with respect to the second eluted enantiomer, viz., − 32.0‰ vs − 29.4‰. These findings suggest the occurrence of isotopic fractionation (as discussed earlier), with opposite trends for co-elutions affecting the initial (front) or final (tail) part of a peak. For this reason, the δ^{13}C values of these two compounds are not reported [Matucha 1991, Cucinotta 2021].

Components	*Es*	Futura 75 *ER%*		Felina 32 *ER%*		Tisza *ER%*	Kompolti *ER%*		Carmagnola *ER%*
***α*-pinene**	(-)	2.9	4.0	3.9	4.0	5.5	2.9	4.6	6.6
	(+)	97.1	96.0	96.1	96.0	94.5	97.1	95.4	93.4
***β*-pinene**	(-)	12.0	16.7	13.5	13.0	16.6	16.4	13.8	21.4
	(+)	88.0	83.3	86.5	87.0	83.4	83.6	86.2	78.6
limonene	(-)	28.7	59.5	39.9	64.4	70.0	63.1	75.3	79.0
	(+)	71.3	40.5	60.1	35.6	30.0	36.9	24.7	21.0
linalool	(-)	29.8	30.6	42.2		-	-		25.1
	(+)	70.2	69.4	57.8		-	-		74.9
***α*-terpineol**	(-)	17.0	41.7	50.8		53.1	-		55.5
	(+)	83.0	58.3	49.2		46.9	-		44.5
(E)-*β*-caryophyllene	(-)	100		100		100	100		100
	(+)	-		-		-	-		-
selina-4(15)-diene	(-/+)	38.8	43.7	40.5	41.4	44.8	40.8	41.0	42.8
	(-/+)	61.2	56.3	59.5	58.6	55.2	59.2	59.0	57.2
selina-3(11)-diene	(-/+)	38.9	44.0	36.6	41.3	44.7	35.1	37.2	40.8
	(-/+)	61.1	56.0	63.4	58.7	55.3	64.9	62.8	59.2
(E)-*β*-caryophyllene oxide	(-)	91.7	97.9	93.9	96.2	98.9	96.8	97.1	98.5
	(+)	8.3	2.1	6.1	3.8	1.1	3.2	2.9	1.5

Table 7.3. Enantiomeric ratios (ER %) ranges (divided for varieties) for genuine Cannabis sativa L. oils

Components	*Es*	Futura 75		Felina 32		Tisza	Kompolti		Carmagnola
		δ^{13}C		δ^{13}C		δ^{13}C	δ^{13}C		δ^{13}C
***α*-pinene**	(-)	-32.5	-26.1	-26.4		-33.8	-	-	-
	(+)	-32.3	-25.9	-30.8	-26.4	-32.9	-32.5	-30.8	-32.2
***β*-pinene**	(-)	-28.4		-	-	-	-	-	-
	(+)	-29.8	-23.0	-28.8	-23.1	-30.5	-30.3	-29.3	-32.2
limonene	(-)	-30.2	-28.0	-31.1		-32.5	-30.8		-33.6
	(+)	-33.8	-27.5	-31.3	-27.8	-32.9	-30.2		-33.2
linalool	(-)	-	-	-30.3		-	-		-32.1
	(+)	-30.3	-29.5	-30.6		-	-		-31.9
***α*-terpineol**	(-)	-30.7		-		-	-		-36.0
	(+)	-30.9	-30.2	-		-	-		-
(E)-*β*-caryophyllene	(-)	-28.0	-23.9	-27.7	-24.2	-28.9	-27.1	-26.8	-27.9
	(+)			-	-	-	-	-	-
selina-4(15)-diene	(-/+)	-29.3	-24.5	-27.8	-23.8	29.7	-29.1	-28.9	-28.7
	(-/+)	-	-	-	-	-	-	-	-
selina-3(11)-diene	(-/+)	-	-	-	-	-	-	-	-
	(-/+)	-29.4	-23.0	-28.9	-24.2	-31.2	-30.3	-29.4	-29.0
(E)-*β*-caryophyllene oxide	(-)	-28.9	-23.2	-28.9	-23.5	-29.7	-29.6	-29.5	-29.9
	(+)	-	-	-	-	-	-	-	-

Table 7.4 δ^{13}C ranges (divided for varieties) for the main components in genuine Cannabis sativa L. oils

7.3.5 Analysis of commercial samples

Nineteen commercial cannabis essential oils purchased from local stores were analysed. Among these, three oils were declared as genuine, while the remaining were labelled as reconstituted. The enantiomeric and $\delta^{13}C$ values determined for these samples are shown in Table 7.5. Among the three commercial oils labelled as genuine, all the samples showed chiral and isotopic behaviour similar to those of a genuine sample. Most chiral and isotopic ratios determined for the reconstituted oil samples were outside the ranges characteristic of the genuine samples. In some oils, the terpene fraction was represented mainly by α-pinene and (E)-β-caryophyllene, as in the case of samples 1–5, while other terpenes were found in very low concentrations or were absent. The enantiomeric ratios in all the reconstituted samples fell outside the range of genuineness: (-)-α-pinene enantiomer was > 70% in samples 1–8, and close to racemic values for samples 9–16, i.e., from 39.8 to 47.7% (while in the genuine samples the range was from 2.9 to 6.6%). The same inverted ratio was observed for β-pinene enantiomers, with values for the dextrorotatory enantiomers ranging from 2.0 to 11.6%, greatly below those of the genuine samples (78.6 to 88.0%). Similarly, (-)-linalool enantiomer was found at higher amount (> 66.0%) in all the commercial samples with respect to the genuine ones (< 42.2%). The enantiomeric ratio of (-)-limonene was similar for samples 1–5 (> 80.0%), while in the other cases very low ratios were observed (< 3.3%). Those values were in all cases outside the characteristic ranges of the genuine samples. Some of the reconstituted samples did not present α-terpineol, apart for samples 6, 10–14 and 16 where it was present almost in a racemic form. Selina-4(15),7(11) and selina-3,7(11) diene were not detected in all the reconstituted samples, while the enantiomeric ratio of β-caryophyllene oxide was in agreement with the genuine oil range. Finally, (E)-β-caryophyllene was determined only in the levo-rotatory form. Concerning the $\delta^{13}C$ values, the values for most components agreed with the isotopic data obtained for the genuine samples, apart for (E)-β-caryophyllene and β-caryophyllene oxide, which were both more negative. The latter evidence suggests the possible addition of exogenous (E)-β-caryophyllene to the commercial samples as one of the major oil terpenes. Such a hypothesis also gives a rationale for the more negative values determined for β-caryophyllene oxide, being it produced upon oxidation of (E)-β-caryophyllene.

Components	*Es*	Commercial Reconstituted EO *ER%*		Commercial Natural EO *ER%*		Commercial Reconstituted EO $\delta^{13}C$		Commercial Natural EO $\delta^{13}C$	
α-pinene	(-)	39.8	82.8	2.6	5.0	-30.4	-28.0	-32.1	-31.1
	(+)	60.2	17.2	97.4	95.0	-31.7	-28.3	-30.7	-30.1
β-pinene	(-)	88.4	98.0	11.9	19.5	-32.0	-28.6	-30.9	-30.2
	(+)	11.6	2.0	88.1	80.5	-31.9	-30.3	-30.3	-28.5
Limonene	(-)	0.9	95.1	42.8	54.7	-32.1	-27.2	-31.6	-30.5
	(+)	99.1	4.9	57.2	45.3	-30.7	-27.8	-32.3	-29.2
linalool	(-)	66.1	98.2	-		-31.5	-24.3	-	
	(+)	33.9	1.8	-		-29.9	-28.7	-	
α-terpineol	(-)	43.2	50.0	-		-30.8	-29.7	-	
	(+)	56.8	50.0	-		-30.6	-30.0	-	
(E)-β-caryophyllene	(-)	100		100		-35.8	-32.1	-28.1	-28.1
	(+)	-		-		-	-	-	-
selina-4(15)-diene	(-/+)	-		39.4	59.5	-		-29.1	-28.5
	(-/+)	-		60.6	42.5	-		-	-
selina-3(11)-diene	(-/+)	-		40.5	42.5	-		-	-
	(-/+)	-		59.5	57.5	-		-28.8	-28.3
(E)-β-caryophyllene oxide	(-)	98.0	100	96.5	98.6	-39.4	-36.6	-28.9	-28.5
	(+)	2.0	-	3.5	1.4	-	-	-	-

Table 7.5 Enantiomeric ratios (ER%) and $\delta^{13}C$ ranges obtained for the commercial Cannabis sativa L. oils, and their origin as declared on the label

7.4 Conclusion

In this research, the enantiomeric ratios and $\delta^{13}C$ values of main terpene constituents of different varieties of Cannabis sativa L. oils were determined, for the first time. A MDGC instrumentation and method were implemented, exploiting a combination of apolar (1D) and chiral (2D) stationary phases, with parallel MS and IRMS detection. The coupling of two separation mechanism allowed, at first instance, to resolve most of the co-elutions observed in a monodimensional analysis performed on any of the two columns.

A more in-depth analysis of the results revealed also the higher accuracy of the data detected/measured by the multidimensional approach, as a consequence of the increased peak separation.

The analysis of a set of commercial oils samples in some cases evidenced enantiomeric ratios and $\delta^{13}C$ values outside of the typical ranges of genuine oils.

Such findings suggest the usefulness of the Es-MDGC-C-IRMS/qMS method, as an effective tool to ascertain the genuineness and quality of these samples.

Current efforts are aimed to expand the dataset of oil samples investigated, in order to increase the statistical confidence of the genuineness ranges established for the key oil components.

References

Badea, S.L., Danet, A.F. Enantioselective stable isotope analysis (ESIA) — a new concept to evaluate the environmental fate of chiral organic contaminants. Sci Total Environ. 514 (2015) 459-466

Bicchi C, Binello A, D'Amato A, Rubiolo P. Reliability of Van den Dool retention indices in the analysis of essential oils. J Chromat Sci. 1999.

Bonaccorsi**,** I., Sciarrone, D., Cotroneo, A., Mondello, L., Dugo, P., Dugo, G. Enantiomeric distribution of key volatile components in Citrus essential oils, RBF 21:5 (2011) 841-849.

Cucinotta, L., De Grazia, G., Salerno, T. M. G., Donnarumma, D., Donato, P., Sciarrone, D., Mondello, L. Overcoming the lack of reliability associated to monodimensional gas chromatography coupled to isotopic ratio mass spectrometry data by heart-cut two-dimensional gas chromatography J. Chromatogr. A 1655 (2021) 462473

Do, T.K.T., Hadji-Minaglou, F., Antoniotti, S., Fernandez, X. Authenticity of essential oils, Trends Anal. Chem. 66 (2015) 146–157.

Dugo, P., Ragonese, C., Russo, M., Sciarrone, D., Santi, L., Cotroneo, A., Mondello, L. Sicilian Lemon Oil: Composition of Volatile and Oxygen Heterocyclic Fractions and Enantiomeric Distribution of Volatile Components, J. Sep. Sci. 33 (2010) 3374-3385.

Fiorini D, Scortichini S, Bonacucina G, Greco NG, Mazzara E, Petrelli R, Torresi J, Maggi F, Cespi M. Cannabidiol-enriched hemp essential oil obtained by an optimized microwave-assisted extraction using a central composite design. Ind Crops Prod. 2020.

Matucha, M., Jockisch, W., Verner, P., Anders, G. Isotope effect in gas—liquid chromatography of labelled compounds, J. Chromatogr. A 588 (1-2) (1991) 251–258

Micalizzi G, Alibrando F, Vento F, Trovato E, Zoccali M, Guarnaccia P, Dugo P, Mondello L. Development of a novel microwave distillation technique for the isolation of Cannabis sativa L. essential oil and gas chromatography analyses for the comprehensive characterization of terpenes and terpenoids, including their enantio-distribution. Molecules. 2021.

Mondello L, Casilli A, Tranchida PQ, Sciarrone D, Dugo P, Dugo G. Analysis of allergens in fragrances using multiple heart-cut multidimensional gas chromatography-mass Spectrometry. LC-GC Europe. 2008;21(3):130–7

Mondello L, Costa R, Sciarrone D, Dugo G. The chiral compound of citrus oils. In: Citrus oils. Composition, advanced analytical techniques, contaminants, and biological activity; Dugo, G, Mondello, L, editors; CRC Press Taylor & Francis Group: Boca Raton, FL, USA, 2010. pp. 349–403

Mosandl A, Hener U, Georg Schmarr H, Rautenschlein M. Chirospecific flavor analysis by means of enantioselective gas chromatography, coupled on-line with isotope ratio mass spectrometry. J High Resolut Chromatogr. 1990.

Mosandl A. Enantioselective capillary gas chromatography and stable isotope ratio mass spectrometry in the authenticity control of flavors and essential oils. Food Rev Int 11:4 (1995) 597–664.

Muccio Z, Wöckel C, An Y, Jackson G.P. Comparison of bulk and compound-specific δ 13 C isotope ratio analyses for the discrimination between cannabis samples. J. Forensic Sci 2012.

Reay MK, Knowles TDJ, Jones DL, Evershed RP. Development of alditol acetate derivatives for the determination of 15 N-enriched amino sugars by gas chromatography–combustion–isotope ratio mass spectrometry. Anal Chem. 2019.

Reichert, S., Fischer, D., Asche, S., Mosandl, A. Stable isotope labelling in biosynthetic studies of dill ether, using enantioselective multidimensional gas chromatography, online coupled with isotope ratio mass spectrometry, Flavour Fragr. J. 15 (2000) 303-308.

Sciarrone, D., Schepis, A., Zoccali, M., Donato, P., Vita, F., Creti, D., Alpi, A., Mondello, L. Multidimensional gas chromatography coupled to combustion- isotope ratio mass spectrometry/quadrupole ms with a low-bleed ionic liquid secondary column for the authentication of truffles and products containing truffle, Anal. Chem. 90 (2018) 6610–6617

Silfer JA, Engel MH, Macko SA, Jumeau EJ. Stable carbon isotope analysis of amino acid enantiomers by conventional isotope ratio mass spectrometry and combined gas chromatography/isotope ratio mass spectrometry. Anal Chem. 1991.

Sommano SR, Chittasupho C, Ruksiriwanich W, Jantrawut P. The cannabis terpenes. Molecules. 2020.

Ternelli M, Brighenti V, Anceschi L, Poto M, Bertelli D, Licata M, Pellati F. Innovative methods for the preparation of medical Cannabis oils with a high content of both cannabinoids and terpenes. J Pharm Biomed Anal. 2020.

Tranchida, P.Q., Sciarrone, D., Dugo, P., Mondello, L. Heart-cutting multidimensional gas chromatography: A review of recent evolution, applications, and future prospects, Anal. Chim. Acta 716 (2012) 66– 75.

Zhang L, Kujawinski DM, Federherr E, Schmidt TC, Jochmann MA. Caffeine in your drink: natural or synthetic? Anal Chem. 2012.

Chapter 8

A thorough compound specific isotopic, enantiomeric and quali-quantitative investigation of Moscato Giallo grapes by means of advanced analytical approaches

8.1 Introduction

Volatile organic compounds (VOCs) in grapevines (*Vitis vinifera* L.) include a wide range of molecules which are directly responsible for their varietal aroma. Dealing with Moscato varieties, in general, volatile composition is mainly represented by terpenoids (monoterpenes and sesquiterpenes), and in less content by volatile phenols, as well as aliphatic volatile compounds (aldehydes and alcohols with a six atom carbon chain). Regarding to terpene composition, they generally occur in two different forms, as free or glycosidically bound compounds. While free terpenes are directly responsible for grape aroma, bound terpenes are linked to sugar moieties and don't immediately contribute to the flavour. Once glicosyde is hydrolysed, aroma perception will be clearly enhanced by the higher amount of volatiles. In general, glycoside forms are higher in concentration with respect to free terpenes in grape berries [Mateo 2000]. Moreover, as extensively reported in literature [Flamini 2005, D'Onofrio 2016], the different terpene composition in grapes is influenced by many factors, including stage of ripening and clearly the variety itself. In the case of Moscato cultivars, aroma is mainly composed by terpenols, as linalool, geraniol, nerol, citronellol and diols, delivering a typical floral flavour. However, their different quantitative distribution is often responsible for the distinct sensorial perception of a specific variety, as in the case of linalool for Moscato Giallo [Flamini 2005, D'Onofrio 2016, Nicolini 2013].

In order to evaluate grape berries' volatile fraction, gas chromatography coupled to mass spectrometry (GC-MS) is usually performed on grape berries extracts. Due to the relative low concentration of terpenes in berries (≤ 1mg/kg), a concentration step is usually needed after extraction. However, nowadays, newer analytical methods allow overcoming this limitation. Recently, Paolini *et al*., described a suitable fast gas-chromatographic approach combined with tandem mass spectrometry for the determination of the main VOCs in oenological products

[Paolini 2018]. The higher sensitivity achieved allows avoiding previous concentration steps, saving time, also in terms of chromatographic run.

However, alongside an extensive quali-quantitative characterization, more specific approaches are aimed to investigate in depth the biochemical pathways of the plant of origin. Among the analytical techniques, enantio selective gas chromatography (Es-GC) is surely one of the most recognized methods to these aims. While terpenes quali-quantitative composition has been extensively investigated in grapes and oenological products, their enantiomeric distribution has been little explored in literature [Luan 2006, Song 2015]. Since plants biosynthesise their chiral metabolites in specific enantiomeric excesses, typical trends can be described by evaluating their enantiomeric separation in a suitable GC column. Once enantiomeric ratios for natural chiral metabolites are determined, this criterion can be used for genuineness assessment as well as for the differentiation among varieties and by other natural matrices.

In parallel, gas chromatography coupled to isotopic ratio mass spectrometry (GC-C-IRMS) is an equally acknowledged approach for the authenticity assessment of a wide range of natural products [Camin 2016]. In detail, in relation to the different uptake of CO_2, the evaluation of $\delta^{13}C$ allows to distinguish between C_3 and C_4 plants, as well as in many cases by synthetic products [Sciarrone 2018].

Due to the capabilities of both techniques to explore specific traits of the plant, the simultaneous detection of enantiomeric and isotopic ratio in an Es-GC-C-IRMS method should be considered the most affordable approach. As a consequence, chiral and isotopic information of the target compounds can be achieved in a single gas chromatographic run. In literature, Mosandl [Mosandl 1990] first demonstrated the suitability of this technique, differentiating synthetic and natural γ-decalactone by the evaluation of the $\delta^{13}C$ of both enantiomers. Nevertheless, in literature, starting from this first application, very few works were published by these means [Silfer 1991, Badea 2015, Reichert 2000, Cucinotta 2022]. In this concern, in spite of the advantages associated to this method, a series of limitations justify the scarce information over the last decades. Whilst the choice of the correct chiral column is surely a basic requirement to guarantee the separation of enantiomers each other, however it may be insufficient, due to possible co-elutions with other interfering compounds.

In this regard, if a minimal co-elution may be not significant for the determination of enantiomeric ratios, since they can be still calculated in single ion monitoring (SIM) or extracted ion modes, differently for isotopic evaluation it represents a critical issue, given that all the organic matter is

burnt to CO_2. An even more limiting problem is related to the different distribution of ^{13}C and ^{12}C isotopes along an entire peak of CO_2. Due to different Van der Vaals forces, ^{13}C isotope precedes ^{12}C of about 150 ms, leading to wrong isotopic determinations if peaks co-elute [Meier Augenstein 1999, Matucha 1991]. As recently reported by our research group [Cucinotta 2021], a co-elution involving the first part of the peak will lead to more negative $\delta^{13}C$ values; differently, more positive $\delta^{13}C$ values will be detected if the co-elution affects the tail. In each case, unreliable results would be obtained. To overcome these limitations, multidimensional gas-chromatography (MDGC) exploited in heart cut mode can provide an improved resolution, prior to the IRMS detection. To these aims, a novel enantio MDGC-C-IRMS/qMS method was developed in order to guarantee a baseline separation of target compounds.

For this application, seventeen grape samples belonging to Moscato Giallo variety were collected in Trentino and Veneto along months of September and October 2021. Alongside a deep quali-quantitative investigation by means of fast GC-QqQ/MS approach, a simultaneous detection of the enantiomeric and isotopic ratio of the main aromatic terpenes was performed. To the best of authors' knowledge, it is the first time that $\delta^{13}C$ values of the main terpene compounds in grape berries are reported in literature.

8.2 Materials and methods

8.2.1 Sample preparation, extraction and concentration

Seventeen different Moscato Giallo grape varieties were collected from Trentino Alto Adige and Veneto along the months of September and October 2021 from local farmers. The choice of a specific grape aromatic variety limited the total amount of samples investigated, although current efforts are done to increase them. For each sample, 200 grape berries were collected with pedicles from bunches and stored at -20°C, prior to the extraction performed by SPE cartridges (ENV+, 1g). For the extraction procedure, primarily 0.2 mL of a mixture of 1-heptanol and ethyl 3-hydroxybutyrate, 0.5 g of gluconolactone and 0.2 mL of nonyl-β-D-glucopyranoside were added, as reported elsewhere in literature [Paolini 2018, Gunata 1985], to 50 mL of the sample homogenate, and diluted to 100 mL with Milli-Q water. Their addition allowed to monitor the amount of both free and conjugated VOCs extracted. Once SPE cartridges were activated with 20 mL of methanol and 25 mL of Milli-Q water, samples were loaded to perform the extraction by adsorption. Free VOCs were eluted with 30 mL of dichloromethane in a 100 mL glass boiling flask, dried with anhydrous sodium sulphate, while an aliquot was picked up for GC-MS/MS

analysis. For the concentration step, 60 mL of pentane were added into the glass boiling flask for the formation of a low boiling azeotropic mixture. Concentration was thus performed in a bath at 40°C until 1.0 mL volume, prior to IRMS analysis. Glycosidic VOCs were eluted with 30 mL of methanol, and this solution was first dried using a rotavapor and then dissolved in 4.5 mL of citrate buffer at pH 5 of an enzyme with glycosidase activity (AR 2000 at 70 mg/mL in water). The solution was thus kept in a bath at 40°C overnight to allow the release of the volatile compounds from the glycosidic bond. After that, 0.2 mL of a mixture of 1-heptanol and ethyl 3-hydroxybutyrate were added, and the VOCs were then extracted with SPE cartridges, and eluted with dichloromethane, as reported for free VOCs. After the extraction an aliquot was picked up for GC-MS/MS analysis, while the concentration step, as for free VOCs, allowed to obtain a final volume of 1.0 mL. For enantio MDGC-C-IRMS analysis, free and bound VOCs were merged in order to obtain a proper signal for IRMS detection.

8.2.2 GC-MS/MS conditions

Volatile organic compounds were analysed by using an Agilent Intuvo 9000 GC system coupled with an Agilent 7000 Series Triple Quadrupole MS equipped with an electron ionisation source operating at 70 eV. The filament current was 50 μA. Separation was obtained by injecting 2 μL in split mode (1:5) into a DB-Wax Ultra Inert (20 m × 0.18 mm id × 0.18 μm film thickness) capillary column with constant He flow of 0.8 mL/min. The injector temperature was set at 250°C. The oven temperature was programmed starting at 40°C for 2 minutes, raised to 55°C by 10°C/min, then raised to 165°C by 20°C/min, and finally raised to 240°C by 40°C/ min and held at this temperature for 5 minutes.

The mass spectra were acquired in dynamic multiple reaction monitoring (dMRM) mode using N_2 as collision gas (flow of 1.5 mL/min) and in Full Scan mode (mass range 33 - 400 m/z). The transfer line and source temperature were set at 250°C and 230°C, respectively.

Data acquisition and analysis were performed using the Agilent Technologies MassHunter Workstation software – Data Acquisition (ver. B.07.06) and the Agilent MassHunter Workstation Software – Quantitative Analysis (ver. B.08.00), respectively.

8.2.3 GC-C-IRMS conditions

GC-C-IRMS analysis were led to evaluate carbon isotopic fractionation for the standards investigated. The instrument was equipped with an auto-sampler (Triplus, Thermo Scientific), a Trace GC Ultra (GC IsoLink + ConFlo IV, Thermo Scientific) interfaced with an isotope ratio mass spectrometer (DELTA V, Thermo Scientific) by means of an open split interface and, in parallel, to a single-quadrupole GC-MS (ISQ Thermo Scientific). GC separation was performed

on a Phenomenex Zebron-Wax 30 m × 0.32 mm i.d. × 0.5 μm d_f with the following temperature program: 40°C (3 min) to 55°C at 3°C/min, to 165°C at 5°C/min, and finally to 240°C (8.5 min) at 10°C min. Injection was performed maintaining injection port at 260°C, and by injecting 2 μL in splitless mode with helium as carrier gas at a flow of 2 mL/min. Ion source and transfer line temperature were maintained at 250°C, while combustion chamber temperature was set to 1000°C.

8.2.4 MDGC-C-IRMS/qMS conditions

The main structure of the MDGC-C-IRMS/qMS prototype was already described in previous works [Sciarrone 2018, Cucinotta 2021, Cucinotta 2022]. Split/splitless injector was maintained at 280°C, in splitless mode for 1 min, with a constant helium flow of 1.0 mL/min at the following pressure program: 184 kPa (1 min) to 275 kPa at 1.89 kPa/min and finally to 330 kPa at 5.68 kPa/min. A SLB-5 ms 30 m × 0.25 mm i.d. × 0.25 μm d_f (Merck Life Science, Darmstadt, Germany) column was used in the 1D with the following temperature program: 40 °C (1 min) to 184 °C at 3°C/min, finally to 330 °C at 15°C/ min. FID1 was maintained at 330°C, with a constant 40.0 mL/min H_2 flow and 400 mL/min air flow rate, with a sampling rate of 80 ms equal to 12.5 Hz. GC2 was equipped with a MEGA-DEX ASX 1 chiral column 25 m × 0.25 mm i.d. × 0.25 μm df (MEGA, Milano, Italy), and the temperature was ramped as follows: 40°C (11 min) to 142 (5 min) °C at 3°C/min and finally to 210°C at 8°C/min. The 2D qMS ion source and interface temperature were maintained at 200 °C; the mass range 40-400 *m/z* was monitored at an acquisition speed of 10 Hz. A pressure program was applied also to the APC device in order to maintain a similar carrier flow in the 2D dimension (≈1 mL/min): 140 kPa (11 min) to 193 kPa at 1.39 kPa/min and finally to 265 kPa at 9.8 kPa/min. After the MDGC separation, the compounds eluted from the second column were splitted through a zero dead-volume tee-union (Valco) to the combustion chamber and therefore to the IRMS system via a 0.85 m × 0.25 mm i.d. uncoated column and to the qMS via a 1.5 m × 0.1 mm i.d. uncoated column. Apart for the IRMS, all data were acquired by the MDGC solution control software package (Shimadzu, Kyoto, Japan) allowed to setup the Deans Switch device parameters and to monitor both the GC1 (FID1) and GC2 (qMS), together. The VisION IRMS (Elementar Analysensysteme GmbH, Langenselbold, Germany) was a bench top 5 kV system equipped with a monitoring gas delivery system. The combustion chamber, maintained at 850°C, was provided with a high performing silicon carbide tube furnace for the quantitative, fractionation-free conversion of the compounds to pure gases (CO_2 and H_2O). The CO_2 produced by pyrolisis of each component was transferred to the IRMS, and the water was removed through a nafion membrane. The following settings were applied to the VisION system: acceleration voltage, 3797.66 V; trap current, 600.000 μA; magnet current, 3700.000 mA. An electron-impact ionization (EI) gas source, a variable field, stigmatically focused electromagnet

for beam separation and multi-channel Faraday collectors set at 44, 45, 46 m/z for beam detection were used. IRMS results were collected by IonOS stable isotope data processing software ver. 3.0.0.5196 (Elementar Analysensysteme GmbH, Langenselbold, Germany); the apex track integration method was exploited to automatically find the correct starting and finishing point of the peaks. All the analysis were led in triplicate and standard deviations for IRMS measurements were found to be under < 0.5.

8.3. Results and discussion

8.3.1 Quali-quantitative analysis by means of fast GC-QqQ/MS

Although Moscato Giallo is broadly recognized as one of the most typical aromatic grape varieties, few information is reported in literature about the characteristic terpenic profile, responsible for the aroma [Flamini 2005]. However, some traits are distinctive with respect to other grape varieties, critical to provide an unambiguous sensorial differentiation. In general, the high concentration of terpenols represent a common characteristic in Moscato specie, while their relative amount allows to distinguish between specific varieties[Flamini 2005, Versini 1993].

In a first step, the quali-quantitative evaluation of the 17 samples of Moscato Giallo grapes was achieved exploiting fast GC-QqQ/MS (see Table 8.1) according to Paolini *et al*. [Paolini 2018], which applied this method to different oenological products as wine and grape must.

After the extraction process the aroma profile of the grapes was evaluated in its entirety, since it is composed by both free (Table 8.1) and bound components (Table 8.2). In details, the targeted analysis revealed the presence of 28 free and 26 glycosidically bound with sugar moieties target compounds.

	Volatile Organic Compounds free forms (mg/Kg)																
	1	**2**	**3**	**4**	**5**	**6**	**7**	**8**	**9**	**10**	**11**	**12**	**13**	**14**	**15**	**16**	**17**
1-hexanol	0,08	0,05	0,09	0,08	0,10	0,13	0,16	0,08	0,08	0,11	0,07	0,05	0,12	0,10	0,06	0,08	0,10
trans-3-hexen-1ol	0,10	0,05	0,07	0,06	0,09	0,10	0,15	0,08	0,08	0,09	0,06	0,04	0,09	0,11	0,03	0,09	0,09
cis-3-hexen-1ol	0,09	0,07	0,10	0,10	0,09	0,12	0,12	0,08	0,09	0,10	0,06	0,07	0,12	0,10	0,08	0,09	0,09
2-phenylethanol	0,01	0,01	0,02	0,01	0,01	0,01	0,01	0,01	0,01	0,01	0,01	0,01	0,01	0,01	0,01	0,01	0,01
benzyl alcohol	0,01	0,02	0,02	0,02	0,01	0,02	0,02	0,01	0,01	0,01	0,02	0,01	0,01	0,02	0,01	0,01	0,02
linalol oxide A-trans	0,11	0,19	0,13	0,12	0,09	0,12	0,17	0,15	0,14	0,08	0,17	0,08	0,10	0,06	0,05	0,09	0,20
linalol oxide B-cis	0,11	0,19	0,09	0,12	0,06	0,16	0,10	0,13	0,13	0,06	0,11	0,05	0,08	0,03	0,03	0,06	0,14
linalool	1,42	1,77	0,99	1,06	0,91	0,99	1,31	1,52	1,23	0,96	1,25	0,69	1,28	0,41	0,26	0,81	1,91
alpha-terpineol	0,01	0,02	0,01	0,01	0,01	0,01	0,01	0,02	0,02	0,01	0,01	0,01	0,01	0,00	0,00	0,01	0,02
terpinen-4-ol	0,01	0,01	0,01	0,01	0,01	0,01	0,01	0,01	0,01	0,01	0,01	0,01	0,01	0,01	0,01	0,01	0,01
beta-citronellol	0,00	0,01	0,01	0,01	0,01	0,01	0,01	0,01	0,00	0,00	0,01	0,00	0,01	0,00	0,00	0,01	0,01
nerol	0,01	0,01	0,01	0,01	0,01	0,01	0,02	0,01	0,01	0,01	0,01	0,01	0,01	0,01	0,02	0,01	0,01
geraniol	0,05	0,06	0,07	0,08	0,03	0,05	0,06	0,04	0,04	0,04	0,05	0,05	0,06	0,06	0,11	0,06	0,06
geranic acid	0,02	0,02	0,03	0,03	0,01	0,02	0,03	0,02	0,01	0,02	0,02	0,02	0,02	0,02	0,02	0,02	0,03
rose oxide I	0,01	0,01	0,01	0,01	0,01	0,01	0,01	0,01	0,01	0,01	0,01	0,01	0,01	0,01	0,01	0,01	0,01
rose oxide II	0,01	0,01	0,01	0,01	0,01	0,01	0,01	0,01	0,01	0,01	0,01	0,01	0,01	0,01	0,01	0,01	0,01
benzaldehyde	0,01	0,01	0,01	0,01	0,01	0,01	0,01	0,01	0,01	0,01	0,01	0,01	0,01	0,01	0,01	0,01	0,01
methyl salycilate	0,01	0,01	0,01	0,01	0,01	0,01	0,01	0,01	0,01	0,01	0,01	0,01	0,01	0,01	0,01	0,01	0,01
zingerone	0,01	0,01	0,01	0,01	0,01	0,01	0,01	0,01	0,01	0,01	0,01	0,01	0,01	0,01	0,01	0,01	0,01
limonene	0,01	0,01	0,01	0,01	0,01	0,01	0,01	0,01	0,01	0,01	0,01	0,01	0,01	0,01	0,01	0,01	0,01
beta-myrcene	0,01	0,02	0,02	0,01	0,01	0,01	0,01	0,02	0,01	0,02	0,02	0,01	0,02	0,01	0,01	0,01	0,02
HO-trienol	0,03	0,05	0,02	0,03	0,01	0,01	0,03	0,02	0,03	0,01	0,01	0,02	0,02	0,01	0,01	0,01	0,03
linalol oxide C-trans	0,30	0,51	0,35	0,35	0,30	0,55	0,48	0,35	0,32	0,32	0,51	0,26	0,34	0,17	0,15	0,25	0,56
linalol oxide D-cis	0,13	0,18	0,12	0,15	0,11	0,20	0,14	0,16	0,14	0,11	0,14	0,11	0,11	0,07	0,08	0,13	0,15
HO-diolo I	0,28	0,41	0,36	0,39	0,15	0,21	0,58	0,36	0,44	0,23	0,30	0,17	0,26	0,18	0,13	0,25	0,74
HO-diolo II	0,25	0,43	0,27	0,25	0,19	0,93	0,42	0,21	0,29	0,27	0,39	0,24	0,29	0,09	0,16	0,14	0,33
8-Hydroxylinalool trans	0,11	0,15	0,13	0,11	0,11	0,10	0,20	0,11	0,12	0,08	0,19	0,08	0,11	0,06	0,05	0,08	0,18
8-Hydroxylinalool cis	0,02	0,04	0,02	0,02	0,03	0,04	0,03	0,03	0,02	0,02	0,02	0,03	0,03	0,02	0,02	0,03	0,04

Table 8.1 quali-quantitative profile of the free volatile organic compounds in Moscato Giallo grape berries

	Volatile Organic Compounds bound forms (mg/Kg)																
	1	**2**	**3**	**4**	**5**	**6**	**7**	**8**	**9**	**10**	**11**	**12**	**13**	**14**	**15**	**16**	**17**
1-hexanol	0,02	0,02	0,02	0,02	0,01	0,01	0,01	0,01	0,02	0,03	0,02	0,02	0,03	0,01	0,02	0,02	0,01
trans-3-hexen-1ol	0,01	0,01	0,01	0,01	0,01	0,01	0,01	0,01	0,01	0,01	0,01	0,01	0,01	0,01	0,01	0,01	0,01
cis-3-hexen-1ol	0,01	0,01	0,01	0,01	0,01	0,01	0,01	0,01	0,01	0,01	0,01	0,01	0,01	0,01	0,01	0,01	0,01
2-phenylethanol	0,04	0,05	0,05	0,03	0,04	0,07	0,04	0,03	0,04	0,06	0,05	0,05	0,05	0,04	0,04	0,05	0,03
benzyl alcohol	0,05	0,06	0,07	0,04	0,05	0,12	0,06	0,04	0,05	0,08	0,08	0,07	0,08	0,07	0,06	0,07	0,06
linalol oxide A-trans	0,08	0,09	0,06	0,07	0,05	0,14	0,09	0,07	0,07	0,08	0,11	0,05	0,09	0,05	0,05	0,05	0,12
linalol oxide B-cis	0,03	0,03	0,02	0,03	0,02	0,05	0,02	0,03	0,03	0,02	0,04	0,02	0,03	0,02	0,01	0,02	0,04
linalool	0,15	0,18	0,10	0,10	0,09	0,21	0,14	0,09	0,09	0,25	0,17	0,13	0,28	0,07	0,14	0,10	0,13
alpha-terpineol	0,03	0,03	0,02	0,02	0,02	0,03	0,03	0,03	0,03	0,03	0,03	0,02	0,04	0,02	0,02	0,03	0,03
terpinen-4-ol	0,01	0,01	0,01	0,01	0,01	0,01	0,01	0,01	0,01	0,01	0,01	0,01	0,01	0,01	0,01	0,01	0,01
beta-citronellol	0,01	0,01	0,01	0,01	0,01	0,01	0,01	0,01	0,01	0,01	0,01	0,01	0,01	0,01	0,01	0,01	0,01
nerol	0,10	0,12	0,14	0,09	0,08	0,25	0,13	0,06	0,10	0,16	0,11	0,16	0,15	0,10	0,20	0,28	0,08
geraniol	0,35	0,54	0,46	0,36	0,33	0,91	0,41	0,22	0,39	0,58	0,39	0,48	0,61	0,41	0,68	1,09	0,25
geranic acid	0,21	0,28	0,24	0,14	0,16	0,36	0,26	0,15	0,21	0,37	0,27	0,24	0,27	0,17	0,28	0,25	0,25
rose oxide I	0,01	0,01	0,01	0,01	0,01	0,01	0,01	0,01	0,01	0,01	0,01	0,01	0,01	0,01	0,01	0,01	0,01
rose oxide II	0,01	0,01	0,01	0,01	0,01	0,01	0,01	0,01	0,01	0,01	0,01	0,01	0,01	0,01	0,01	0,01	0,01
benzaldehyde	0,01	0,01	0,01	0,01	0,01	0,01	0,01	0,01	0,01	0,01	0,01	0,01	0,01	0,01	0,01	0,01	0,01
methyl salycilate	0,01	0,01	0,01	0,01	0,01	0,01	0,01	0,01	0,01	0,01	0,01	0,01	0,01	0,01	0,01	0,01	0,01
zingerone	0,01	0,01	0,01	0,01	0,01	0,01	0,01	0,01	0,01	0,01	0,01	0,01	0,01	0,01	0,01	0,01	0,01
HO-trienol	0,03	0,03	0,01	0,01	0,01	0,01	0,04	0,02	0,02	0,01	0,02	0,02	0,01	0,02	0,02	0,03	0,01
linalol oxide C- trans	0,02	0,01	0,01	0,01	0,01	0,02	0,03	0,02	0,02	0,02	0,02	0,02	0,02	0,02	0,02	0,02	0,03
linalol oxide D- cis	0,02	0,04	0,03	0,02	0,02	0,03	0,03	0,03	0,03	0,04	0,03	0,05	0,03	0,02	0,03	0,03	0,04
HO-diolo I	0,27	0,37	0,30	0,25	0,16	0,31	0,51	0,16	0,32	0,29	0,47	0,24	0,37	0,22	0,24	0,19	0,47
HO-diolo II	0,02	0,03	0,01	0,01	0,01	0,08	0,02	0,01	0,01	0,04	0,03	0,02	0,03	0,01	0,02	0,02	0,02
8-Hydroxylinalool trans	0,35	0,46	0,37	0,29	0,22	0,52	0,60	0,22	0,49	0,54	0,49	0,42	0,51	0,27	0,29	0,38	0,45
8-Hydroxylinalool cis	0,17	0,24	0,16	0,15	0,11	0,83	0,20	0,10	0,20	0,25	0,17	0,20	0,24	0,13	0,20	0,23	0,15

Table 8.2 Quali-quantitative profile of the bound volatile organic compounds in Moscato Giallo grape berries

With respect to previous literature findings [Flamini 2005, Versini 1993], a higher amount of the free fraction was found with respect to the glycosidic forms in most of the samples even if their relative distribution may depend by several factors, as the ripening stage of berries or breeding.

Dealing with terpenols, linalool was the main compound in almost all the Moscato Giallo samples. In detail, the free form was much more concentrated than its relative bound form, responsible for the typical floral aroma. Only in Sample 16, geraniol was unexpectedly higher in concentration, both in the glycosidic and free forms. Differently from the linalool distribution, the geraniol-bound form was higher in concentration than the free one in all the samples investigated. To the best of our knowledge, among the few recent references about Moscato volatiles in grapes, data dealt with the principal aroma components of the different varieties [Flamini 2005, Versini 1993]. Only the

report by Nicolini *et al*. [Nicolini 2013] provided an in-depth study on the relative composition of the volatile terpenol fractions of different oenological products. According to this study, a similar relative composition should be expected between grape and wine [Nicolini 2013]. The data achieved of all the grape samples investigated in the present study were consistent with these findings, confirming a similar volatile profile between Moscato Giallo grape and wine. In detail, higher concentrations of the linalool oxide pyranoid forms were observed with respect to the furanoid ones and of the *trans* oxide derivatives with respect to the *cis* ones. Dealing with diols, 3, 7-octadiene-2,6-diol-2,6-dimethyl (ho-diolo I) was always predominant with respect to 1,7-octadiene-3,6-diol-2,6-dimethyl (ho-diolo II), as well as for 8-hydroxylinalool *trans* with respect to the *cis* form.

According to the quali/quantitative results of the volatile fraction, the main terpenols were further investigated by means of isotopic and chiral analyses (Section 8.3.3).

8.3.2 Evaluating the carbon isotopic fractionation along the concentration process

While for quali-quantitative analysis, samples were analysed after the extraction process, for the isotopic analysis an additional concentration step was required. Given the lower natural relative abundance of about 100 times of ^{13}C than ^{12}C, an isotopic ratio mass spectrometer suffers of renowned higher detection limits than a common MS, which have often limited its application. As a direct consequence, scarce information are reported in literature about the $\delta^{13}C$ value for samples having very low concentrated key compounds, as in the case of terpenes in Moscato grapes. To these aims, a concentration process was mandatory after the extraction procedure in order to obtain a proper amount of analytes for isotopic analysis. As reported in section 8.2.1, an azeotropic mixture was prepared adding 60 mL of pentane to the CH_2Cl_2 extract and brought to a boil in a bath at 40°C until 1.5 mL volume. Concentration allowed to increase the relative amount of terpenes prior to IRMS detection, by reducing solvent total volume. However, since evaporation requires the overcoming of intermolecular forces, solute losses may happen besides solvent evaporation. This phenomenon may clearly involve in carbon isotopic fractionation, leading to a different $^{13/12}C$ distribution. Isotopic fractionation during evaporation may be considered the result of a preferential removal of molecules containing the lighter isotope (^{12}C), with respect to the heavier one (^{13}C) [Bouchard 2008, Shin 2010]. It's clear how such conditions may largely affect the reliability of the isotopic measurements for the key components investigated. To these aims, preliminary tests needed to be led before the analysis of real samples. In this concern, a mixture of three terpene standards, namely eucalyptol, geraniol and linalool, was prepared in CH_2Cl_2 with the

aim to simulate sample concentration process. While eucalyptol was chosen for its relative lower boiling temperature, linalool and geraniol were investigated being among the main terpenes in Moscato Giallo samples. During the boiling process, aliquots were picked up at different times (t_1, t_2…t_5) until the final volume (t_6). Each solution was thus analysed in triplicates (SD < 0.5 ‰) to monitor possible isotopic shifts with respect to isotopic data of the starting solution (t_0) (Figure 8.1).

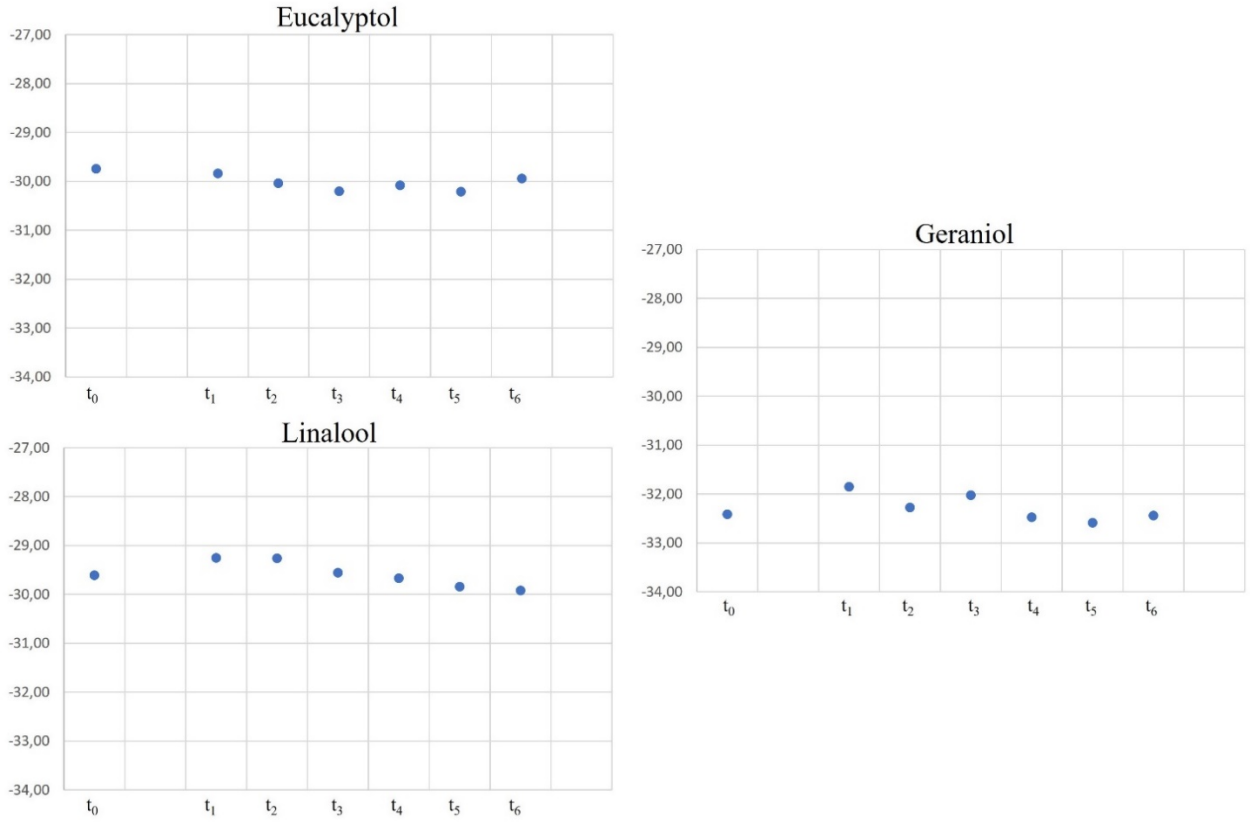

Figure 8.1 Correlation between the $\delta^{13}C$ value along the concentration step for eucalyptol, linalool and geraniol; t_0: starting volume, t_6: final volume (≈ 1.5 mL)

As showed in all the graphs, no relevant isotopic differences (always < ±0.5 ‰) were found with respect to the starting solution (t_0) for all the terpenes. These findings confirmed the lack of isotopic fractionation along the concentration step, allowing the isotopic measurements of real samples.

8.3.3 Monodimensional GC chiral analysis and the development of an enantio MDGC-C-IRMS/qMS approach

For quali-quantitative analysis the coupling of tandem mass spectrometry to monodimensional GC provided an increased resolution power (Section 8.3.1), thanks to the selection of specific MRM transitions for the target analytes. Differently, for isotopic ratio mass spectrometry it was unfeasible, since the $\delta^{13}C$ is determined after the combustion of all the organic matter to carbon

dioxide. Unlike other conventional MS approaches, where it is still possible to operate in selected ion monitoring or exploiting extracted ion mode, for IRMS detection the oxidation of key compounds to CO_2 will delete any structural information. Moreover, a partial peak integration would compromise the reliability of the measurement, due to the renowned chromatographic isotopic effect along a peak of CO_2 [Cucinotta 2021, Matucha 1991]. Dealing with monodimensional conditions (GC-C-IRMS), this configuration would lead to a series of limitations in the case of co-elutions. Recently our research group demonstrated the limitations of a monodimensional Es-GC approach hyphenated to an isotopic ratio mass spectrometer in the analysis of real samples [Cucinotta 2022]. Although the choice of a specific chiral column may guarantee the baseline separation of target enantiomers each other, co-elutions may involve with adjacent achiral components. This case was evident also in Moscato Giallo grape samples. Figure 8.2 shows co-elutions occurring in a monodimensional chiral profile for some specific samples. Although the selected chiral column, namely the MEGA DEX ASX-1 phase, allowed the separation of the enantiomers of a chiral couple each other, co-elutions occurred with other interfering peaks. As visible in Figure 8.2A, although linalool enantiomers were efficiently separated each other, a co-elution involved with an interfering peak for 3S-linalool. The same issue was evident for (E)-3S-linalool-8-hydroxy, which strongly co-elute with another interfering compound on the tail. In this concern, despite the potential to simultaneously determine isotopic and chiral ratio of key compounds, the presence of overlapping compounds severally limits the reliability of both the measurements.

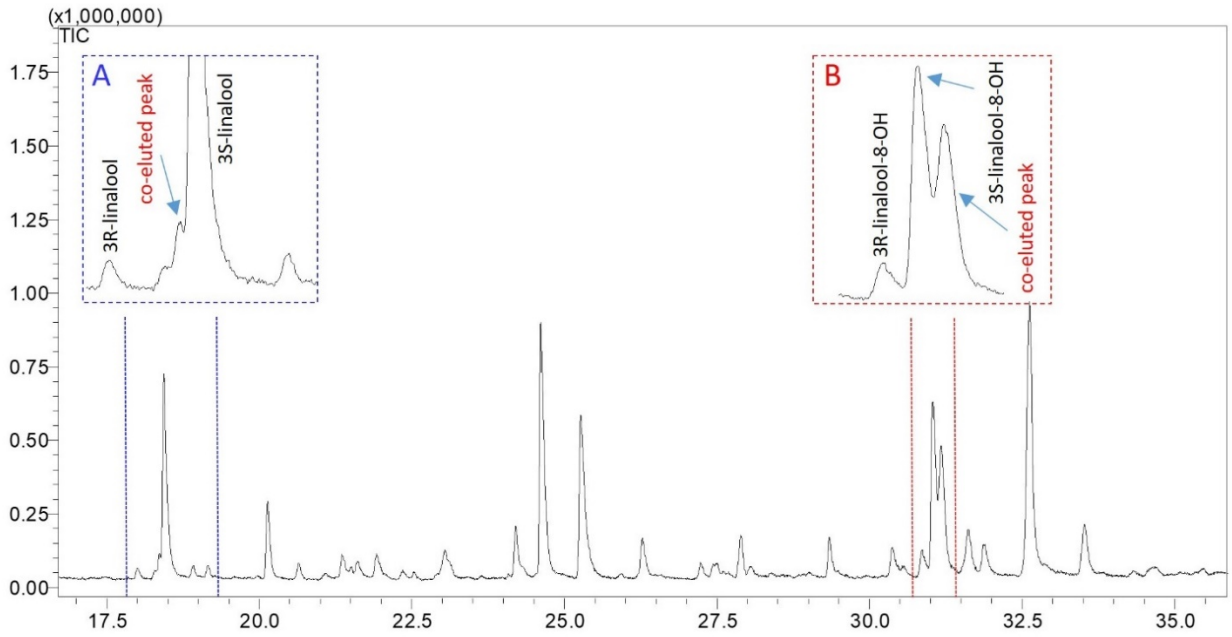

Figure 8.2: Monodimensional chiral GC/MS analysis of a Moscato Giallo grape extract: dashed (blue) lines highlight a co-elution for 3S-linalool; dashed (red) lines highlight a co-elution for 3S-linalool-8-OH

As already demonstrated in a previous work [Cucinotta 2021], also a little co-elution for IRMS detection may involve in unreliable isotopic results, as well as in a reduced repeatability. In detail, a co-elution on the tail will involve in a wrong more positive $\delta^{13}C_{VPDB}$ with respect to conditions of baseline separation, as for the case of (E)-3S-linalool-8-hydroxy, due to the depletion of ^{12}C at that level. Conversely, a co-elution on the first part of the peak, as for the case of 3S-linalool, will reduce the amount of ^{13}C at that level, resulting in a wrong more negative $\delta^{13}C_{VPDB}$ value. It is noteworthy how these drawbacks have involved in very few literature references in this field [Mosandl 1990, Badea 2015]. Consequently, due to the limitations of a monodimensional approach, a multidimensional GC method was developed to achieve an efficient separation. In this concern, with the aim to guarantee not only a baseline resolution from the interfering compounds, but also the separation of each chiral terpene in its two enantiomers, an appropriate chiral column was chosen. Multidimensional conditions were thus optimized employing an apolar column in the ^{1}D and the chiral cyclodextrin stationary phase in the ^{2}D. The high reproducibility in terms of retention times on apolar columns [Bicchi 1999] allowed to choose specific and narrow cut windows for the transfer of target terpenols after the ^{1}D FID stand-by analysis (Figure 8.3) for each sample. Pressure conditions, both for AFC and APC, as well as related linear velocities were optimized in order to guarantee a complete transfer of the heart cut fractions from ^{1}D to ^{2}D, mandatory to avoid isotopic fractionation. Among the different components, the most

representative Moscato Giallo terpenes were selected for multiple heart cuts, for further separation on the ^{2}D chiral column, namely linalool, linalool oxide trans pyranoid, geraniol, 3, 7-dimethylocta-1, 7-dien-3, 6-diol and (E)-linalool-8-hydroxy. After the ^{2}D separation, eluate from the chromatographic system was split to the IRMS and to the qMS. Parallel ^{2}D qMS detection allowed to confirm the identity of the compounds transferred from the ^{1}D, by comparing MS experimental spectra on spectral similarity databases (FFNSC 4.0).

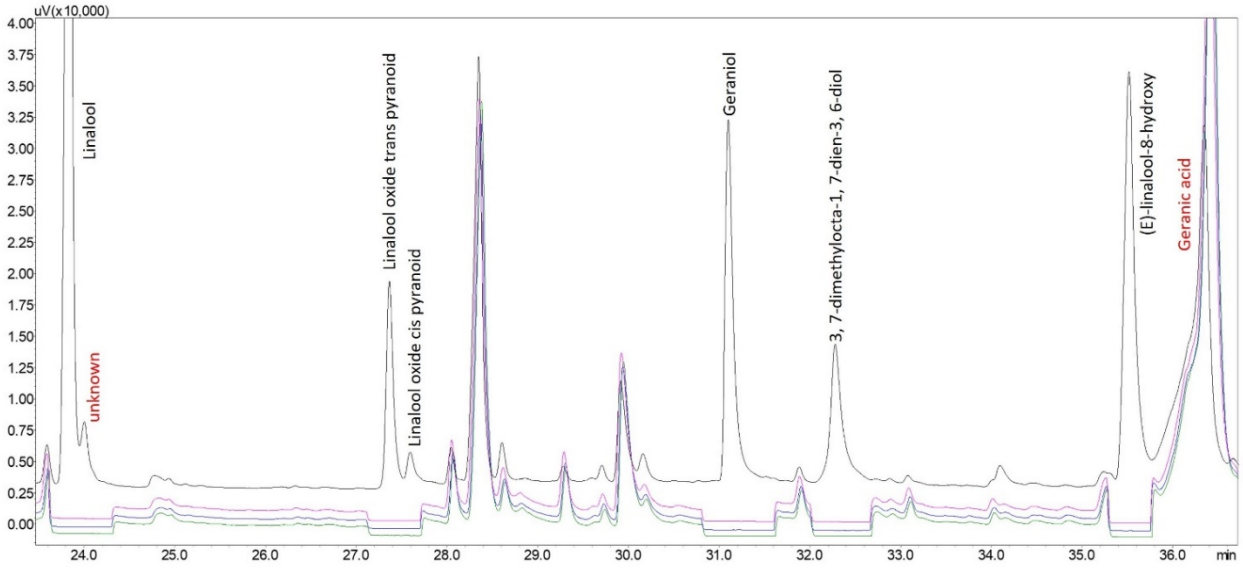

Figure 8.3 Comparison between a ^{1}D stand-by analysis (black trace) and ^{1}D cut ones (pink, blue, green traces) for a Moscato grape extract.

Figure 8.4 shows the ^{2}D profile after the multidimensional separation. Although the selected terpenols were co-eluted in the ^{1}D stand-by on the apolar column (Figure 8.3), an efficient separation was achieved (Figure 8.4). The complementary selectivity of the selected stationary phases allowed overcoming the limitations of a monodimensional analysis, achieving the simultaneous determination of both enantiomeric and isotopic ratio. As illustrated, both the enantiomers of linalool were properly resolved from the main co-eluted compound in the ^{1}D stand-by analysis, allowing the correct determination of both isotopic and enantiomeric ratio. Similarly, linalool oxide cis and trans pyranoid were baseline separated each other. For the enantiomers of 3, 7-dimethylocta-1, 7-dien-3, 6-diol, unfortunately an incomplete separation did not allow the determination of δ^{13}C value, but only of enantiomeric one. On the other side, linalool-E-8-hydroxy enantiomers were well separated each other and from the co-eluted peaks in the monodimensional chiral profile (Figure 8.2).

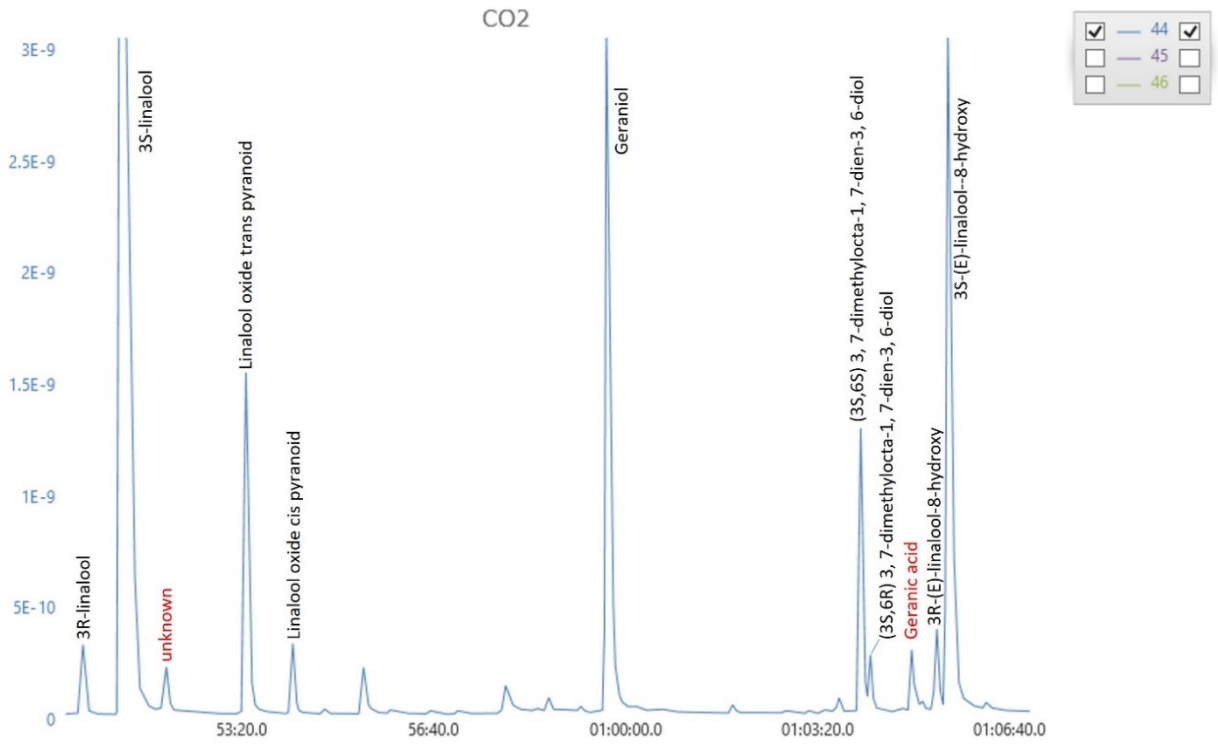

Figure 8.4 ^{2}D IRMS profile of a Moscato grape extract after the multidimensional separation

8.3.4 Enantiomeric and isotopic results in Moscato Giallo samples

Once the enantio MDGC-C-IRMS/qMS approach was optimized, seventeen Moscato Giallo grape extracts were analysed by these means. As reported in section 8.3.2 for standards, the extraction process involved the same additional concentration step prior to IRMS detection. Since no differences were expected in terms of isotopic distribution, in this research, free and bound forms were simultaneously evaluated unifying the solutions before the enantio MDGC-C-IRMS analysis. Dealing with chiral compounds, similar trends were found for all the target terpenes in all the Moscato Giallo samples investigated (Table 8.3). Previous works by Mosandl and co-workers on chiral terpenes allowed to assign the specific identity of each enantiomer investigated [Luan 2004, Luan 2006].

	Linalool			3,7-dimethylocta-1,7-dien-3,6-diol			(E)-linalool-hydroxy		
Sample (Es)	3R	3S	EE	3S,6S	3S,6R	EE	3R	3S	EE
1	2.21	97.79	95.58	82.30	17.70	64.60	8.09	91.91	83.82
2	2.41	97.59	95.18	85.22	14.78	70.44	7.08	92.92	85.84
3	3.79	96.21	92.42	88.03	11.97	76.06	8.22	91.78	83.56
4	3.26	96.74	93.48	86.09	13.91	72.18	9.22	90.78	81.56
5	3.24	96.76	93.52	83.00	17.00	66.00	7.59	92.41	84.82
6	3.93	96.07	92.14	76.02	23.98	52.04	3.75	96.25	92.50
7	2.56	97.44	94.88	82.35	17.65	64.70	7.00	93.00	86.00
8	2.33	97.67	95.34	84.07	15.93	68.14	9.46	90.54	81.08
9	2.64	97.36	94.72	86.15	13.85	72.30	9.62	90.38	80.76
10	4.74	95.26	90.52	80.68	19.32	61.36	6.56	93.44	86.88
11	2.56	97.44	94.88	85.71	14.29	71.42	7.04	92.96	85.92
12	3.66	96.34	92.68	85.59	14.41	71.18	7.89	92.11	84.22
13	3.10	96.90	93.80	81.82	18.18	63.64	8.07	91.93	83.86
14	4.50	95.50	91.00	83.92	16.08	67.84	11.05	88.95	77.90
15	4.10	95.90	91.80	78.31	21.69	56.62	8.24	91.76	83.52
16	5.60	94.40	88.80	85.00	15.00	70.00	10.37	89.63	78.96
17	2.49	97.51	95.02	82.14	17.86	64.28	8.33	91.67	83.34

Table 8.3 Enantiomeric data for the main terpenes investigated in the seventeen Moscato Grape samples. EE: enantiomeric excess

For each chiral couple investigated, an evident enantiomeric excess (>50%) was always registered for one of the two enantiomers, outlining a typical behaviour. Linalool was found to be predominant in the 3S form (95.26-97.79%), as well as (E)-linalool-hydroxy (88.95-96.25%). For 3, 7-dimethylocta-1, 7-dien-3, 6-diol, the 3S, 6S form was predominant (76.02-88.03%) than the 3S, 6R enantiomer; in this case, unfortunately, no data were collected for IRMS due to the incomplete separation involving the enantiomers. These chiral results about Moscato Giallo samples were found generally in agreement with the previous report from Luan *et al*. about other Moscato grape varieties. Dealing with IRMS detection, as well as for chiral data, $\delta^{13}C_{VPDB}$ values were recorded after the ^{2}D separation. All the signals above 0.5 nA, inside the uncertainty of the

instrument signal, were acquired in triplicates showing a standard deviation always < 0.5 ‰; on the other hand, signals below this threshold were not taken in consideration. Due also to the drawbacks highlighted in Section 8.3.2, this is the first time that $\delta^{13}C_{VPDB}$ values for key terpenes in grapes, as well as in oenological products, are reported in literature. Moreover, considering the evident enantiomeric excess registered for one of the two enantiomers (Table 8.3), $\delta^{13}C_{VPDB}$ was evaluated only for the main ones of each couple. Although the coupling of a chiral selector with IRMS detection has few witnesses in literature, no significant $\delta^{13}C_{VPDB}$ shifts should be expected between the enantiomers of the same chiral molecule, being the products of the same biosynthetic pathway. Accordingly, carbon isotopic ratio of the enantiomers 3S-linalool, (E)-3S-linalool-hydroxy, 2S, 5S-linalool oxide cis pyranoid and the achiral geraniol were acquired, as visible in Table 8.4.

	3S-linalool	2S,5R-linalool oxide trans pyranoid	geraniol	(E)-3S-linalool-hydroxy
Sample	$\delta^{13}C_{VPDB}$	$\delta^{13}C_{VPDB}$	$\delta^{13}C_{VPDB}$	$\delta^{13}C_{VPDB}$
1	-35.0	-34.2	-33.0	-33.9
2	-33.1	-32.5	-31.0	-29.8
3	-36.8	-35.9	-34.5	-33.2
4	-37.7	-37.4	-35.7	-34.5
5	-35.4	-34.3	-33.0	-33.0
6	-38.2	-36.9	-37.1	-36.1
7	-39.6	-38.8	-36.5	-36.6
8	-34.8	-33.9	-33.2	-32.9
9	-37.7	-37.2	-35.5	-34.0
10	-35.7	-34.7	-33.2	-33.7
11	-37.1	-36.9	-35.3	-33.9
12	-37.5	-36.9	-35.6	-34.7
13	-35.7	-34.7	-33.4	-32.8
14	-38.8	-37.4	-35.9	-35.2
15	-36.4	-36.0	-33.5	-34.8
16	-40.5	-39.2	-36.4	-35.5
17	-35.7	-35.2	-33.8	-33.4

Table 8.4 $\delta^{13}C_{VPDB}$ value for the main enantio terpenes in the seventeen Moscato grape samples

Dealing with isotopic results, although different absolute $\delta^{13}C_{VPDB}$ values were found among the samples investigated, a typical relative trend was found among the terpenes in terms of isotopic distribution. These findings were satisfactory since mono-varietal samples were investigated. Due to the high closeness in terms of geographical origin, no relevant differences were found, as expected, among samples from Trentino and Veneto for isotopic data. In detail, 3S-linalool registered always the most negative $\delta^{13}C_{VPDB}$ value in all the samples investigated, covering a range from -33.1 ‰ (Sample 2) to -40.5 ‰ (Sample 16). Beside 3S-linalool, geraniol and (E)-3S-linalool-hydroxy had alternatively the most positive values in Moscato Giallo samples. As reported by a review from van Leeuwen *et al*., [van Leeuwen 2014] most of the components derived from C_3 plants show $\delta^{13}C_{VPDB}$ values inside the range from -24 to -34 ‰. In this concern, since synthetic standards from coal have $\delta^{13}C_{VPDB}$ values from -25 ‰ to -30 ‰, some overlappings may involve with respect to the range of modern C_3 plants, making authenticity assessment more difficult. Differently, as shown in Table 8.4, most of the $\delta^{13}C_{VPDB}$ values registered for grapes, especially for 3S-linalool, fell outside from this range. However, these unusual negative isotopic data were immediately explained considering monoterpenes biosynthesis in grapes. In a previous research, Luan *et al*., [Luan 2002] demonstrated how monoterpenes biosynthesis in grapes occurs by means of the mevalonate-independent 1-deoxy- d-xylulose 5-phosphate/2C-methyl- d-erythritol 4-phosphate (DOXP/MEP) pathway in plastids. However, this metabolic way is not considered as the preferred pathway for isoprenoid biosynthesis, whose is typically performed by means of the mevalonate acid pathway. Moreover, the differences in these two metabolic pathways reflect in a different isotopic fractionation for the secondary metabolites [Hayes 2001]. Dealing with carbon isotopes, Hayes [Hayes 2001] described how a higher depletion of ^{13}C for isoprenoids is observed in the MEP pathway with respect to the same ones synthetized by mevalonate acid pathway. These findings were able to explain such negative isotopic values registered for terpenes in grape berries. In agreement, samples with target volatiles having more negative $\delta^{13}C_{VPDB}$ values with respect to typical C_3 distribution may be very useful for authenticity assessment [Strojnik 2019, Cuchet 2019]. Dealing with fruit aromas, Strojnik *et al*., [Strojnik 2019] provided a clear differentiation for VOCs in apple aromas, since synthetic standards from coal showed much more positive $\delta^{13}C_{VPDB}$ values with respect to natural samples. In this concern, future studies will deal with the analysis of commercial oenological products for authenticity aims.

8.4 Conclusions

In this study, a full characterization of the terpenic profile in Moscato Giallo grapes was achieved by means of the coupling of different analytical approaches. Fast GC-QqQ/MS provided a suitable quali-quantitative investigation of the key volatiles in grapes in reduced times. Dealing with simultaneous isotopic and chiral analysis, monodimensional Es-GC-C-IRMS analysis demonstrated to be unsuitable to these aims. A MDGC method was thus developed, combining an apolar column in the ^{1}D and a chiral stationary phase in the ^{2}D one, allowing an improved separation of the target terpenols prior to the IRMS and qMS detection. In these concern, the analysis of Moscato Giallo grapes revealed a typical behaviour for both enantiomeric and isotopic ratios. Current efforts are aimed to increase the database of grapes investigated, in order to evaluate specific statistical trends, confirming the genuineness range established for natural samples.

Future studies will deal with the analysis of the Moscato Giallo wines obtained by the same grapes used in this work, in order to evaluate isotopic and enantiomeric behaviour along winemaking.

References

Badea, S.L., Danet, A.F. Enantioselective stable isotope analysis (ESIA) — a new concept to evaluate the environmental fate of chiral organic contaminants. Sci Total Environ. 514 (2015) 459-466

Bicchi, C., Binello, A., D'Amato, A., Rubiolo, P. Reliability of Van den Dool Retention Indices in the Analysis of Essential Oils. J Chromat Sci. 1999

Bouchard, D., Hohener P., Hunkeler, D. Carbon isotope fractionation during volatilization of petroleum hydrocarbons and diffusion across a porous medium: A column experiment. Environ Sci Technol. 42 (2008) 7801-7806

Camin, F., Bontempo, L., Perini, M., Piasentier, E. Stable isotope ratio analysis for assessing the authenticity of food of animal origin, Compr. Rev. Food Sci. Food Saf. 15 (5) (2016) 868–877

Cuchet A., Jame, P., Anchisi, A., Schiets, F., Oberlin, C., Lefèvre, J.C., Carénini, E., Casabianca, H. Authentication of the naturalness of wintergreen (Gaultheria genus) essential oils by gas chromatography, isotope ratio mass spectrometry and radiocarbon assessment. Ind Crops Prod 142 (2019) 111873

Cucinotta, L., De Grazia, G., Salerno, T. M. G., Donnarumma, D., Donato, P., Sciarrone, D., Mondello, L. Overcoming the lack of reliability associated to monodimensional gas chromatography coupled to isotopic ratio mass spectrometry data by heart-cut two-dimensional gas chromatography J. Chromatogr. A 1655 (2021) 462473

Cucinotta, L., De Grazia, G., Micalizzi, G., Bontempo, L., Camin, F., Mondello, L., Sciarrone, D. Simultaneous evaluation of the enantiomeric and carbon isotopic ratios of Cannabis sativa L. essential oils by multidimensional gas chromatography Anal Bioanal Chem. 414:18 (2022) 5733-5738

D'Onofrio, C., Matarese, F., Cuzzola, A. Study of the terpene profile at harvest and during berry development of Vitis vinifera L. aromatic varieties Aleatico, Brachetto, Malvasia di Candia aromatica and Moscato bianco, J. Sci. Food Agric. 97 (2016) 2898-2907

Flamini, R. Some advances in the knowledge of grape, wine and distillates chemistry as achieved by mass spectrometry, J. Mass Spectrom. 40 (2005) 705-713

Gunata, Y.Z., Bayonove, C.L., Baumes R.L., Cordonnier, R.E. The aroma of grapes I. Extraction and determination of free and glycosidically bound fractions of some grape aroma components. J. Chromatogr. A 331 (1985) 83-90

Hayes, J.M. Fractionation of the isotopes of carbon and hydrogen in biosynthetic processes. Reviews in Mineralogy and Geochemistry. 43:1 (2001) 225-277

Luan, F., Wüst, M. Differential incorporation of 1-deoxy-d-xylulose into (3S)-linalool and geraniol in grape berry exocarp and mesocarp. Phytochem. 60 (2002) 451-459

Luan, F., Hampel, D., Mosandl, A., Wüst, M. Enantioselective Analysis of Free and Glycosidically Bound Monoterpene Polyols in Vitis vinifera L. Cvs. Morio Muscat and Muscat Ottonel: Evidence for an Oxidative Monoterpene Metabolismin Grapes, J. Agric. Food Chem. 52 (2004) 2036−2041

Luan, F., Mosandl, A., Gubesch, M., Wust, M. Enantioselective analysis of monoterpenes in different grape varieties during berry ripening using stir bar sorptive extraction- and solid phase extraction-enantioselective-multidimensional gas chromatography-mass spectrometry, J. Chromatogr. A 1112 (2006) 369-374

Mateo, J.J., Jimenez, M. Monoterpenes in grape juice and wines, J. Chromatogr. A, 881 (2000) 557-567

Matucha, M., Jockisch, W., Verner, P., Anders, G. Isotope effect in gas—liquid chromatography of labelled compounds, J. Chromatogr. A 588 (1-2) (1991) 251–258

Meier-Augenstein, W. Applied gas chromatography coupled to isotope ratio mass spectrometry, J. Chromatogr. A, 842 (1999) 351-371.

Mosandl, A., Hener, U., Georg Schmarr, H., Rautenschlein, M. Chirospecific Flavor Analysis by Means of Enantioselective Gas Chromatography, Coupled On-Line with Isotope Ratio Mass Spectrometry, J. High Resolut. Chromatogr. 13 (1990) 528-530

Nicolini, G., Moser, S., Borin, G., Tonidandel, L., Roman, T., Larcher, R. Gli aromi del Moscato Giallo nelle sue interpretazioni in Trentino e nei Colli Euganei. L'Enologo Nov. 2013

Paolini, M., Tonidandel, L., Moser, S., Larcher, R. Development of a fast gas chromatography–tandem mass spectrometry method for volatile aromatic compound analysis in oenological products, J. Mass Spectrom. 53 (2018) 801–810.

Reichert, S., Fischer, D., Asche, S., Mosandl, A. Stable isotope labelling in biosynthetic studies of dill ether, using enantioselective multidimensional gas chromatography, online coupled with isotope ratio mass spectrometry, Flavour Fragr. J. 15 (2000) 303-308.

Sciarrone, D., Schepis, A., Zoccali, M., Donato, P., Vita, F., Creti, D., Alpi, A., Mondello, L. Multidimensional gas chromatography coupled to combustion- isotope ratio mass spectrometry/quadrupole ms with a low-bleed ionic liquid secondary column for the authentication of truffles and products containing truffle, Anal. Chem. 90 (2018) 6610–6617

Shin, W.J., Lee, K.S. Carbon isotope fractionation of benzene and toluene by progressive evaporation 24:11 (2010) 1636-1640

Silfer, J.A., Engel, M.H., Macko, S.A., Jumeau, E.J. Stable carbon isotope analysis of amino acid enantiomers by conventional isotope ratio mass spectrometry and combined gas chromatography/isotope ratio mass spectrometry. Anal Chem. 63 (1991) 370-374

Song, M., Xia, Y., Tomasino, E. Investigation of a Quantitative Method for the Analysis of Chiral Monoterpenes in White Wine by HS-SPME-MDGC-MS of Different Wine Matrices, 20 (2015) 7359-7378

Strojnik, L., Stopar, M., Zlatič, E., Kokalj, D., Gril, M. N., Ženko, B., Žnidaršič, M., Bohanec, M., Boshkovska, B. M., Luštrek, M., Gradišek, A., Potočnik, D., Ogrinc, N. Authentication of key aroma compounds in apple using stable isotope approach Food Chem. 277 (2019) 766-773

Van Leeuwen, K., Prenzler, P.D., Ryan, D., Camin, F. Gas Chromatography-Combustion-Isotope Ratio Mass Spectrometry for Traceability and Authenticity in Foods and Beverages. 13 (2014) 814-837

Versini, G., Dalla Serra, A, Monetti A, De Micheli, L., Mattivi, F. Free and bound grape aroma profiles variability within the family of Muscat called varieties. Connaissance aromatique des cepeges etqualite des vins, (1993) 12-18

Chapter 9

Chiral isotopic fractionation in lemon essential oil: a new tool for authenticity assessment?

9.1 Introduction:

Authenticity assessment for essential oils is an everlasting challenge between quality controllers and frauds, in continuous competition. Because of increasing consumers' request, as in the case of citrus cold-pressed products, their commercialization is spreading ever more all over the world. Among citrus oils, lemon essential oil has a larger economic impact in the flavour and fragrance industry. The essential oil, mainly obtained through cold pressed extraction by the peel of the fruit, is widely employed in different fields, from renowned food and beverages applications, as well as aromatherapy to newer pharmacological approaches, due to the antioxidant properties of its components [Dosoky 2018]. Regarding the volatile fraction, it is mainly made up of olefinic monoterpenes, such as β-pinene, limonene, γ-terpinene, and in minor amounts by aldehydes, such as citral (neral+geranial), although they largely contribute to the flavour [Mondello 2010].

Chemical composition can be easily investigated by means of gas chromatography coupled to flame ionization detection (GC-FID) and gas chromatography coupled to mass spectrometry (GC/MS), although it may vary quantitatively in relation to seasonal production [Mondello 2010]. Thus, whilst an initial screening can be achieved by conventional quali-quantitative analysis, a full evaluation can be done by means of more sophisticated analytical approaches. Enantio-selective gas-chromatography (Es-GC) has been extensively described in the literature for its capability to evaluate the genuineness and quality of essential oils [Schurig 2001]. In dealing with citrus fruit essential oils, specific enantiomeric excesses are registered for key compounds, as in the case of (+)-limonene (>95%) with respect to its levorotatory form [Mondello 2010]. Clear differences from genuine ranges allow the unveiling of fraudulent additions, by these means. However, the target component having a pronounced enantiomeric excess may be selected by other sources, making authenticity assessment harder. Complementarily, gas chromatography coupled to isotopic ratio mass spectrometry (GC-C-IRMS) is largely recognized as a powerful tool for authenticity assessment analysis. The different CO_2 uptake by the plant and the related biochemical pathways allow to distinguish among C_3, C_4 and CAM plants, as well as from synthetic sources [Meier

Augenstein 1999, Sciarrone 2018, Camin 2016]. In the literature, Schipilliti *et al*. reported $\delta^{13}C$ values of the main terpenes in lemon essential oils, allowing in some cases to discern fraudulent additions, as well as to distinguish from different geographical origins [Schipilliti 2012]. Since both techniques deeply investigate the genuineness of natural products, a simultaneous detection by means of enantio-selective gas chromatography coupled to isotopic ratio mass spectrometry (Es-GC-C-IRMS) may be considered a suitable technique for authenticity aims. Such an approach was first demonstrated by Mosandl and co-workers for the differentiation of natural and synthetic products [Mosandl 1990], and after by a few more research groups [Silfer 1991, Badea 2015]. By employing a single gas chromatographic method, it would be able to detect the enantiomeric excesses and $\delta^{13}C$ values of the target compounds, simultaneously. Despite these undeniable advantages, even in terms of total time analysis, some drawbacks have severally limited its widespread diffusion. Dealing with medium-high complexity samples, compounds with very similar physic-chemical properties may involve in co-elutions along a chromatogram. Even more, this issue may be accentuated by a chiral separation. Although the selection of a suitable cyclodextrine-based stationary phase can efficiently resolve the enantiomers of a single chiral couple each other, overlapping with interfering or achiral components may involve. However, if a partial co-elution may not largely affect the calculation of enantiomeric excesses since diagnostic m/z fragments can be still monitored in extracted ion modes, conversely it represents several matters for isotopic evaluation. As already reported by our research group, the uneven distribution of carbon isotopes along an entire peak of CO_2 leads to unreliable more positive or negative $\delta^{13}C$ values with respect to conditions of baseline separation [Matucha 1991, Cucinotta 2021]. To overcome these limitations, multidimensional gas-chromatography (MDGC) may represent the suitable analytical approach, thanks to the higher peak resolution achieved by the employment of two columns with different selectivity. Enantio-selective multidimensional gas chromatography (Es-MDGC), exploited in heart-cut mode, was first reported by Schomburg *et al*. [Schomburg 1984], allowing to select of specific window times in the first achiral dimension for a further chiral separation in the second one. Starting from this first study, several works were led by these means, also in the field of citrus essential oils [Sciarrone 2010, Hong 2017]. In this regard, Sciarrone *et al*., [Sciarrone 2010] demonstrated the capability of an Es-MDGC system to solve co-elutions with respect to a conventional Es-GC in mandarin essential oils, achieving more reliable quantitative results. Dealing with lemon essential oils, Hong *et al*., [Hong 2017] employed an Es-MDGC system for the detection of four specific chiral couples. Conversely, very few works have dealt with the simultaneous determination of both the enantiomeric excess and the $\delta^{13}C$ value for target compounds [Reichert 2000, Cucinotta 2022], due to the need for a baseline resolution prior to

IRMS detection. To these aims, in this research, a novel Es-MDGC-C-IRMS/qMS approach was developed, employing an apolar and a chiral stationary phase in the first and second dimensions, respectively. By these means, it was possible to simultaneously evaluate the enantiomeric excess and the $\delta^{13}C$ ratio of the enantiomers of the main chiral terpenes in lemon essential oils for the first time in literature, and the $\delta^{13}C$ ratio of the main achiral compounds. In this concern, the baseline separation of pinenes enantiomers, namely (-) and (+)-α and β-pinene, allowed to register their specific $\delta^{13}C$ ratios, laying the foundation for new considerations in the field of essential oil authenticity assessment.

9.2 Materials and Methods

9.2.1 Samples

Twenty genuine cold-pressed lemon essential oils were provided by local producers in the season 2021/2022 and stored at +4 °C. Prior to the GC analysis, all the samples were diluted 1:10 in *n*-hexane. A C_7-C_{30} *n*-alkane mix, kindly provided by Merck Life Science (Darmstadt, Germany), was used for the calculation of linear retention index (LRI) values. For the calibration of the $\delta^{13}C$ ratio with respect to VPDB scale, the CO_2 reference gas was calibrated using three certified alkanes from Indiana mix A7, namely hexadecane (**$\delta^{13}C$** -26.15 ‰), octadecane (**$\delta^{13}C$** -32.70 ‰) and eicosane (**$\delta^{13}C$** -40.91 ‰) (Indiana University, Bloomington, IN). Isotopic ratio measurements of the samples of interest were done by the following formula:

$$\delta^{13}C = \frac{Rsample - Rstandard}{Rstandard}$$

where *R* represents the abundance ratio of the heavier carbon isotope against the lighter one ($^{13}C/^{12}C$).

9.2.2 MDGC-C-IRMS/qMS conditions

The MDGC-C-IRMS/qMS prototype was already described in previous works [Cucinotta 2021, Cucinotta 2022], and briefly consists of two GC-2010 Plus gas chromatographers (defined as GC1 and GC2), connected by means of a heated transfer line (Shimadzu Europa, Duisburg, Germany). GC1 was equipped with a split/splitless injector, a flame ionization detector (FID) and a Deans-switch (DS) transfer device, connected to an advanced pressure control unit (APC), which supplied the same carrier gas (He) (Shimadzu Europa, Duisburg, Germany) allowing to divert the first column eluent to the FID or to the second column in the GC2. The latter was hyphenated in parallel to a QP2010 Ultra quadrupole mass spectrometer (Shimadzu Europa, Duisburg, Germany) and to

a VisION IRMS system by means of a GC V furnace system (Elementar Analysensysteme GmbH, Langenselbold, Germany) maintained at 830 °C. For the current application, the split/splitless injector was maintained at 280 °C, at a split ratio 10:1, delivering to the ^{1}D column, an SLB-5 ms 30 m × 0.25 mm i.d. × 0.25 μm df (Merck Life Science, Darmstadt, Germany), a constant helium flow of 1.0 mL/min. A pressure program was used, from 185 kPa (5 min) to 261 kPa at 1.89 kPa/min, to 330 kPa at 7.28 kPa/min.The GC1 oven was ramped as follows: 50 °C (5 min) to 170 °C at 3 °C/min, finally to 250 °C (4 min) at 15 °C/min. The FID (330 °C; H_2 flow, 40.0 mL/ min; air flow rate, 400 mL/min; sampling rate, 80 ms equal to 12.5 Hz) was connected to the DS device via a 0.25 m × 0.18 mm i.d. stainless steel uncoated column and used to monitor the ^{1}D eluent. GC2 was equipped with a MEGA-DEX ASX 1 chiral column 25 m × 0.25 mm i.d. × 0.25 μm df (MEGA, Milano, Italy), and the temperature was ramped as follows: 40 °C (10 min) to 82 °C at 2 °C/min, to 220 °C (4.9 min) at 7 °C/min. The ^{2}D column was connected at one side to the DS device and at the other side to a zero dead-volume tee-union (Valco). The effluent was split to the combustion chamber and to the IRMS system via a 0.85 m × 0.25 mm i.d. uncoated column and to the qMS via a 2 m × 0.1 mm i.d. uncoated column. A pressure program was applied to the APC device in order to maintain a constant carrier flow also in the ^{2}D column (≈1 mL/min): 140 kPa (10 min) to 189 kPa at 1.39 kPa/min, to a final pressure of 265 kPa at 8.04 kPa/min. The qMS ion source and interface temperature were maintained at 200 °C; the mass range 40-400 *m/z* was monitored at an acquisition speed of 10 Hz. The target compounds were identified by searching their qMS spectra against the FFNSC 4.0 mass spectral library database (Shimadzu Europa, Duisburg, Germany), using a double filter based on spectral similarity and on a range of Linear Retention Index (LRI). The VisION IRMS (Elementar Analysensysteme GmbH, Langenselbold, Germany) was a bench top 5 kV system equipped with an integrated monitoring gas delivery system. The combustion chamber was provided with a high performing silicon carbide tube furnace for the quantitative, fractionation-free conversion of the compounds to pure gases (CO_2 and H_2O). The CO_2 produced by pyrolisis of each component was transferred to the IRMS, while the water produced was removed through a Nafion membrane. The system was designed with reduced dead volumes to maintain the chromatographic integrity of the separated compounds, preserving the chromatographic resolution at the IRMS. An auxiliary He line (sample line He), automatically controlled through a second channel of the APC unit, was used in the furnace to allow a proper control over the open split conditions for the IRMS. The following settings were applied to the VisION system: acceleration voltage, 3795.007 V; trap current, 600.000 μA; magnet current, 3700.000 mA. The APC was operated in constant flow mode, to maintain the open split in a steady state. An electron-impact ionization (EI) gas source, a variable field, stigmatically

focused electromagnet for beam separation and multi-channel Faraday collectors for beam detection were used. IRMS data were collected by IonOS stable isotope data processing software ver. 3.0.0.5196 (Elementar Analysensysteme GmbH, Langenselbold, Germany); the ratio offset integration method was exploited to automatically find the correct starting and finishing point of the peaks. All the analyses were led at least in triplicate and standard deviations for IRMS measurements were found to be under < 0.5.

9.3. Results and discussion

9.3.1 Development of an Es-MDGC-C-IRMS approach

As discussed in the introduction section, natural matrices are often characterized by the presence of components with very wide concentration ranges, from present in traces to very abundant compounds that can exceed 30-50% of the total composition. Consequently, different analytical conditions are conventionally chosen with the aim of finding a compromise between these two concentration extremes. In dealing with IRMS detection, it is necessary to pay even more attention not to introduce insufficient quantities of analytes, due to the detection limits, obviously being lower than the common mass spectrometers. This issue is related to the approximately 100 times lower natural relative abundance of ^{13}C compared to that of ^{12}C. On the other hand, the introduction of concentrated solutions may overload the chromatographic system. Considering a conventional GC-C-IRMS approach, this issue can arouse the overlap of adjacent peaks or partial co-elutions linked to peak broadening, and thus the inability to obtain baseline separated peaks. To overcome these problems, in a previous research regarding the GC-C-IRMS analyses on lemon essential oils [Schipilliti 2012], three chromatographic runs were performed to achieve a reliable $\delta^{13}C$ ratio measurement of high, medium and trace amount compounds, respectively. To this aim, different on-column amounts of lemon essential oil were injected in the three runs: a low sample amount was injected to measure the principal components, while an higher and a very high sample amounts were injected to measure the low concentrated and trace components of the oil, respectively. Whilst such a method ensures a reliable evaluation of the target compounds, on the other hand, it was time-consuming, especially when several samples, as in the case of a citrus essential oil, are required to be analysed. It is clear that such an approach involved also in an increased consumption of solvent and sample, as well as an increased consumption of helium as carrier gas. In this concern, the current research aimed first to reduce the total analysis time and cost by developing a single chromatographic method. Moreover, following the results obtained in a previous study on Cannabis Sativa *L.* essential oils [Cucinotta 2022], the main aim was not only to detect the $\delta^{13}C$

ratio of the terpenes of interest but also the enantiomeric ratio of the chiral volatiles, simultaneously in a single chromatographic run. However, although the coupling of a chiral separation to isotopic ratio mass spectrometry can offer two crucial pieces of information for authenticity assessment in a single analysis, very few references are present in the literature [Karl 1994, Faber 1995, Frank 1995, Juchelka 1998, Reichert 2000, Cucinotta 2022]. Such a lack is closely related to a series of limitations which have drastically limited the spread of this approach. Among these, the insufficient chromatographic resolution surely represents the main issue. In this concern, although the selected chiral phase can efficiently resolve all the enantiomers of the selected chiral terpenes, co-elutions may involve achiral components, or between target achiral components. Dealing with citrus essential oils, different research works were carried out by employing an enantio-multidimensional gas chromatographic system prior to mass spectrometric detection [Hong 2017, Sciarrone 2010]. As extensively reported in the literature, the insufficient resolution represents an even more serious limitation for IRMS detection, since it involves unreliable isotopic results [Matucha 1991, Cucinotta 2021]. For these reasons, coupling multidimensional gas chromatography to isotopic ratio mass spectrometry represents the best choice since a baseline separation is mandatory prior to the detection. Differently from MS detection where diagnostic fragments can still be monitored by means of extracted ion mode or single ion monitoring (SIM), for IRMS, this is not achievable due to the conversion of all the organic components to CO_2 prior to the detection. This matter is even more evident due to the renowned chromatographic isotopic effect of the CO_2 in GC, which leads to unreliable results in the case of co-elution. Limitations about monodimensional Es-GC-C-IRMS analysis for lemon essential oils are shown in Figure 9.1.

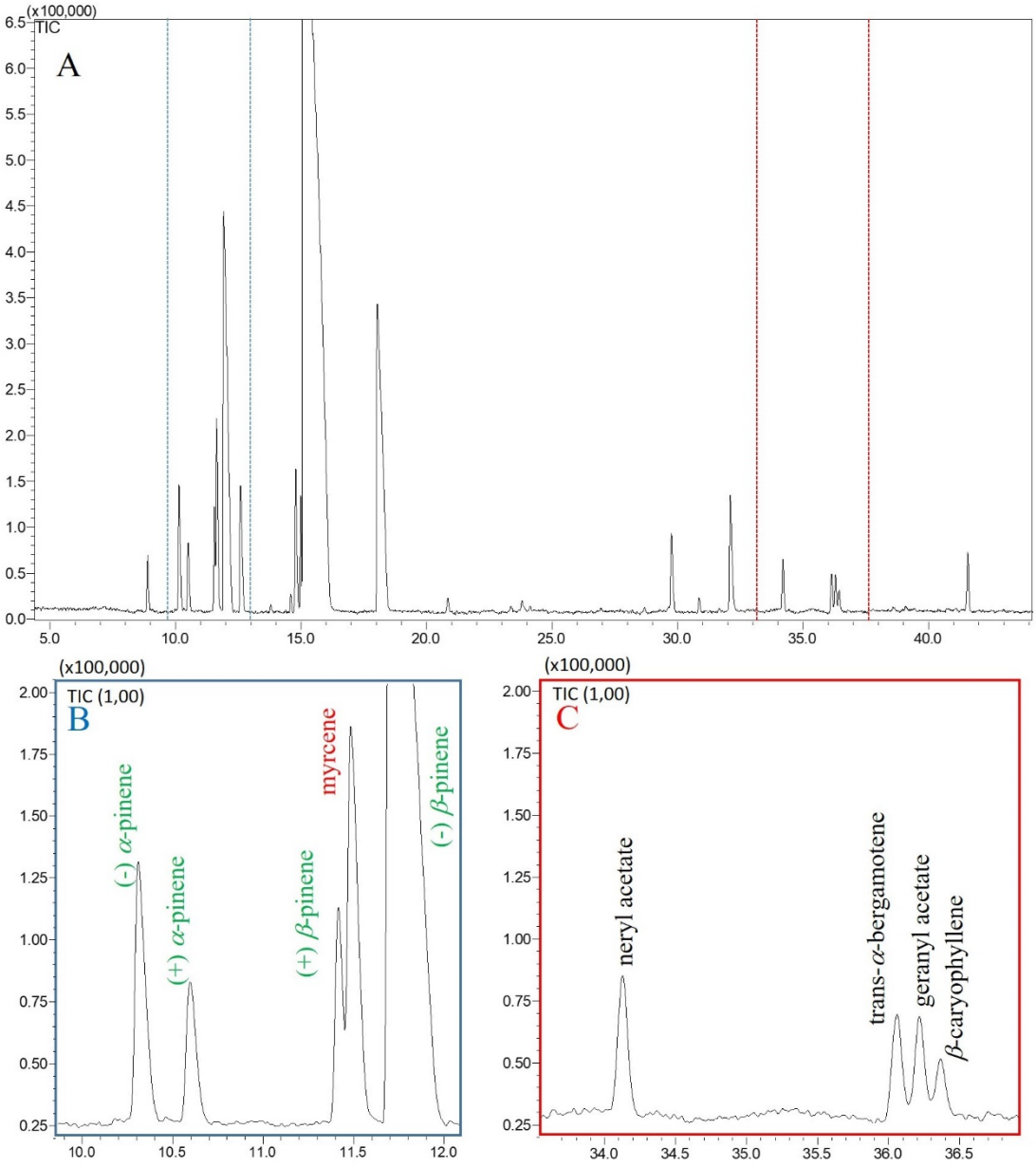

Figure 9.1 (A) monodimensional GC-MS chiral profile of a lemon essential oil investigated, showing different critical co-elutions (B and C)

Figure 9.1A shows the monodimensional chiral GC-MS chromatogram achieved for a lemon essential oil, while Figure 9.1B and 9.1C show specific critical zones. As visible, (+) β-pinene co-elutes with myrcene (Figure 9.1B), making unreliable the determination of the enantiomeric ratio of β-pinene, and even more the $\delta^{13}C$ value of (+) β-pinene. Figure 9.1C shows co-elution involving target achiral components, namely trans-α-bergamotene, geranyl acetate and β-caryophyllene, whose $\delta^{13}C$ would have been surely wrong with such a monodimensional configuration. To overcome these limitations, a multidimensional gas chromatographic approach was developed. Since no qualitative information were available after the ^{1}D detector (FID), the

identity of each peak of interest was confirmed based on the elution order observed in monodimensional GC-MS analysis employing the same apolar stationary phase. Furthermore, the experimental LRIs of the peaks obtained after a ^{1}D stand-by analysis were matched to the theoretical values, within a ±10 units tolerance [Cucinotta 2022]. Due to the high repeatability in terms of retention times on the apolar column, narrow-cut windows were chosen for the transfer of the selected terpenes from the ^{1}D to the ^{2}D. Figure 9.2 shows a data comparison between a st-by (black trace) and a cut analysis (pink trace) for a lemon essential oil.

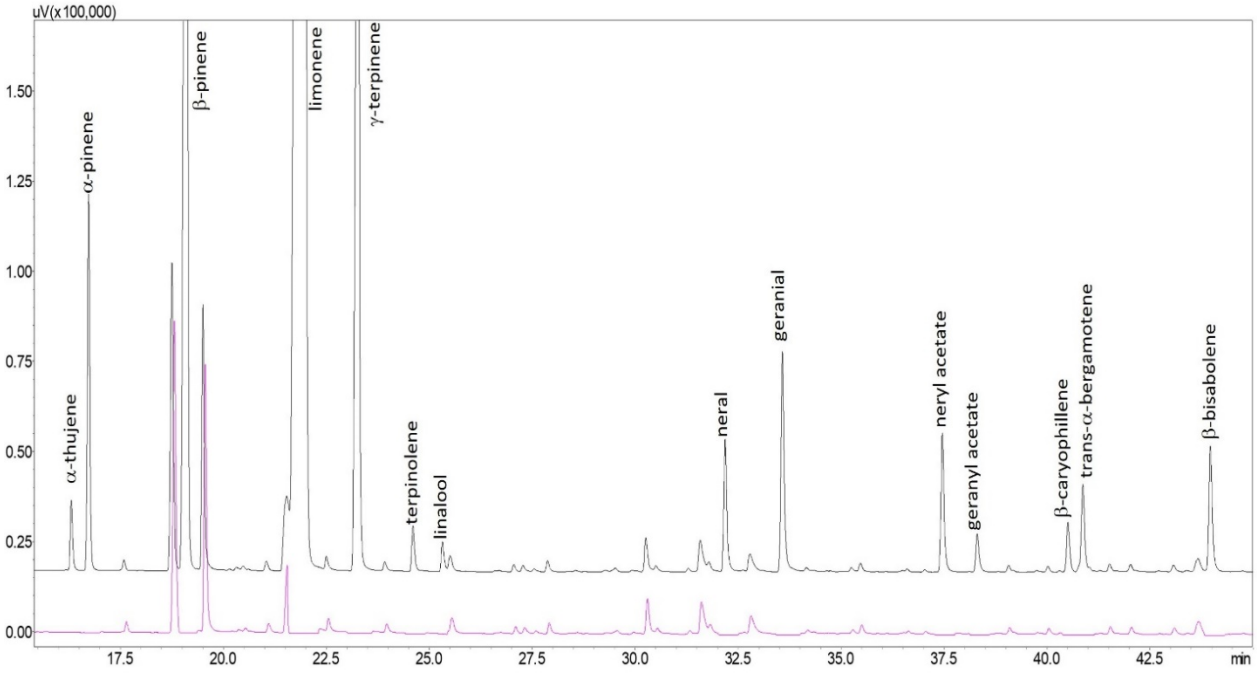

Figure 9.2 Data comparison between ^{1}D st-by (black trace) and ^{1}D cut analysis (pink trace) in the MDGC configuration

Fourteen cut windows were selected transferring from the ^{1}D to the ^{2}D α-thujene, α-pinene, β-pinene, limonene, γ-terpinene, terpinolene, linalool, α-terpineol, neral, geranial, neryl acetate, geranyl acetate, β-caryophyllene, trans-α-bergamotene and β-bisabolene. Figure 9.3 shows the ^{2}D IRMS chromatogram obtained after the chiral separation. Thanks to this approach, all the target components were efficiently baseline resolved, allowing a reliable simultaneous determination of the enantiomeric and isotopic data.

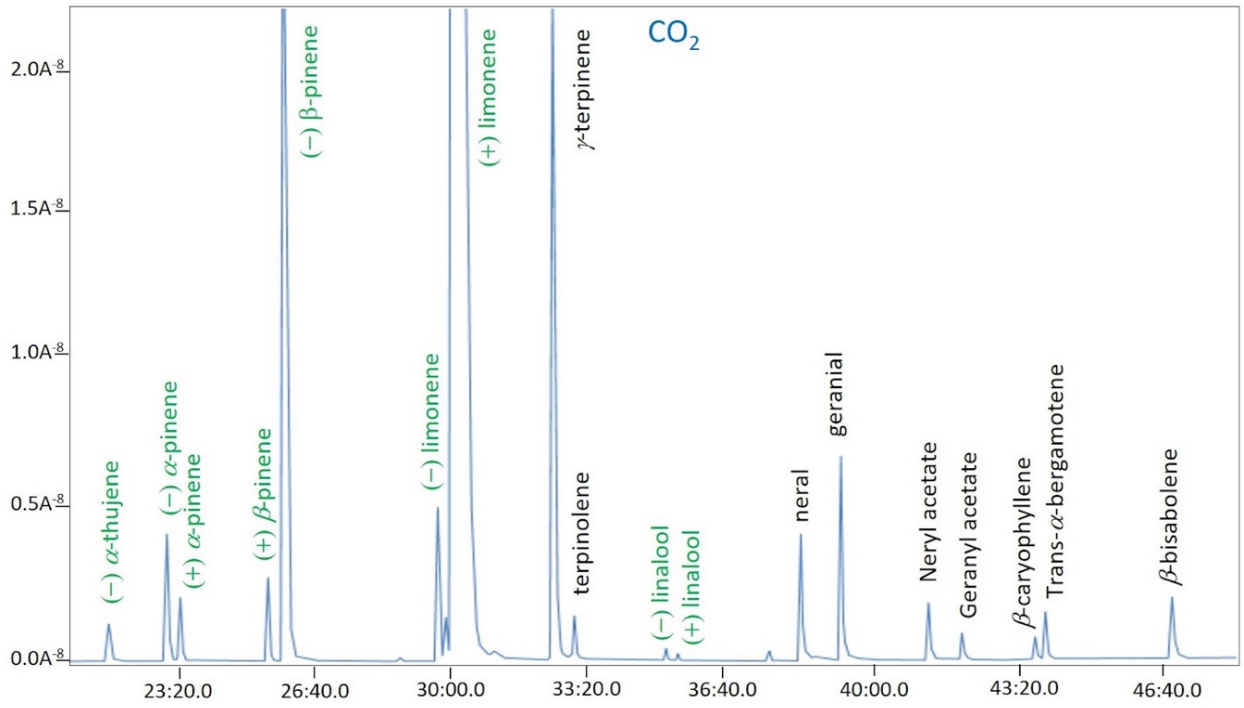

Figure 9.3: ^{2}D IRMS profile of the selected terpene components of a lemon essential oil. Green: enantiomeric terpene, Black: achiral terpene.

Enantiomeric ratios were determined for the chiral terpene, namely α-thujene, α-pinene, β-pinene, limonene and linalool. With respect to previous research works reported in Citrus oils book, similar enantiomeric trends were found for all the components investigated (see Figure 9.4)

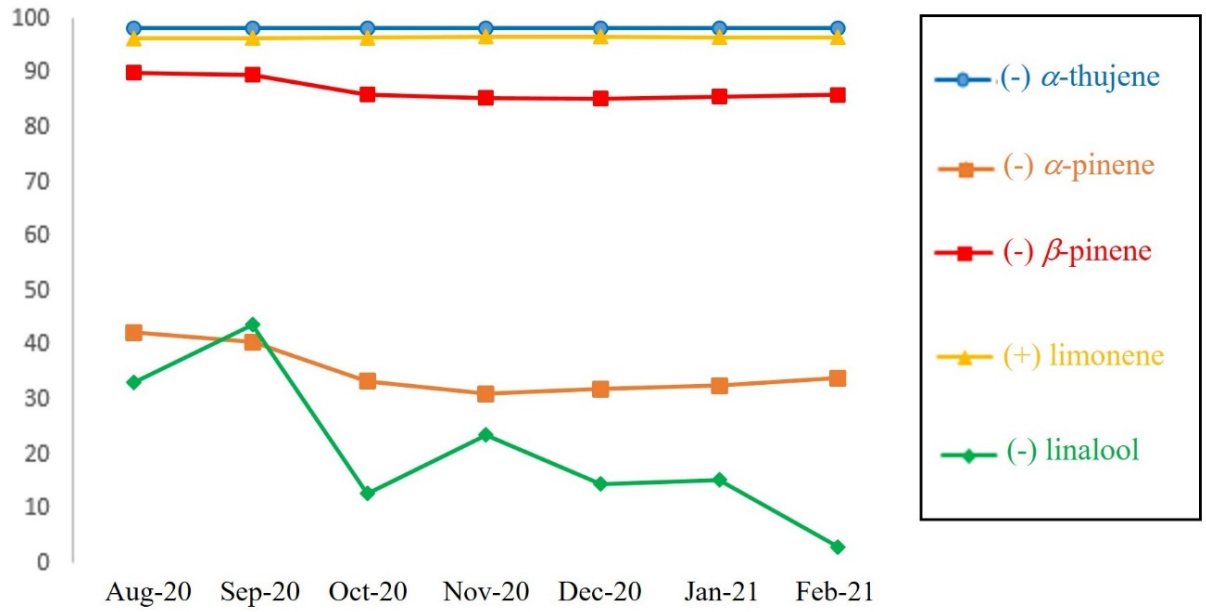

Figure 9.4 chiral trend along the sampling from August 2020 to February 2021

Enantiomeric excesses have been reported for the levorotatory form for most of the components investigated, namely α-thujene, α-pinene, β-pinene, linalool, while only for limonene the dextrorotatory form was the more abundant.

In detail, (+) limonene (see Table 1) was always found with an enantiomeric excess higher than 96% with respect to the levorotatory form. Due to the employment of a MDGC system, and the related higher separation power, data were found more in agreement with the study of Gionfriddo *et al*., with respect to the last communication reported in Citrus Oil book. Both (-) α-pinene and (-) β-pinene were in excess with respect to the dextrorotatory form from August 2020 to February 2021, with the higher enantiomeric excess registered in the months of August and September 2020. Dealing with α-thujene, as well as for limonene, an evident enantiomeric excess (98%) was registered for the levorotatory form.

About IRMS data, the δ^{13}C ratio of γ-terpinene was determined herein for the first time in literature, although it represents one of the main components in lemon essential oil. Only the signals higher than 0.5 nA were considered for the determination of δ^{13}C ratio: (+) α-thujene, (-) and (+) α-pinene, (-) and (+) β-pinene, (+) limonene, γ-terpinene, terpinolene, neral, geranial, neryl acetate, geranyl acetate, β-caryophyllene, trans-α-bergamotene and β-bisabolene were evaluated. Due to the very low signals detected, (-) and (+) linalool were not taken in consideration. About the genuine lemon essential oils analysed, most of the results were found in agreement with previous literature data on enantiomeric and isotopic ratios [Mondello 2010, Schipilliti 2012]. However, dealing with the δ^{13}C ratio of specific enantiomers, an unexpected isotopic data was found for the enantiomers of both α and β-pinene in all the samples investigated. With respect to previous findings in the field of essential oils, a different δ^{13}C ratio was observed among the enantiomers of the same chiral couple as reported in Table 9.1.

Target components	**LRI theor 5ms**	**LRI exp 5ms**	**Enantiomeric ratio range**	**δ^{13}C range**
(+) α-thujene	927	930	<1.0	nd
(–) α-thujene			>99.0	-25.8 -28.4
(–) *α*-pinene	933	935	64.10-71.64	-27.7 -30.0
(+) *α*-pinene			35.90-28.36	-29.8 -31.7
(+) *β*-pinene	978	980	4.96-7.79	-27.9 -30.6
(–) *β*-pinene			95.04-92.21	-25.0 -27.3
(–) limonene	1030	1032	1.65-1.95	nd
(+) limonene			98.35-98.05	-25.9 -28.0
γ-terpinene	1058	1060	-	-27.8 -30.9
terpinolene	1086	1090	-	-24.9 -30.2
(-) linalool	1101	1103	55.58-75.66	nd
(+) linalool			44.42-24.34	nd
neral	1238	1242	-	-25.7 -28.3
geranial	1268	1272	-	-25.9 -28.3
neryl acetate	1361	1363	-	-29.2 -32.5
geranyl acetate	1380	1382	-	-29.6 -32.5
trans-*α*-bergamotene	1432	1434	-	-28.8 -31.8
β-bisabolene	1508	1511	-	-28.6 -31.3

Table 9.1 Main information about the key terpenes investigated in lemon essential oils. *LRI exp. were calculated and compared to LRI theor. on SLB-5ms column.

As visible in Figure 9.5, a higher isotopic fractionation was involved for the dextrorotatory enantiomers of both *α* and *β*-pinene with respect to the levorotatory forms.

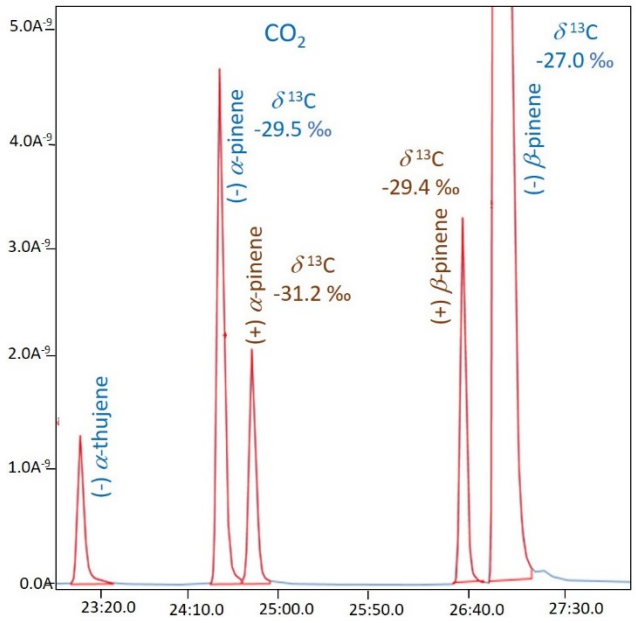

Figure 9.5 2D IRMS view relative to the separation of α, β-pinene enantiomers and the evident chiral isotopic fractionation registered

A deep discussion related to these results is provided in the next paragraph.

9.3.2 Chiral terpene isotopic fractionation

In the field of flavour and fragrances Mosandl's research group has played a pioneering role reporting in the literature for the first time the coupling of enantio-selective gas chromatography to isotopic ratio mass spectrometry [Mosandl 1990]. Their studies focused on the analysis of key odorants evaluating both the enantiomeric and isotopic ratios, to differentiate genuine and adulterated samples. Moreover, besides the capability to detect the enantiomeric ratio of a chiral couple, as shown in the previous section, this technique allows evaluating of the δ^{13}C ratio of each enantiomer. Despite of the results obtained in this research for lemon essential oils (see section 3.1), most of the studies reported consistent δ^{13}C ratio values of chiral components [Karl 1994, Faber 1995, Frank 1995, Juchelka 1998, Reichert 2000, Cucinotta 2022]. This theme was discussed in various research works, since two enantiomers were intended as products synthesized in the same enzymatic pathway, then expecting identical ^{13}C levels. Therefore, the detection of enantiomers with different δ^{13}C ratios was considered as a symptom of oil reconstitution [Frank 1995]. Only one report about genuine dill oil analysis, reported different isotopic data for the enantiomers of a key volatile produced in a specific part of the plant [Faber 1997]. In this concern, whilst the enantiomers of limonene produced in dill herbs had very similar δ^{13}C ratios, contrarily the enantiomers of limonene produced in dill buds were found to have an unexpected difference in terms of δ^{13}C ratio higher than 3‰. However, from a biochemical point of view, a review of

Rodney Croteau [Croteau 1987] resumed the typical biosynthetic steps of the main terpene components starting from the same achiral precursor geranyl pyrophosphate (GPP). As clearly reported, after the conversion of GPP to an allylic cation, the generation of a chiral centre leads to two parallel pathways involved in terpene biosynthesis. Starting from the two newly formed chiral reaction intermediates, different metabolic pathways are involved in the biosynthesis of the specific enantiomers, as in the case of (-) and (+) α-pinene [Croteau 1987, Philipps 2003]. After that, Lucker *et al*., provided new interesting insights about terpene biosynthesis in lemon essential oils [Lucker 2002]. The authors demonstrated how four different terpene synthases of flavedo were responsible for the production of more than 90% of the characteristic components in the oil. Moreover, the same group highlighted how the resulting enantiomeric excess needed to be considered as the sum of the products of the different enzymes which are responsible for the production of specific monoterpenes in a different concentration and with specific enantiomeric excesses. More recently, a very close link between terpene biosynthesis and carbon isotopic fractionation was provided by a research work of Tan *et al*. [Tan 2018]. In this study, the authors evaluated carbon isotopic fractionation along terpene biosynthesis. Due to a series of carbon-carbon bonds formation and breaking, kinetic carbon isotope effects are involved. These phenomena clearly lead to a distinct isotopic value for each terpene product, which is directly related to its individual biosynthetic pathways. Coming back to the lemon oils analysed, these findings were able to explain the isotopic differences between the enantiomers of the same chiral component, since they needed to be considered as products of different metabolic pathways. In this study, a higher isotopic fractionation was evident for the levorotatory forms with respect to dextro ones for α and β pinene in all the lemon samples analysed as shown in Figure 9.6. As visible, although a certain variability was observed depending by the moment of the production season, a constant trend was observed for all the samples with the dextrorotatory forms characterized by a higher isotopic fractionation (more negative $\delta^{13}C$ ratio values) with respect to the levorotatory form.

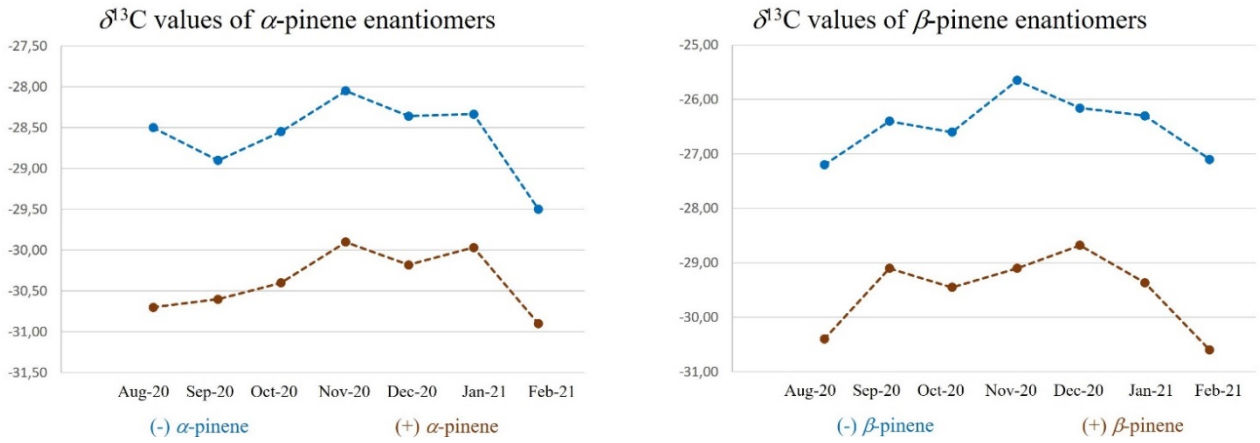

Figure 9.6 δ^{13}C ratio trends of α and β-pinene enantiomers in the lemon essential oils analysed.

However, besides the reasons behind the chiral isotopic fractionation, it's clear that the sum of these findings may open a series of perspectives in the field of the analysis of essential oils. From a biochemical point of view, the detection of a chiral isotopic fractionation process may be useful also to trace the biosynthetic pathways of the plants, as shown by Faber for dill [Faber 1997]. On the other hand, this type of detection can provide an additional distinctive trait of the plant, whose investigation is needed, even more for authenticity assessment aims.

9.4 Conclusions

The current study reports for the first time the simultaneous achievement of both enantiomeric and isotopic data, by employing a prototype system coupling enantio-selective multidimensional gas chromatography to isotopic ratio mass spectrometry. With respect to previous IRMS methods, the total time analysis was clearly reduced, since both the information were obtained after a single gas chromatographic run. Moreover, the baseline separation of the enantiomers of chiral components provided the capability to evaluate new interesting information about their carbon isotopic ratio. The different δ^{13}C ratios found between the α and β-pinene enantiomers suggest a characteristic isotopic fractionation related to a specific biosynthetic pathway of the lemon plant. This finding paves the way for newer considerations in the field of authenticity assessment since different essential oil types may present typical chiral isotopic fractionation processes. Future studies will be devoted to expand this approach also to different citrus fruits to deeply investigate their authenticity.

References

Badea, S.L., Danet, A.F. Enantioselective stable isotope analysis (ESIA) — a new concept to evaluate the environmental fate of chiral organic contaminants. Sci Total Environ. 514 (2015) 459-466

Camin, F., Bontempo, L., Perini, M., Piasentier, E. Stable Isotope Ratio Analysis for Assessing the Authenticity of Food of Animal Origin, Compr. Rev. Food Sci. Food Saf. 15(5) (2016) 868−77.

Croteau, R. Biosynthesis and Catabolism of Monoterpenoids Chem. Rev. 87 (1987) 929-954

Cucinotta, L., De Grazia, G., Salerno, T. M. G., Donnarumma, D., Donato, P., Sciarrone, D., Mondello, L. Overcoming the lack of reliability associated to monodimensional gas chromatography coupled to isotopic ratio mass spectrometry data by heart-cut two-dimensional gas chromatography J. Chromatogr. A 1655 (2021) 462473

Cucinotta, L., De Grazia, G., Micalizzi, G., Bontempo, L., Camin, F., Mondello, L., Sciarrone, D. Simultaneous evaluation of the enantiomeric and carbon isotopic ratios of Cannabis sativa L. essential oils by multidimensional gas chromatography Anal Bioanal Chem. 414:18 (2022) 5733-5738

Dosoky, N. S., Setzer, W. N. Biological Activities and Safety of *Citrus* spp. Essential Oils, Int J Mol Sci 19:7 (2018) 1966 doi: 10.3390/ijms19071966

Faber, B., Krause, B., Dietrich, A., Mosandl, A. Gas Chromatography-Isotope Ratio Mass Spectrometry in the Analysis of Peppermint Oil and Its Importance in the Authenticity Control J. Essent. Oil Res. 7:2 (1995) 123-131

Faber, B., Bangert, K., Mosandl, A. GC–IRMS and Enantioselective Analysis in Biochemical Studies in Dill (Anethum graveolens L.) Flavour Fragr. J. 12 (1997) 305–314

Frank, C., Dietrich, A., Kremer, U., Mosandl, A. GC-IRMS in the Authenticity Control of the Essential Oil of Coriandrum sativum L. J. Agric. Food Chem. 43 (1995) 1634-1637

Hong, J. H., Khan, N., Jamila, N., Hong, Y. S., Nho, E. Y., Choi, J. Y., Lee, C. M., Kim, K. S. Determination of Volatile Flavour Profiles of *Citrus* spp. Fruits by SDE-GC–MS and Enantiomeric Composition of Chiral Compounds by MDGC–MS Phytochem. Anal. 28 (2017) 392–403

Juchelka, D., Beck, T., Dettmar, F., Mosandl. A., Multidimensional gas chromatography coupled on-line with isotope ratio mass spectrometry (MDGC-IRMS). J. High Resolut. Chromatogr. 1998, 21, 145

Karl, V., Dietrich, A., Mosandl, A. Gas Chromatography - Isotope Ratio Mass Spectrometry Measurements-of Some Carboxylic Esters from Different Apple Varieties Phytochem. Anal. 5 (1994) 32-37

Lucker, J., El Tamer, M. K., Schwab, W., Verstappen, F. W. A., van der Plas, L. H. W., Bouwmeester, H. J., Verhoeven, H. A. Monoterpene biosynthesis in lemon (Citrus limon) cDNA isolation and functional analysis of four monoterpene synthases Eur. J. Biochem. 269 (2002) 3160–3171

Matucha, M., Jockisch, W., Verner, P., Anders, G. Isotope effect in gas—liquid chromatography of labelled compounds, J. Chromatogr. A 588 (1-2) (1991) 251–258

Meier-Augenstein, W. Applied gas chromatography coupled to isotope ratio mass spectrometry, J. Chromatogr. A, 842 (1999) 351-371.

Mondello, L., Dugo, G. Citrus Oils. Composition, Advanced Analytical Techniques, Contaminants, and Biological Activity; Dugo, G, Mondello, L, editors; CRC Press Taylor & Francis Group: Boca Raton, FL, USA, 2010.

Mondello, L., Costa, R., Sciarrone, D., Dugo, G. The chiral compound of citrus oils. In: Citrus Oils. Composition, Advanced Analytical Techniques, Contaminants, and Biological Activity; Dugo, G, Mondello, L, editors; CRC Press Taylor & Francis Group: Boca Raton, FL, USA, 2010. pp. 349–403

Mosandl, A., Hener, U., Georg Schmarr, H., Rautenschlein, M. Chirospecific flavor analysis by means of enantioselective gas chromatography, coupled on-line with isotope ratio mass spectrometry. J High Resolut Chromatogr. 1990

Phillips, M. A., Wildung, M. R., Williams, D. C., Hyatt, D. C. , Croteau, R. cDNA isolation, functional expression, and characterization of (+)-α-pinene synthase and (-)-α-pinene synthase from loblolly pine (Pinus taeda): Stereocontrol in pinene biosynthesis, Arch Biochem Biophys, 411 (2003) 267–276

Reichert, S., Fischer, D., Asche, S., Mosandl, A. Stable isotope labelling in biosynthetic studies of dill ether, using enantioselective multidimensional gas chromatography, online coupled with isotope ratio mass spectrometry, Flavour Fragr. J. 15 (2000) 303-308.

Schipilliti, L., Dugo, P., Bonaccorsi, I., Mondello, L. Authenticity control on lemon essential oils employing Gas Chromatography–Combustion-Isotope Ratio Mass Spectrometry (GC–C-IRMS), Food Chem. 131 (2012) 1523-1530

Schomburg, G., Husmanm, H., Hubinger, E., Konig, W.A. Multidimensional capillary gas chromatography – enantiomeric separations of selected cuts using a chiral second column, J. High Resolut. Chromatogr. 7 (1984) 404-410

Schurig, V. Separation of enantiomers by gas chromatography J. Chromatogr. A, 906 (2001) 275-299

Sciarrone, D., Schipilliti, L., Ragonese, C., Tranchida, P. Q., Dugo, P., Dugo, G., Mondello, L. Thorough evaluation of the validity of conventional enantio-gas chromatography in the analysis of volatile chiral compounds in mandarin essential oil: A comparative investigation with multidimensional gas chromatography J. Chromatogr. A 1217 (2010) 1101–1105

Sciarrone, D., Schepis, A., Zoccali, M., Donato, P., Vita, F., Creti, D., Alpi, A., Mondello, L. Multidimensional Gas Chromatography Coupled to Combustion- Isotope Ratio Mass Spectrometry/Quadrupole MS with a Low-Bleed Ionic Liquid Secondary Column for the Authentication of Truffles and Products Containing Truffle, Anal. Chem. 90 (2018) 6610−6617.

Silfer, J.A., Engel, M.H., Macko, S.A., Jumeau, E.J. Stable carbon isotope analysis of amino acid enantiomers by conventional isotope ratio mass spectrometry and combined gas chromatography/isotope ratio mass spectrometry. Anal Chem. 63 (1991) 370-374

Tan, W., Bartram, S., Boland, W. Mechanistic studies of sesquiterpene cyclases based on their carbon isotope ratios at natural abundance, Plant, Cell and Environment 41 (2018) 39–49

Publications

1) **Lorenzo Cucinotta**, Gemma De Grazia, Tania Maria Grazia Salerno, Danilo Donnarumma, Paola Donato, Danilo Sciarrone, Luigi Mondello
   "Overcoming the lack of reliability associated to monodimensional gas chromatography coupled to isotopic ratio mass spectrometry data by heart-cut two-dimensional gas chromatography", J. Chromatogr. A 1655 (2021) 462473 https://doi.org/10.1016/j.chroma.2021.462473
2) **Lorenzo Cucinotta**, Gemma De Grazia, Giuseppe Micalizzi, Luana Bontempo, Federica Camin, Luigi Mondello, Danilo Sciarrone
   "Simultaneous evaluation of the enantiomeric and carbon isotopic ratios of Cannabis sativa L. essential oils by multidimensional gas chromatography", Anal Bioanal Chem 414 (2022) 5643–5656 https://doi.org/10.1007/s00216-022-04035-1
3) Marco Calvi, Luana Bontempo, Sarah Pizzini, **Lorenzo Cucinotta**, Federica Camin, Barbara Stenni
   "Isotopic Characterization of Italian Industrial Hemp (Cannabis sativa L.) Intended for Food Use: A First Exploratory Study", Separations, 9(6) (2022) 136; https://doi.org/10.3390/separations9060136
4) Gemma De Grazia, **Lorenzo Cucinotta**, Archimede Rotondo, Paola Donato, Luigi Mondello, Danilo Sciarrone
   "Expanding the Knowledge Related to Flavors and Fragrances by Means of Three-Dimensional Preparative Gas Chromatography and Molecular Spectroscopy", Separations 9(8) (2022) 202; https://doi.org/10.3390/separations9080202